A STUDY OF CONTROL SYSTEM RADII FOR APPROXIMATIONS OF INFINITE DIMENSIONAL SYSTEMS

by

Kimberly L. Oates

Thesis submitted to the Faculty of the

Virginia Polytechnic Institute and State University

in partial fulfillment of the requirements for the degree of

MASTER OF SCIENCE

in

Mathematics

APPROVED:

John A. Burns

John A. Burns, Chairman

Eugene M. Cliff   Terry L. Herdman

Eugene M. Cliff   Terry L. Herdman

August, 1991

Blacksburg, Virginia

A STUDY OF CONTROL SYSTEM RADII FOR APPROXIMATIONS OF INFINITE DIMENSIONAL SYSTEMS

by

Kimberly L. Oates

Committee Chairman: John A. Burns

Mathematics

(Abstract)

In this paper we investigate several aspects of computing control system radii for finite element approximations of control systems governed by partial differential equations. Finite element approximations of the heat equation (parabolic), the wave equation (hyperbolic) and the equations of thermoelasticity (mixed) are used as test cases. Balanced realizations, reduced order models and other transformed models are also studied.

Acknowledgements

I would like to thank my advisor, Dr. John Burns, for his constant encouragement and guidance. He has been a wonderful friend as well as an advisor and has made my last two years invaluable. I can't thank him enough for everything he has done for me.

Thanks are also due to Dr. Eugene Cliff and Dr. Terry Herdman for serving on my committee. They were always encouraging and offered a lot of support.

I'd also like to thank Jin and Donna for their technical typing.

I wish to acknowledge the financial support I received from the Air Force Office of Scientific Research under grant AFOSR-89-0001 and the Defense Advanced Research Projects Agency under contract F49620-87-C-0116.

Next, I'd like to thank the group at ICAM for all of their friendships. It was a pleasure to work with everyone at ICAM.

Finally, I'd like to thank my family for their support. Also, I want to thank Harold for always being there to listen, having patience through the hard times and always giving me the encouragement I needed.

TABLE OF CONTENTS

Chapter I. Introduction

1.1. Introduction.

The development of numerical methods for control of systems governed by partial differential equations often involves a two stage approximation. The first stage typically makes use of finite element, finite difference or Galerkin schemes to produce a finite dimensional, also termed lumped parameter, model to be used as a "design model". Once this finite dimensional "approximating" control system is constructed, numerical or linear algebra algorithms are used to solve the corresponding finite dimensional control problem. This approach to control design for infinite dimensional systems can work well (see [5,7,11,18,19,24,25]) or not at all, depending on the particular approximation scheme used to construct the lumped model [6]. Also, the numerical conditioning of the finite dimensional control problem will depend on the choice of the approximation scheme as well as the type of control problem to be solved, e.g. LQR optimal control, H^∞-control, pole placement, etc..

In recent years, it has been noted that control system radii often provide a measure of the conditioning of specific control problems (see [1,10,12,13,23]). Consequently, it is interesting to investigate these radii for those special finite dimensional systems that result from Galerkin type approximations of partial differential equations. In this paper, we investigate numerically and theoretically a number of problems involving control system radii for Galerkin approximations of three infinite dimensional control systems. The main goals of the numerical experiments are to provide insight into the usefulness of system radii and to investigate some open problems concerning the computation of these radii.

In this chapter, we present a standard example, the heat equation, to illustrate the basic approach that ultimately produces finite dimensional approximate models used in the control design. Two methods, finite elements and finite differences, are used to construct finite dimensional lumped models. This process is described in detail for the heat equation. References are provided for the problems described by the wave equation and the equations of thermoelasticity.

Example 1.1.1. Consider the system governed by the heat equation

$$\frac{\partial}{\partial t}y(t,x) = \frac{\partial^2}{\partial x^2}y(t,x) + b(x)u(t), \tag{1.1.1}$$

$0 < x < 1$, $t > 0$, with Dirichlet boundary conditions

$$y(t,0) = y(t,1) = 0 \tag{1.1.2}$$

and initial condition

$$y(0,x) = T(x). \tag{1.1.3}$$

Here we assume $b(\cdot)$ and $T(\cdot)$ are given and belong to $L_2(0,1)$. The linear quadratic regulator (LQR) problem is to find a control $u_*(\cdot) \in L_2(0,+\infty)$ to minimize the cost function

$$J(u(\cdot)) = \frac{1}{2}\int_0^\infty \{\int_0^1 |y(t,x)|^2 dx + R|u(t)|^2\}dt, \tag{1.1.4}$$

where $R > 0$ is a constant. Observe that

$$J(u(\cdot)) = \frac{1}{2}\int_0^\infty \{\|y(t,\cdot)\|^2_{L_2} + R|u(t)|^2\}dt \tag{1.1.5}$$

is a quadratic functional of $y(t,\cdot)$ and $u(\cdot)$.

It is useful to formulate the control problem (1.1.1)–(1.1.4) as an infinite dimensional control problem. This framework provides the basis for computational and theoretical results. We shall formulate (1.1.1)–(1.1.3) as a distributed parameter system in the Hilbert space $Z = L_2(0,1)$.

Let $\mathcal{A}$ denote the operator defined on Z by $\mathcal{D}(\mathcal{A}) = H^2(0,1) \cap H_0^1(0,1)$ and for $\varphi \in \mathcal{D}(\mathcal{A})$

$$\mathcal{A}\varphi = \frac{\partial^2}{\partial x^2}\varphi.$$

The operator $\mathcal{A}$ generates a C_0-semigroup $S(t)$ on Z. An explicit representation of $S(t)$ can be found by separation of variables (see [27]). In particular,

$$[S(t)T(\cdot)](x) = \sum_{k=1}^{\infty} e^{-\lambda_k t}\langle T(\cdot), \varphi_k(\cdot)\rangle \varphi_k(x), \tag{1.1.6}$$

where $\lambda_k = k^2\pi^2$, $\varphi_k(x) = \sqrt{2}\sin(k\pi x)$ and $\langle \cdot, \cdot \rangle$ denotes the standard inner product on $L_2(0,1)$.

Define the input operator $\mathcal{B} : \mathbb{R}^1 \to L_2(0,1)$ by

$$[\mathcal{B}u](x) = b(x)u \tag{1.1.7}$$

and note that $\mathcal{B}$ is a continuous linear operator. It can be shown [9,10,15] that the heat equation (1.1.1)–(1.1.3) is equivalent to the infinite dimensional system in $Z = L_2(0,1)$ governed by

$$\dot{z}(t) = \mathcal{A}z(t) + \mathcal{B}u(t) \tag{1.1.8}$$

with initial data

$$z(0) = T(\cdot) \in L_2(0,1). \tag{1.1.9}$$

If one defines the "output operator" $\mathcal{C} : Z \to Z$ by $\mathcal{C}z = z$, i.e. the identity operator, then the output to (1.1.8)–(1.1.9) is given by

$$y(t) = \mathcal{C}z(t) \tag{1.1.10}$$

and the cost functional (1.1.5) can be written as

$$J(u(\cdot)) = \frac{1}{2}\int_0^{\infty} \{\langle y(t), y(t)\rangle + \langle Ru(t), u(t)\rangle\}dt \tag{1.1.11}$$

or, equivalently, as

$$J(u(\cdot)) = \frac{1}{2}\int_0^{\infty} \{\langle Qx(t), x(t)\rangle + \langle Ru(t), u(t)\rangle\}dt, \tag{1.1.12}$$

where $\mathcal{Q} = \mathcal{C}^*\mathcal{C}$. Unless otherwise stated, we shall assume that $\mathcal{Q} = \mathcal{C}^*\mathcal{C}$ and $\mathcal{C}$ is a bounded linear operator. In the numerical experiments it is, as for the heat equation here, always the case that $\mathcal{Q} = \mathcal{C} = I$.

It is important to note that $\mathcal{A}$ is self-adjoint and dissipative, i.e.

$$\langle \mathcal{A}z, z\rangle \leq 0 \tag{1.1.13}$$

for all $z \in \mathcal{D}(\mathcal{A})$. Many finite element and finite difference schemes will produce approximations A_N of $\mathcal{A}$ that will also be self-adjoint and dissipative. This feature can be exploited when one computes certain system radii.

1.2. Finite Dimensional Approximation.

The infinite dimensional control problem (1.1.8)–(1.1.12) can be approximated by a finite dimensional control problem if one can construct appropriate approximations of the operators $\mathcal{A}, \mathcal{B}, \mathcal{C}$ and $\mathcal{Q}$. Finite element and finite difference schemes produce such finite dimensional approximations that satisfy various convergence properties. Although we shall not address these theoretical issues, it is important to note that care must be taken to insure that a particular scheme has the proper convergence properties. The interested reader is referred to [6,17,18,19] and the references therein for a discussion of this issue. All of the schemes used in this paper have been analyzed and applied to the LQR problems considered below.

For this paper, it suffices to assume that approximating operators $\mathcal{A}_N, \mathcal{B}_N, \mathcal{C}_N$ and $\mathcal{Q}_N$, for $N = 1, 2, \ldots$, have been constructed. The distributed parameter control system, denoted by Σ,

$$\dot{z}(t) = \mathcal{A}z(t) + \mathcal{B}u(t), \qquad z(0) = z_0 \tag{1.2.1}$$

$$y(t) = \mathcal{C}z(t) \tag{1.2.2}$$

with cost functional

$$J(u(\cdot)) = \frac{1}{2}\int_0^\infty \{\langle \mathcal{Q}z(t),\ z(t)\rangle + \langle Ru(t),\ u(t)\rangle\}dt \tag{1.2.3}$$

is then approximated by the lumped parameter "design model"

$$\dot{z}^N(t) = \mathcal{A}_N z^N(t) + \mathcal{B}_N u(t), \qquad z^N(0) = z_0^N \tag{1.2.4}$$

$$y^N(t) = \mathcal{C}_N z^N(t) \tag{1.2.5}$$

with cost functional

$$J_N(u(\cdot)) = \frac{1}{2}\int_0^\infty \{\langle \mathcal{Q}_N z^N(t),\ z^N(t)\rangle + \langle Ru(t),\ u(t)\rangle\}dt. \tag{1.2.6}$$

Fundamental questions regarding the convergence of control laws computed using the design model to the optimal control laws for the infinite dimensional system Σ have been the subject of several papers (see [6,7,17,18,19]). We shall concentrate on the control system properties of the design model. There are numerous ways of approximating infinite dimensional systems. These methods include modal expansions, finite differences and finite elements. In many cases these methods lead to system matrices with a very special structure. For example, the matrices produced may be symmetric, banded, block tridiagonal, etc.. It is possible to use the structure of these matrices in the design and analysis of the control problem. Since there are many ways of approximating an infinite dimensional system, it is important to identify those methods that are robust. For example, if the infinite dimensional system Σ is controllable, then the approximating system should also be controllable. Likewise, if Σ is stabilizable, then (1.2.4) should be stabilizable. The important system properties should be preserved under the approximations (see [8,9,10,11]).

For the heat equation, it is known that certain finite element and finite difference schemes preserve controllability, observability, stabilizability and detectability of the infinite dimensional system [9,10]. We now present a detailed description of these two schemes. The basic approach extends to the other systems discussed in Chapter III.

Let $N \geq 1$ and divide the interval $[0,1]$ into $N+1$ subintervals $[x_i, x_{i+1}]$, where $x_i = \frac{i}{N+1}$ for $i = 0, 1, \ldots, N+1$. We shall construct approximations $\mathcal{A}_N, \mathcal{B}_N, \mathcal{C}_N$ and $\mathcal{Q}_N$ for the operators $\mathcal{A}, \mathcal{B}, \mathcal{C}$ and $\mathcal{Q}$ of the infinite dimensional control system (1.2.4)–(1.2.6). Recall that $\mathcal{A}$ denotes the operator defined on $L_2(0,1)$ by $\mathcal{D}(\mathcal{A}) = H^2(0,1) \cap H_0^1(0,1)$ and for $\varphi \in \mathcal{D}(\mathcal{A})$

$$\mathcal{A}\varphi = \frac{\partial^2}{\partial x^2}\varphi.$$

First we describe the finite difference method. Using forward differences we approximate $\varphi'(x_i)$ by $\varphi'(x_i) \cong \frac{[\varphi(x_i) - \varphi(x_{i-1})]}{h}$ where $h = \frac{1}{N+1}$. Thus, the second derivative is approximated by the formula

$$\varphi''(x_i) \cong \frac{\varphi(x_{i+1}) - 2\varphi(x_i) + \varphi(x_{i-1})}{h^2}. \tag{1.2.7}$$

In order to construct approximations of the operators of the infinite dimensional system, we define subspaces of $Z = L_2(0,1)$ that are spaces of piecewise linear splines. Let $h_i^N(x)$ denote the "hat" function which is piecewise linear, continuous on $[0,1]$ and satisfies $h_i(x_j) = \delta_{ij}$, where $\delta_{ij} = 1$ if $i = j$ and $\delta_{ij} = 0$ otherwise. The $N+2$ dimensional subspace Z^N of Z is spanned by $\{h_0^N(\cdot), h_1^N(\cdot), \ldots, h_N^N(\cdot), h_{N+1}^N(\cdot)\}$ and the N dimensional space $Z_0^N =$ span $\{h_1^N(\cdot), h_2^N(\cdot), \ldots, h_N^N(\cdot)\}$ is a subspace of $H_0^1(0,1)$. One way to think of the finite difference scheme is to view elements $\varphi(\cdot) \in H_0^1(0,1)$ as being approximated by $\varphi^N(\cdot) \in Z_0^N$ using interpolation, i.e.,

$$\varphi(x) \approx \varphi^N(x) = \sum_{i=1}^{N} \varphi(x_i) h_i^N(x). \tag{1.2.8}$$

The central difference formula (1.2.7) applied to (1.2.8) becomes

$$\varphi''(x) \approx [\mathcal{A}_N^D \varphi^N(\cdot)](x) \triangleq \sum_{i=1}^{N} \frac{[\varphi(x_{i+1}) - 2\varphi(x_i) + \varphi(x_{i-1})]}{h^2} h_i^N(x). \tag{1.2.9}$$

The finite dimensional approximation $\mathcal{A}_N^D$ of the infinite dimensional operator $\mathcal{A}$ has the matrix representation A_N^D on Z_0^N given by

$$A_N^D = \frac{1}{h^2}\begin{bmatrix} -2 & 1 & 0 & 0 & 0 & \cdots & 0 \\ 1 & -2 & 1 & 0 & 0 & \cdots & 0 \\ 0 & 1 & -2 & 1 & 0 & \cdots & 0 \\ 0 & 0 & 1 & -2 & 1 & \cdots & 0 \\ \vdots & \vdots & \vdots & \ddots & \ddots & & \vdots \\ \vdots & \vdots & \vdots & & \ddots & \ddots & 1 \\ 0 & 0 & 0 & \cdots & \cdots & 1 & -2 \end{bmatrix}. \tag{1.2.10}$$

Likewise, if $T(\cdot)$ and $b(\cdot)$ belong to $H^1(0,1)$, we construct B_N^D and T_0^N by

$$B_N^D = col(b(x_1), b(x_2), \ldots, b(x_N)) \tag{1.2.11}$$

and

$$T_0^N = col(T(x_1), T(x_2), \ldots, T(x_N)). \tag{1.2.12}$$

If $z^N(t)$ denotes the vector

$$z^N(t) = col(y(t,x_1), y(t,x_2), \ldots, y(t,x_N)), \tag{1.2.13}$$

then the infinite dimensional system Σ is "approximated" by the N-dimensional system Σ_N^D,

$$\dot{z}^N(t) = A_N^D z^N(t) + B_N^D u(t), \qquad z_0^N(0) = T_0^N, \tag{1.2.14}$$

$$y^N(t) = I_N z^N(t) \tag{1.2.15}$$

where I_N is the $N \times N$ identity matrix. The cost functional $J_N(\cdot)$ is determined by setting $Q_N^D = I_N$. The problem governed by (1.2.14)–(1.2.15) is determined by the system matrices A_N^D, B_N^D, C_N^D and the weighting matrix Q_N^D. We shall abuse notation and use

$$\Sigma = (\mathcal{A}, \mathcal{B}, \mathcal{C}) \tag{1.2.16}$$

and

$$\Sigma_N^D = (A_N^D, B_N^D, C_N^D) \tag{1.2.17}$$

to represent (1.1.8)–(1.1.10) and (1.2.14)–(1.2.15), respectively. The initial data is not represented in (1.2.16)–(1.2.17). The main emphasis of this paper is concerned with control system properties that are independent of initial data and hence the information provided by (1.2.16)–(1.2.17) is usually sufficient for the issues considered here.

The finite difference model Σ_N^D does not always make sense if $b(\cdot)$ or $T(\cdot)$ does not belong to $H_0^1(0,1)$. The finite element scheme is more general. In particular, the basic idea is to approximate functions $\varphi(\cdot) \in H_0^1(0,1)$ by its "least squares projection" onto Z_0^N. This leads to a Galerkin or finite element method.

Since $y(t,\cdot)$ belongs to $H_0^1(0,1)$, we assume an approximation of the form

$$y(t,x) \cong y^N(t,x) = \sum_{i=1}^{N} z_i^N(t) h_i^N(x) \tag{1.2.18}$$

and note that $y^N(t,0) = y^N(t,1) = 0$. It is not possible to directly substitute $y^N(t,x)$ into the heat equation since $h_i^N(x)$ does not have a second derivative. Therefore, one replaces the heat equation by its weak form (see [10,30]) and approximates this form of the heat equation. Basically, the idea is to multiply both sides of the heat equation by a "test function", $\psi(\cdot)$ belonging to $H_0^1(0,1)$, and integrate by parts to produce the variational form of (1.1.1)–(1.1.3).

Multiplying (1.1.1) by $\psi(x)$ and integrating over $[0,1]$ yields

$$\int_0^1 \frac{\partial}{\partial t} y(t,x)\psi(x)dx = \int_0^1 \frac{\partial^2}{\partial x^2} y(t,x)\psi(x)dx + \left[\int_0^1 b(x)\psi(x)dx\right] u(t). \tag{1.2.19}$$

If one integrates by parts the first term on the right hand side of (1.2.19), it follows that

$$\int_0^1 \frac{\partial}{\partial t} y(t,x)\psi(x)\,dx = -\int_0^1 \frac{\partial}{\partial x} y(t,x)\frac{d}{dx}\psi(x)\,dx + \left[\int_0^1 b(x)\psi(x)\,dx\right] u(t) \tag{1.2.20}$$

must hold for all $\psi(\cdot) \in H_0^1(0,1)$. Thus, if $y(t,x)$ satisfies the heat equation (1.1.1)–(1.1.3), then (1.2.20) holds for all $\psi(\cdot) \in H_0^1(0,1)$. Moreover, the Fundamental Lemma of the Calculus of Variations [16] implies that if (1.2.20) holds for all $\psi(\cdot) \in H_0^1(0,1)$, then $y(t,x)$ must be a solution of (1.1.1)–(1.1.3).

Since $y^N(t,x)$ belongs to $H_0^1(0,1)$, it can be substituted into (1.2.20) replacing $y(t,x)$. Moreover, $h_j^N(\cdot)$ belongs to $H_0^1(0,1)$ so (1.2.20) can be approximated by

$$\begin{aligned}\int_0^1 \frac{\partial}{\partial t} y^N(t,x) h_j^N(x) dx = &- \int_0^1 \frac{\partial}{\partial x} y^N(t,x) \frac{d}{dx} h_j^N(x)\, dx \\ &+ \left[\int_0^1 b(x) h_j^N(x) dx\right] u(t)\end{aligned} \tag{1.2.21}$$

for each $j = 1, 2, \ldots, N$. However, since

$$y^N(t,x) = \sum_{i=1}^{N} z_i^N(t) h_i^N(x)$$

it follows that (1.2.21) is equivalent to

$$\begin{aligned}\sum_{i=1}^{N} \dot{z}_i^N(t) \left[\int_0^1 h_i^N(x) h_j^N(x)\, dx\right] = &- \sum_{i=1}^{N} z_i^N(t) \left[\int_0^1 \frac{d}{dx} h_i^N(x) \frac{d}{dx} h_j^N(x)\, dx\right] \\ &+ \left[\int_0^1 b(x) h_j^N(x) dx\right] u(t)\end{aligned} \tag{1.2.22}$$

for $j = 1, 2, \ldots, N$. Equation (1.2.22) represents N equations in N "variables" that has the form

$$\frac{d}{dt} M_N^E \begin{bmatrix} z_1^N(t) \\ z_2^N(t) \\ \vdots \\ z_N^N(t) \end{bmatrix} = -K_N^E \begin{bmatrix} z_1^N(t) \\ z_2^N(t) \\ \vdots \\ z_N^N(t) \end{bmatrix} + G_N^E u(t) \tag{1.2.23}$$

where the mass matrix, M_N^E; stiffness matrix, K_N^E, and input matrix, G_N^E, are given by

$$M_N^E = \left[\int_0^1 h_i^N(x) h_j^N(x) dx\right]^T, \tag{1.2.24}$$

$$K_N^E = \left[\int_0^1 \frac{d}{dx} h_i^N(x) \frac{d}{dx} h_j^N(x) dx\right]^T, \tag{1.2.25}$$

and

$$G_N^E = \left[\int_0^1 b(x) h_j^N(x) dx\right]^T, \tag{1.2.26}$$

respectively.

After computing the integrals, it follows that

$$M_N^E = \frac{1}{6(N+1)} \begin{bmatrix} 4 & 1 & 0 & 0 & 0 & \cdots & 0 \\ 1 & 4 & 1 & 0 & 0 & \cdots & 0 \\ 0 & 1 & 4 & 1 & 0 & \cdots & 0 \\ 0 & 0 & 1 & 4 & 1 & \cdots & 0 \\ \vdots & \vdots & \vdots & \ddots & \ddots & & \vdots \\ \vdots & \vdots & \vdots & & \ddots & \ddots & 1 \\ 0 & 0 & 0 & \cdots & \cdots & 1 & 4 \end{bmatrix}, \tag{1.2.27}$$

$$K_N^E = (N+1) \begin{bmatrix} 2 & -1 & 0 & 0 & 0 & \cdots & 0 \\ -1 & 2 & -1 & 0 & 0 & \cdots & 0 \\ 0 & -1 & 2 & -1 & 0 & \cdots & 0 \\ 0 & 0 & -1 & 2 & -1 & \cdots & 0 \\ \vdots & \vdots & \vdots & \ddots & \ddots & & \vdots \\ \vdots & \vdots & \vdots & & \ddots & \ddots & -1 \\ 0 & 0 & 0 & \cdots & \cdots & -1 & 2 \end{bmatrix}, \tag{1.2.28}$$

and

$$G_N^E = \begin{bmatrix} \langle b(\cdot),\ h_1^N(\cdot)\rangle \\ \langle b(\cdot),\ h_2^N(\cdot)\rangle \\ \vdots \\ \langle b(\cdot), h_N^N(\cdot)\rangle \end{bmatrix}. \tag{1.2.29}$$

Consequently, the finite dimensional model becomes (see [10] for details)

$$M_N^E \dot{z}^N(t) = -K_N^E z^N(t) + G_N^E u(t), \qquad z^N(0) = z_0^N, \tag{1.2.30}$$

where $z_0^N = col(\langle T(\cdot), h_1^N(\cdot)\rangle, \langle T(\cdot), h_2^N(\cdot)\rangle, \ldots, \langle T(\cdot), h_N^N(\cdot)\rangle)$. Let

$$A_N^E = -[M_N^E]^{-1} K_N^E, \tag{1.2.31}$$

$$B_N^E = [M_N^E]^{-1} G_N^E, \tag{1.2.32}$$

$$C_N^E = M_N^E \tag{1.2.33}$$

and Σ_N^E denote the following "finite element model"

$$\dot{z}^N(t) = A_N^E z^N(t) + B_N^E u(t), \qquad z^N(0) = z_0^N \tag{1.2.34}$$

$$y^N(t) = C_N^E z^N(t). \tag{1.2.35}$$

The mass matrix, M_N^E, approximates the identity operator, thus $Q_N^E = C_N^E = M_N^E$ is the appropriate weight in $J_N(\cdot)$.

Although both Σ_N^D and Σ_N^E are often used as (open-loop) approximations of Σ, care should be exercised when using Σ_N^D or Σ_N^E in control design (see [7,10]). Questions concerning open-loop convergence, convergence of control laws, preservation of system properties, etc., are all important and have been discussed in the literature cited above. We turn now to the central issue of this paper: the analysis of the systems, Σ_N.

Chapter II. Control System Radii

2.1. Control System Concepts.

In this section we let $\Sigma_n = (A, B, C)$ denote the linear time invariant finite dimensional system

$$(\Sigma_n) \qquad \begin{aligned} \dot{x}(t) &= Ax(t) + Bu(t) && (2.1.1) \\ y(t) &= Cx(t) && (2.1.2) \end{aligned}$$

of dimension n. In particular, A is an $n \times n$ real matrix and B and C are $n \times m$ and $l \times n$ real matrices, respectively. Here $x(t)$ denotes the state vector, $y(t)$ is the output and $u(t)$ is the input or control.

Given initial data x_0 in $\mathbb{R}^n$ and a control $u(t)$ and $L_2(0, t_1)$, the solution to (2.1.1) with $x(0) = x_0$ is given by the variation of parameter formula

$$x(t) = e^{At}x_0 + \int_0^t e^{A(t-s)}Bu(s)ds \tag{2.1.3}$$

where e^{At} is the matrix exponential of A. In particular, e^{At} is the C_0-semigroup generated by A (see [27]).

We say that (2.1.1) can be steered from x_0 to x_1 if there is a $t_1 > 0$ and a control $u(\cdot)$ in $L_2(0, t_1)$ such that $x(0) = x_0$ and $x(t_1) = x_1$ where $x(t)$ is defined by (2.1.3).

We shall need the following basic definitions of controllability, observability, stabilizability and detectability. Although these definitions are not presented in the most general form, they are sufficient for the linear time invariant system considered here.

Definition 2.1.1. The system Σ_n is controllable if given $x_0, x_1 \in \mathbb{R}^n$, $t_1 > 0$, there is a control $u(\cdot) \in L_2(0, t_1)$ such that $u(\cdot)$ steers $x(t)$ from x_0 to x_1 at time t_1.

Definition 2.1.2. The linear system Σ_n is observable if $u(t) \equiv 0$ and $y(t) \equiv 0$ for $0 \le t \le \hat{t}$ implies that $x_0 = 0$.

Definition 2.1.3. The linear system Σ_n is exponentially stabilizable if there is a $m \times n$ matrix K and positive numbers M and α such that if $u(t)$ is defined by

$$u(t) = -Kx(t), \tag{2.1.4}$$

then the closed loop system

$$\dot{x}_c(t) = [A - BK]x_c(t) \tag{2.1.5}$$

has solutions $x_c(t)$ satisfying

$$\|x_c(t)\| \leq Me^{-\alpha t}\|x_c(0)\| \tag{2.1.6}$$

for all $t \geq 0$.

Definition 2.1.4. The linear system Σ_n is detectable if there exists a $n \times k$ matrix F and positive numbers N and δ such that if $z_c(t)$ satisfies

$$\dot{z}_c(t) = (A^T - C^T F^T)z_c(t) \tag{2.1.7}$$

then

$$\|z_c(t)\| \leq Ne^{-\delta t}\|z_c(0)\| \tag{2.1.8}$$

for all $t \geq 0$.

Although there are several equivalent notions of matrix norms, we shall always use the spectral norm.

Definition 2.1.5. Let M be a $p \times q$ complex matrix. The spectral norm of M is defined by

$$\|M\| = \sup_{\|x\|_2 = 1} \|Mx\|_2, \tag{2.1.9}$$

where $\|x\|_2$ denotes the standard Euclidean norm on $\mathbb{C}^p$ and $\mathbb{C}^q$. Note that $\mathbb{C}^p$ consists of all p–tuples where each p–tuple is a complex number.

The following theorems provide the basic link between the system properties and the system matrices. Proofs of these results may be found in [20,29].

Theorem 2.1.1. *The linear system Σ_n is controllable if and only if the controllability matrix*

$$CM = [B, AB, A^2B, \ldots, A^{n-1}B] \tag{2.1.10}$$

has rank n.

Theorem 2.1.2. *The linear system Σ_n is observable if and only if the observability matrix*

$$OM = \begin{bmatrix} C \\ CA \\ CA^2 \\ \vdots \\ CA^{n-1} \end{bmatrix} = [C^T, A^TC^T, (A^2)^TC^T, \ldots, (A^{n-1})^TC^T]^T \tag{2.1.11}$$

has rank n.

The following theorem may be found in [2]. We give the proof here because it provides some insight into the theorems on controllability radii that follow.

Theorem 2.1.3. *Let*

$$H(\lambda) = [\lambda I - A,\ B]. \tag{2.1.12}$$

The linear system Σ_n is controllable if and only if rank $H(\lambda) = n$ for all $\lambda \in \mathbb{C}$.

Proof: First assume that Σ_n is controllable, then by Theorem 2.2.1 $rank[B, AB, A^2B, \ldots, A^{n-1}B] = n$. If $v^*B = 0$ for some $v^* \neq 0$, then $v^*[AB, A^2B, \ldots, A^{n-1}B] \neq 0$. Therefore, there is a p such that $1 \leq p \leq n-1$ and $v^*A^pB \neq 0$. Thus, one of the vectors A^*v, $(A^*)^2v, \ldots, (A^*)^{n-1}v$ is not orthogonal to the column space spanned by B. Suppose v is an eigenvector of A^*. Then $(\lambda - A^*)v = 0$. Therefore $\lambda v = A^*v$ and so $B^*\lambda v = B^*A^*v$. However, recall that $v^*B = 0$ and thus $B^*\lambda v = 0$. Consequently, $B^*A^*v = 0$ or $v^*AB = 0$ which requires all vectors A^*v, $(A^*)^2v, \ldots, (A^*)^{n-1}v$ to be orthogonal to the column space spanned by B. Therefore v must not be an eigenvector of A^*. Thus, $(\lambda I - A^*)v \neq 0$ for all λ, so $v^*(\lambda I - A) \neq 0$ for all λ, and hence $rank\ H(\lambda) = rank[\lambda I - A,\ B] = n$.

Conversely, if $rank\ H(\lambda) = n$, then we first show that A^* has no nontrivial eigenvector orthogonal to the column space of B. The proof of the converse will follow from this fact. Hence we assume A^* has a nontrivial invariant subspace, S, orthogonal to the column space of B. We will show that there is an eigenvector of A^* which is in S. Let v be a nonzero vector in S. Thus v, $A^*v, \ldots, (A^*)^{n-1}v$ are orthogonal to the column space of B. If m denotes the smallest integer k such that v, $A^*v, \ldots, (A^*)^k v$ are linearly dependent, then there exits $a_0, a_1, \ldots, a_k$, $\sum_{i=0}^{k} |a_i| \neq 0$ and $a_0 v + a_1 A^* v + \cdots + a_m (A^*)^m v = 0$. Let μ be a root of $a_0 + a_1 z + \cdots + z^m = 0$ so that $a_0 + a_1\mu + \cdots + \mu^m = 0$. Let $b_0, b_1, \ldots, b_{m-1}$ be such that

$$
\begin{aligned}
b_{m-1} &= -1 \\
b_{m-2} &= -a_{m-1} + \mu b_{m-1} \\
b_{m-3} &= -a_{m-2} + \mu b_{m-2} \\
&\vdots \\
b_0 &= -a_1 + \mu b_1.
\end{aligned}
$$

Then $\mu b_0 = -\mu a_1 - \mu^2 a_2 - \cdots - \mu^m = a_0$ and it follows that

$$
\begin{aligned}
a_0 &= \mu b_0 \\
a_1 &= \mu b_1 - b_0 \\
a_2 &= \mu b_2 - b_1 \\
&\vdots \\
a_{m-1} &= \mu b_{m-1} - b_{m-2}.
\end{aligned}
$$

Therefore, $\mu b_0 v + (\mu b_1 - b_0)A^*v + \cdots + (\mu b_{m-1} - b_{m-2})(A^*)^{m-1}v - b_{m-1}(A^*)^m v = 0$ and hence $(\mu I - A^*)(b_0 v + b_1 A^* v + \cdots + b_{m-1}(A^*)^{m-1} v) = 0$. Consequently, a nonzero eigenvector of A^* is orthogonal to the column space of B. However, we know A^* has no eigenvector orthogonal to the column space of B. So, by contradiction, A^* has no nontrivial invariant subspace orthogonal to the column space of B.

Now suppose $v^* B = 0$ for some $v \neq 0$. Then either v or A^*v or $\ldots$ or $(A^*)^n v$ is not orthogonal to the column space of B. Suppose $(A^*)^k v$ is not orthogonal to the column space of B, then $[(A^*)^k v]^* B \neq 0$. Therefore, $v^* A^k B \neq 0$ and hence $v^*[B, AB, \ldots, A^{n-1}B] \neq 0$. Therefore, it follows that $rank\ H(\lambda) = rank[B, AB, \ldots, A^{n-1}] = n$ and this completes the proof of the theorem.

If $K(\lambda)$ denotes the matrix

$$K(\lambda) = [\lambda I - A^T,\ C^T], \tag{2.1.13}$$

then Theorem (2.1.2) yields the following result.

Theorem 2.1.4. *The linear system Σ_n is observable if and only if $rank\ K(\lambda) = n$ for all $\lambda \in \mathbb{C}$.*

The above proof may be modified to yield the following results.

Theorem 2.1.5. *The linear system Σ_n is stabilizable if and only if $rank\ H(\lambda) = n$ for all $\lambda \in \mathbb{C}$ with $Re(\lambda) \geq 0$.*

Theorem 2.1.6. *The linear system Σ_n is detectable if and only if $rank\ K(\lambda) = n$ for all $\lambda \in \mathbb{C}$ with $Re(\lambda) \geq 0$.*

It should be noted that controllability is a generic property. In particular, if the system Σ_n is controllable, then Σ_n remains controllable under sufficiently small perturbations of A and B. It is important to know the size of the smallest perturbations that change the controllability of a system. As noted in [1,12,14,21,22,23] this can be useful in the numerical analysis of algorithms for control design. If the distance between a controllable system and an uncontrollable system is large then "small" errors in data defining the system, matrices A, B and C, will not destroy controllability. Numerical algorithms which assume a specific system property such as controllability or stabilizability can be expected to be numerically ill-conditioned if the system is nearly uncontrollable (or nearly unstabilizable). The basic idea is discussed in the papers by Laub [21,23] and Demmel [12,13]. We turn now to the precise definitions of system radii.

2.2. System Radii.

As noted previously, if the distance between a controllable (observable, stabilizable, detectable) system and an uncontrollable (unobservable, unstabilizable, undetectable) system is small, then the control problem may be numerically impossible to solve. System radii may provide some measure of ill-conditioning. As noted by Laub [21,23] and Demmel [12,13] the "condition number of the control problem" is often inversely proportional to the distance from that problem to the nearest ill-posed problem. Therefore, if the distance from the control problem to the nearest ill-posed problem is small then one would expect the condition number to be large, hence ill-conditioned.

Let Γ be the set of all complex "systems" of dimension (n, m, k). Thus, $\Sigma = (A, B, C) \in \Gamma$ if A, B and C are $n \times n$, $n \times m$ and $l \times n$ complex matrices, respectively. In particular,

$$\Gamma = \{\Sigma = (A, B, C) | A \in \mathbb{C}^{n\times n},\ B \in \mathbb{C}^{n\times m},\ C \in \mathbb{C}^{l\times n}\}. \tag{2.2.1}$$

Let $\Omega \subset \Gamma$ denote the subset of real systems,

$$\Omega = \{\Sigma = (A, B, C) \in \Gamma | A \in \mathbb{R}^{n\times n},\ B \in \mathbb{R}^{n\times m},\ C \in \mathbb{R}^{l\times n}\}. \tag{2.2.2}$$

Let $\Sigma^1 = (A_1, B_1, C_1)$ and $\Sigma^2 = (A_2, B_2, C_2)$ belong to Γ. We define the distance between Σ^1 and Σ^2 by

$$\delta(\Sigma^1, \Sigma^2) = \|(A_1 - A_2, B_1 - B_2, C_1 - C_2)\|_2. \tag{2.2.3}$$

If $\Sigma \in \Gamma$ and S is a subset of Γ, then the distance between Σ and S is defined by

$$d(\Sigma, S) = \inf\{\delta(\Sigma, \Sigma^j) \mid \Sigma^j \in S\}. \tag{2.2.4}$$

Let $N_c \subseteq \Gamma$ be the set of all complex systems that are not controllable, $N_o \subseteq \Gamma$ be the set of all complex systems that are not observable, $N_s \subseteq \Gamma$ be the set of all complex systems that are not stabilizable and $N_d \subseteq \Gamma$ be the set of all complex systems that are not detectable, or equivalently,

$$N_c = \{\Sigma \in \Gamma | (A, B) \text{ is not controllable}\}, \tag{2.2.5}$$

$$N_o = \{\Sigma \in \Gamma | (A, C) \text{ is not observable}\}, \tag{2.2.6}$$

$$N_s = \{\Sigma \in \Gamma | (A, B) \text{ is not stabilizable}\} \tag{2.2.7}$$

and

$$N_d = \{\Sigma \in \Gamma | (A, C) \text{ is not detectable}\}. \tag{2.2.8}$$

Given $\Sigma \in \Gamma$, we define the (complex) controllability radii, γ_c; observability radii, γ_o; stabilizability radii, γ_s, and detectability radii, γ_d by

$$\gamma_c = \gamma_c(\Sigma) = d(\Sigma, N_c), \tag{2.2.9}$$

$$\gamma_o = \gamma_o(\Sigma) = d(\Sigma, N_o), \tag{2.2.10}$$

$$\gamma_s = \gamma_s(\Sigma) = d(\Sigma, N_s), \tag{2.2.11}$$

and

$$\gamma_d = \gamma_d(\Sigma) = d(\Sigma, N_d). \tag{2.2.12}$$

These radii provide numerical bounds on the errors that can be tolerated in the data defining the system matrices A, B and C and still guarantee the respective system property. Also, these radii provide some measure of the numerical ill-conditioning of the various control design algorithms used to solve the control problems defined by $\Sigma = (A, B, C)$.

We note that system radii are useful only if they can be computed. One of the main goals of this paper is to investigate this issue for systems that result from finite dimensional approximations of infinite dimensional systems. Let $\sigma_{\min}(M)$ denote the minimum singular value of the matrix M. The following theorems may be found in [14].

Theorem 2.2.1. *If Σ is controllable, then*

$$\gamma_c = \gamma_c(\Sigma) = \min_{\lambda \in \mathbb{C}} \{\sigma_{\min}[H(\lambda)]\}. \tag{2.2.13}$$

Alternatively,

$$\gamma^2(\Sigma) = \min_{(x,y)\in U} [\phi(x,y)]$$

where

$$\phi(x,y) = \{\|A^T x\|^2 + \|A^T y\|^2 + \|B^T x\|^2 + \|B^T y\|^2\} \\ - \{[x^T A x + y^T A y]^2 + [x^T(A^T - A)y]^2\} \tag{2.2.14}$$

and

$$U = \{(x,y) \in \mathbb{R}^n \times \mathbb{R}^n \mid \|x\| + \|y\| = 1\}. \tag{2.2.15}$$

Theorem 2.2.2. *If Σ is stabilizable, then*

$$\gamma_s = \gamma_s(\Sigma) = \min_{Re(\lambda)\geq 0} \{\sigma_{\min}[H(\lambda)]\}. \tag{2.2.16}$$

Even with the above theorem, γ_c and γ_s may be difficult to compute, especially for large systems. Note that the measures, γ_c and γ_s, allow for complex perturbations of A, B and C because $H(\lambda)$ must have maximal rank for all complex λ. Therefore, it may happen that the minimum-norm rank reducing perturbation $(\delta(A), \delta(B), \delta(C))$ is complex. Thus, one must include complex matrices in Γ. Sometimes it is desirable to allow only real perturbations. Therefore, we define the (real) radii by

$$\omega_c = \omega_c(\Sigma) = d(\Sigma, N_c \cap \Omega), \tag{2.2.17}$$

$$\omega_o = \omega_o(\Sigma) = d(\Sigma, N_o \cap \Omega), \tag{2.2.18}$$

$$\omega_s = \omega_s(\Sigma) = d(\Sigma, N_s \cap \Omega), \tag{2.2.19}$$

and

$$\omega_d = \omega_d(\Sigma) = d(\Sigma, N_d \cap \Omega). \tag{2.2.20}$$

The following result may be found in [20].

Theorem 2.2.3. *If Σ is controllable, then Σ is stabilizable.*

Theorem 2.2.3 implies that the distance from a system Σ to an uncontrollable system is always less than or equal to the distance from the system Σ to an unstabilizable system. In other words,

$$\gamma_c \leq \gamma_s \tag{2.2.21}$$

and

$$\omega_c \leq \omega_s. \tag{2.2.22}$$

Note also that restricting the system to be real and allowing only real perturbations yields

$$\gamma_c \leq \omega_c \tag{2.2.23}$$

and

$$\gamma_s \leq \omega_s. \tag{2.2.24}$$

There may be a significant difference between the various measures.

Much work has been done on the problem of expressing these measures by computable representations. Some of the attempts to find representations for ω_c and ω_s have produced erroneous results. Boley and Lu [4] gave the following characterization

$$\omega_c = \min_{\lambda \in \mathbf{R}} \{\sigma_{\min}[H(\lambda)]\}.$$

The following is a counterexample and may be found in [10].

Example 2.2.1. Let $0 < \epsilon \leq \frac{1}{2}$ and define

$$A = \begin{bmatrix} 0 & -1 \\ 1 & 0 \end{bmatrix} \qquad \text{and} \qquad B = \begin{bmatrix} \epsilon \\ 0 \end{bmatrix}.$$

Note that $\omega_c = \epsilon \leq \frac{1}{2}$ since

$$[B, AB] = \begin{bmatrix} \epsilon & 0 \\ 0 & \epsilon \end{bmatrix}$$

and a system is controllable when $rank[B, AB] = n$. Note that in general for an arbitrary A, $\omega_c \leq \epsilon$.

Observe that

$$H(\lambda)[H(\lambda)]^T = \begin{bmatrix} \lambda^2 + 1 + \epsilon^2 & \lambda \\ 0 & 1 + \lambda^2 \end{bmatrix}.$$

Therefore we can see that the minimum singular value of $H(\lambda)$, which is the minimum of the positive square roots of the eigenvalues of the matrix $H(\lambda)[H(\lambda)]^T$, is $\sqrt{\lambda^2+1}$. So $\sigma_{\min}[H(\lambda)] = \sqrt{\lambda^2+1}$ and $\underset{\lambda\in\mathbf{R}}{min}\{\sigma_{\min}[H(\lambda)]\} = 1$. Thus $w_c \leq \frac{1}{2} < 1 = \underset{\lambda\in\mathbf{R}}{min}\{\sigma_{\min}[H(\lambda)]\}$. In other words, for this example we have $\omega_c < \underset{\lambda\in\mathbf{R}}{min}\{\sigma_{\min}[H(\lambda)]\}$.

The following results may be found in the papers by Burns and Peichl [2,10].

Theorem 2.2.4. *Assume that $\Sigma = (A, B, C) \in \Gamma$ is controllable.*

(i) If $A = A^*$, then

$$\gamma_c = \min_{\lambda\in\mathbf{R}}\{\sigma_{\min}[H(\lambda)]\}. \tag{2.2.25}$$

(ii) If $A = -A^*$, then

$$\gamma_c = \min_{\lambda\in\mathbf{R}}\{\sigma_{\min}[H(i\lambda)]\}. \tag{2.2.26}$$

(iii) If $\Sigma = (A, B, C) \in \Omega$ and $A = A^T$, then

$$\gamma_c = \omega_c = \min_{\lambda\in\mathbf{R}}\{\sigma_{\min}[H(\lambda)]\}. \tag{2.2.27}$$

Theorem 2.2.5. *Assume that $\Sigma = (A, B, C) \in \Gamma$ is stabilizable and let $\mathbb{R}^+ = \{\lambda \in \mathbb{R} | \lambda > 0\}$.*

(i) If $A = A^*$, then

$$\gamma_s = \min_{\lambda\in\mathbf{R}^+}\{\sigma_{\min}[H(\lambda)]\}. \tag{2.2.28}$$

(ii) If $A = -A^*$, then

$$\gamma_s = \min_{\lambda\in\mathbf{R}}\{\sigma_{\min}[H(i\lambda)]\}. \tag{2.2.29}$$

(iii) If $\Sigma = (A, B, C) \in \Omega$ and $A = A^T$, then

$$\gamma_s = \omega_s = \min_{\lambda\in\mathbf{R}^+}\{\sigma_{\min}[H(\lambda)]\}. \tag{2.2.30}$$

Corollary 2.2.1. *If $\Sigma = (A, B, C) \in \Omega$ is stabilizable, $A = A^T$ and $x^T Ax \leq 0$ for all $x \in \mathbb{R}^n$, then*

$$\omega_s = \gamma_s = \sigma_{\min}[H(0)] = \sigma_{\min}[A, B]. \tag{2.2.31}$$

Corollary 2.2.1 has applications to a wide variety of models that result from finite element and finite difference approximations of the heat equation. Many finite element and finite difference approximations of the heat equation produce real, symmetric A matrices that satisfy $x^T Ax \leq 0$. It is important to note that none of the system radii are invariant under general similarity transformations. In particular, let $T \in \mathbb{R}^{n \times n}$ be nonsingular. If $\tilde{A} = T^{-1}AT$, $\tilde{B} = T^{-1}B$ and $\tilde{C} = CT$, then it may happen that

$$\gamma_c(A, B) \neq \gamma_c(\tilde{A}, \tilde{B}),$$

$$\gamma_s(A, B) \neq \gamma_s(\tilde{A}, \tilde{B}),$$

$$\gamma_o(A, C) \neq \gamma_o(\tilde{A}, \tilde{C})$$

and

$$\gamma_d(A, C) \neq \gamma_d(\tilde{A}, \tilde{C}).$$

If T is unitary, then all of the measures are preserved under transformations.

2.3. Balancing and Model Reduction.

In this section, we review the basic concepts of balancing and model reduction. The reader is referred to the papers [22,26] for complete details.

Given a system $\Sigma = (A, B, C)$ and a nonsingular mapping $T : \mathbb{R}^n \to \mathbb{R}^n$, the transformation

$$w(t) = T^{-1}x(t) \tag{2.3.1}$$

produces a state space model of the form

$$\dot{w}(t) = [T^{-1}AT]w(t) + [T^{-1}B]u(t) \tag{2.3.2}$$

$$y(t) = [CT]w(t) \tag{2.3.3}$$

which has the same input–output relation as the system $\Sigma = (A, B, C)$. In particular if

$$\tilde{A} = T^{-1}AT, \tag{2.3.4}$$

$$\tilde{B} = T^{-1}B, \tag{2.3.5}$$

and

$$\tilde{C} = CT, \tag{2.3.6}$$

then $\Sigma = (A, B, C)$ and $\tilde{\Sigma} = (\tilde{A}, \tilde{B}, \tilde{C})$ share the same system properties. For example, Σ is controllable if and only if $\tilde{\Sigma}$ is controllable, etc..

Since we are interested in the LQR problem, we note that the transformation (2.3.4)–(2.3.6) produces an equivalent LQR problem provided J is replaced by

$$\tilde{J}(u(\cdot)) = \frac{1}{2}\int_0^\infty \left\{ \langle \tilde{Q}w(t), w(t)\rangle + \langle Ru(t), u(t)\rangle \right\} dt \tag{2.3.7}$$

where

$$\tilde{Q} = T^T Q T. \tag{2.3.8}$$

If one solves the LQR problem defined by (2.3.2)–(2.3.3) and (2.3.7)–(2.3.8) for the optimal gain $\tilde{K}$, then the optimal gain K for the original LQR problem is given by

$$K = \tilde{K}T^{-1}. \tag{2.3.9}$$

Proofs of the above statements follow by direct substitution of $w(t) = T^{-1}x(t)$ into the fundamental equations.

We shall be interested in several transformations. However, one transformation often used in control system design is the balancing transformation. In order to define this transformation, we first note that the system is required to be exponentially stable. If Σ is exponentially stable, then the controllability and observability grammians are given by

$$W_c^2 = \int_0^\infty e^{At} B B^T e^{A^T t}\, dt \tag{2.3.10}$$

and

$$W_o^2 = \int_0^\infty e^{A^T t} C^T C e^{At}\, dt, \tag{2.3.11}$$

respectively. It follows that W_c^2 and W_o^2 are the unique symmetric, positive definite matrices which satisfy

$$A W_c^2 + W_c^2 A^T = -BB^T \tag{2.3.12}$$

and

$$A^T W_o^2 + W_o^2 A = -C^T C, \tag{2.3.13}$$

(see [26]). The following definition can be found in [26].

Definition 2.3.1. A system $\hat{\Sigma} = (\hat{A}, \hat{B}, \hat{C})$ is said to be (internally) balanced if there exist a diagonal matrix

$$\hat{\Lambda} = diag\,\{\sigma_1^2, \sigma_2^2, \ldots, \sigma_n^2\} \tag{2.3.14}$$

such that $\hat{W}_c^2 = \hat{W}_o^2 = \hat{\Lambda}$.

If Σ is controllable and observable, then there exists a nonsingular transformation T_b such that $\hat{\Sigma} = (\hat{A}, \hat{B}, \hat{C})$ defined by $\hat{A} = T_b^{-1} A T_b$, $\hat{B} = T_b^{-1} B$ and $\hat{C} = C T_b$ is balanced (see [26] for details) and $\hat{\Lambda} = \hat{W}_c^2 = \hat{W}_o^2 = diag\,\{\sigma_1^2, \sigma_2^2, \ldots, \sigma_n^2\}$ where $\sigma_1^2, \sigma_2^2, \ldots, \sigma_n^2$ are the Hankel singular values for Σ.

MATLAB was used for our numerical experiments. The file BALREAL.M, using Laub's algorithm, constructs the balanced system $\hat{\Sigma} = (\hat{A}, \hat{B}, \hat{C})$ given the exponentially stable system $\Sigma = (A, B, C)$. A vector is also produced containing the diagonal of $\hat{\Lambda}$ ordered such that $\sigma_1^2 \geq \sigma_2^2 \geq \cdots \geq \sigma_n^2$. The balancing matrix T_b is also returned. We note that in MATLAB 386, BALREAL.M returns the incorrect T_b. However, it is rather simple to modify BALREAL.M so that the correct transformation T_b is returned (remove the line $t = t(i,i)$ and replace it with $t = t * In(:,i)$ where $In = eye(n)$). Note also that the correct transformation T_b is needed to construct $\hat{Q}$ from Q and K from $\hat{K}$.

After balancing the system Σ it is possible to apply a model reduction technique to the balanced system $\hat{\Sigma}$. The basic idea is to eliminate those states corresponding to the "smallest singular values σ_j^2." If the last k singular values $\sigma_n^2, \sigma_{n-1}^2, \ldots, \sigma_{n-k+1}^2$ are "small" compared to $\sigma_1^2, \sigma_2^2, \ldots, \sigma_{n-k}^2$, then the model reduction scheme proceeds as follows. The system

$$\dot{w}(t) = \hat{A}w(t) + \hat{B}u(t) \tag{2.3.15}$$

$$y(t) = \hat{C}w(t) \tag{2.3.16}$$

is partitioned into the system

$$\begin{bmatrix} \dot{w}_1(t) \\ \dot{w}_2(t) \end{bmatrix} = \begin{bmatrix} \hat{A}_{11} & \hat{A}_{12} \\ \hat{A}_{21} & \hat{A}_{22} \end{bmatrix} \begin{bmatrix} w_1(t) \\ w_2(t) \end{bmatrix} + \begin{bmatrix} \hat{B}_1 \\ \hat{B}_2 \end{bmatrix} u(t) \tag{2.3.17}$$

$$y(t) = \begin{bmatrix} \hat{C}_1 & \hat{C}_2 \end{bmatrix} \begin{bmatrix} w_1(t) \\ w_2(t) \end{bmatrix} \tag{2.3.18}$$

where $w_2(t)$ is a vector of dimension k corresponding to the "smallest" singular values. Therefore,

$$\dot{w}_1(t) = \hat{A}_{11}w_1(t) + \hat{A}_{12}w_2(t) + \hat{B}_1u(t) \tag{2.3.19}$$

and

$$\dot{w}_2(t) = \hat{A}_{21}w_1(t) + \hat{A}_{22}w_2(t) + \hat{B}_2u(t). \tag{2.3.20}$$

The next step in model reduction is to set $\dot{w}_2(t) = 0$. Hence (2.3.20) becomes

$$w_2(t) = -\hat{A}_{22}^{-1}\hat{A}_{21}w_2(t) - \hat{A}_{22}^{-1}\hat{B}_2u(t) \tag{2.3.21}$$

and by substitution

$$\dot{w}_1(t) = A_R w_1(t) + B_R u(t) \tag{2.3.22}$$

and

$$y(t) = C_R w(t) + D_R u(t) \tag{2.3.23}$$

where

$$A_R = \hat{A}_{11} - \hat{A}_{12}\hat{A}_{22}^{-1}\hat{A}_{21},$$

$$B_R = \hat{B}_1 - \hat{A}_{12}\hat{A}_{22}^{-1}\hat{B}_2,$$

$$C_R = \hat{C}_1 - \hat{C}_2\hat{A}_{22}^{-1}\hat{A}_{21}$$

and

$$D_R = \hat{C}_2\hat{A}_{22}^{-1}\hat{B}_2.$$

This process leads to the reduced order system $\Sigma_R = (A_R, B_R, C_R, D_R)$. Observe that we have an extra term, $D_R u(t)$, in our reduced output equation.

Again, we are concerned with solving the LQR problem for the reduced order model. In order to do so, the cost function J must be modified to account for the term $D_R u(t)$ in the output.

If (2.3.21) is substituted into the cost function J, then the integrand becomes

$$\begin{aligned}
\langle \hat{Q}w, w\rangle + \langle Ru, u\rangle &= \begin{bmatrix} w_1 & w_2 \end{bmatrix} \begin{bmatrix} \hat{Q}_{11} & \hat{Q}_{12} \\ \hat{Q}_{21} & \hat{Q}_{22} \end{bmatrix} \begin{bmatrix} w_1 \\ w_2 \end{bmatrix} + u^T R u \\
&= w_1^T Q_R w_1 + w_1^T N_R u + u^T R_R u \\
&= \langle Q_R w_1, w_1\rangle + \langle w_1, N_R u\rangle + \langle R_R u, u\rangle.
\end{aligned}$$

Consequently, the appropriate cost function for the reduced order LQR problem has the form

$$J_R(u(\cdot)) = \frac{1}{2}\int_o^\infty \{\langle Q_R w_1(t), w_1(t)\rangle + \langle w_1(t), N_R u(t)\rangle + \langle R_R u(t), u(t)\rangle\}\, dt \tag{2.3.24}$$

where

$$Q_R = \hat{Q}_{11} - \hat{Q}_{12}\hat{A}_{22}^{-1}\hat{A}_{21} - \hat{A}_{21}^T(\hat{A}_{22}^{-1})^T\hat{Q}_{21} + \hat{A}_{21}^T(\hat{A}_{22}^{-1})^T\hat{Q}_{22}\hat{A}_{22}^{-1}\hat{A}_{21},$$

$$N_R = \hat{A}_{21}^T(\hat{A}_{22}^{-1})^T[\hat{Q}_{22}^T + \hat{Q}_{22}]\hat{A}_{22}^{-1}\hat{B}_2 - [\hat{Q}_{12} + \hat{Q}_{21}^T]\hat{A}_{22}^{-1}\hat{B}_2$$

and

$$R_R = \hat{B}_2^T(\hat{A}_{22}^{-1})^T\hat{Q}_{22}\hat{A}_{22}^{-1}\hat{B}_2 + R.$$

If K_R denotes the optimal gain matrix for the reduced order LQR problem, then we construct a "suboptimal" gain for the full order balanced system by augmenting K_R with k zero columns, i.e.,

$$\hat{K}_b = \begin{bmatrix} K_R & \vdots & 0 & \vdots & 0 & \vdots & \cdots & 0 \end{bmatrix}. \tag{2.3.25}$$

In the next chapter, we present the results of several numerical experiments based on using balancing and model reduction to compute optimal feedback laws. We note, however, that the reduced order LQR problem has cross terms and that these terms should be accounted for so that the reduced LQR problem provides an accurate approximation to the full LQR problem.

Chapter III. Numerical Experiments

3.1. Introduction.

In this chapter we present the results of several numerical experiments for three different control systems. The goal of this effort is to provide some insight into the problem of computing system radii for finite element approximations of parabolic, hyperbolic and hybrid systems. We restrict our attention to finite element approximations and refer the reader to [9,10] where finite difference schemes are discussed and compared with finite element models.

MATLAB was used to construct the basic finite element models. Various MATLAB routines from the Control Toolbox were used for balancing, model reduction and solving the LQR control problems.

3.2. The Heat Equation.

The problem we consider here is the control problem for the heat equation discussed in Chapter I. In particular, we consider the problem

$$\frac{\partial}{\partial t}y(t,x) = \frac{\partial^2}{\partial x^2}y(t,x) + xu(t), \tag{3.2.1}$$

$0 < x < 1$, $t > 0$, with Dirichlet boundary conditions

$$y(t,0) = y(t,1) = 0 \tag{3.2.2}$$

and cost function

$$J(u(\cdot)) = \frac{1}{2}\int_0^\infty \{\|y(t,\cdot)\|^2_{L^2} + R|u(t)|^2\}\,dt \tag{3.2.3}$$

where $R = 1.0 \times 10^{-6}$.

If one applies the finite element method to this system then the approximate control problem is governed by the "raw finite element" model (1.2.34)–(1.2.35). In particular, if $A_N = A_N^E$, $B_N = B_N^E$ and $C_N = C_N^E = Q_N$ are defined by (1.2.31)–(1.2.33), then the finite element system (of dimension N) is given by

$$\Sigma_N = (A_N, B_N, C_N). \tag{3.2.4}$$

We shall also make use of the balanced realization of (3.2.4) which we denote by

$$\hat{\Sigma}_N = (\hat{A}_N, \hat{B}_N, \hat{C}_N). \tag{3.2.5}$$

If k is an integer with $1 \leq k \leq N$, then the reduced order model obtained by eliminating k states of the balanced system $\hat{\Sigma}_N$ is denoted by

$$\hat{\Sigma}_N^k = (\hat{A}_N^k, \hat{B}_N^k, \hat{C}_N^k, \hat{D}_N^k). \tag{3.2.6}$$

Observe that $\hat{\Sigma}_N^k$ has dimension $N - k$.

We shall make use of the matrices

$$H_N(\lambda) = [\lambda I - A_N, B_N], \tag{3.2.7}$$

$$K_N(\lambda) = [\lambda I - A_N^T, C_N^T], \tag{3.2.8}$$

$$\hat{H}_N(\lambda) = [\lambda I - \hat{A}_N, \hat{B}_N] \tag{3.2.9}$$

and

$$\hat{K}_N(\lambda) = [\lambda I - \hat{A}_N^T, \hat{C}_N^T]. \tag{3.2.10}$$

Moreover, the functions that compute the corresponding minimum singular values are denoted by

$$\mathcal{F}_N(\lambda) = \sigma_{\min}[H_N(\lambda)], \tag{3.2.11}$$

$$\mathcal{G}_N(\lambda) = \sigma_{\min}[K_N(\lambda)], \tag{3.2.12}$$

$$\hat{\mathcal{F}}_N(\lambda) = \sigma_{\min}[\hat{H}_N(\lambda)] \tag{3.2.13}$$

and

$$\hat{\mathcal{G}}_N(\lambda) = \sigma_{\min}[\hat{K}_N(\lambda)], \tag{3.2.14}$$

respectively.

Observe that since A_N is symmetric, real and dissipative, Theorem 2.2.4, part (iii) yields

$$\gamma_c^N = \gamma_c(\Sigma_N) = \min_{\lambda \in \mathbf{R}} \mathcal{F}_N(\lambda), \tag{3.2.15}$$

and by duality,

$$\gamma_o^N = \gamma_o(\Sigma_N) = \min_{\lambda \in \mathbf{R}} \mathcal{G}_N(\lambda). \tag{3.2.16}$$

We note that the balanced system matrix $\hat{A}_N$ is not symmetric and hence Theorem 2.2.4 cannot be applied to compute the radii

$$\hat{\gamma}_c^N = \gamma_c(\hat{\Sigma}_N)$$

and

$$\hat{\gamma}_o^N = \gamma_o(\hat{\Sigma}_N).$$

All of the numerical results presented in this paper are based on an algorithm for computing $\mathcal{F}_N(\lambda)$, $\mathcal{G}_N(\lambda)$, $\hat{\mathcal{F}}_N(\lambda)$ and $\hat{\mathcal{G}}_N(\lambda)$ for λ in a specified rectangle in the complex plane. The particular code (CONT2.M) used in the calculations is a modified version of a code first developed by Gunther Peichl. No attempt was made to use optimization packages to compute the various radii. It will become clear from the plots of the surfaces $z = \mathcal{F}_N(\lambda)$, $z = \mathcal{G}_N(\lambda)$, etc., that standard optimization algorithms have trouble with problems of the type considered here. In particular, $\mathcal{F}_N(\lambda)$, $\mathcal{G}_N(\lambda)$, $\hat{F}_N(\lambda)$ and $\hat{\mathcal{G}}_N(\lambda)$ can have multiple local minima and "corners". *Table 3.2.1* contains values for γ_c^N, γ_o^N, $\hat{\gamma}_c^N$ and $\hat{\gamma}_o^N$ for increasing values of N. Observe that, as noted in [9], γ_c^N and γ_o^N converge to 0 as $N \to \infty$. Moreover, the same appears to be true for $\hat{\gamma}_c^N$

and $\hat{\gamma}_o^N$. Balancing does improve γ_c^N but greatly reduces γ_o^N. In particular, $\hat{\gamma}_o^N$ is two orders of magnitude smaller than γ_c^N, γ_o^N or $\hat{\gamma}_c^N$. Hence, $\hat{\Sigma}_N$ is nearly unobservable. Note that the MATLAB algorithm BALREAL.M in the Control Toolbox failed to balance the raw finite element model Σ_N for $N \geq 16$. This can be partially explained by the fact that γ_c^{16} and γ_o^{16} are "small" and hence Σ_{16} is near an uncontrollable and unobservable system. Consequently, one would expect that balancing Σ_{16} is a numerically ill–conditioned problem.

Figures 3.2.1, 3.2.4, 3.2.7 and *3.2.10* show that, as expected from Theorem 2.2.4, the controllability and observability radii are given by (3.2.15) and (3.2.16), respectively. The minimum always occurs on the (negative) real axis and is near an eigenvalue of A_N (see [2,10]). *Figure 3.2.2* contains the plot of $\mathcal{F}_4(\lambda)$ for real λ satisfying $240 \leq \lambda \leq 0$. *Figure 3.2.3* is a scaled version of *3.2.2*. Similar plots for $\mathcal{G}_4(\lambda)$, $\mathcal{F}_8(\lambda)$ and $\mathcal{G}_8(\lambda)$ are given in *Figures 3.2.5, 3.2.6, 3.2.8, 3.2.9* and *3.2.11*. The same series of plots for the balanced case are presented in *Figures 3.2.12–3.2.24*.

It is interesting to note that although Theorem 2.2.4 can not be applied to the balanced system $\hat{\Sigma}_N$, the minima of $\hat{\mathcal{F}}_N(\lambda)$ and $\hat{\mathcal{G}}_N(\lambda)$ also occur on the (negative) real axis. Observe that for the raw finite element model the minimum defining γ_c^N and γ_o^N occurs near the eigenvalue of largest magnitude. However, this is not the case for the balanced system $\hat{\Sigma}_N$, where for $N > 4$, $\hat{\gamma}_o^N$ is obtained near an eigenvalue of smaller magnitude.

We ran several numerical experiments of this type with similar results. Based on these numerical results we concluded that balancing the raw finite element model as a first step to model reduction can be numerically ill–conditioned. Also, even though Theorem 2.2.4 does not apply to the balanced system $\hat{\Sigma}_N$, we conjecture that the minimum of $\hat{\mathcal{F}}_N(\lambda)$ and $\hat{\mathcal{G}}_N(\lambda)$ occurs on the real axis. We leave this as a conjecture and note that a similar observation will be made for certain transformed finite element models for the wave equation.

Table 3.2.1 – Controllability and Observability Radii				
N	γ_c^N	$\hat{\gamma}_c^N$	γ_o^N	$\hat{\gamma}_o^N$
2	.47131	.33469	.16667	.22899
4	.25881	.22885	.07940	.06555
8	.11759	.15311	.03927	.00663
10	.08838	.13509	.03153	.00196
12	.06942	.12229	.02639	.00060
14	.05634	.11264	.02271	.00020
16	.04688	—	.01994	—

We also computed stabilizability and detectability radii, γ_s^N and γ_d^N, for increasing values of N. *Table 3.2.2* contains these radii for the raw finite element model and the balanced model. Observe that $\hat{\gamma}_s^N = \hat{\gamma}_d^N$ for all values of N. Moreover, it appears that γ_s^N, γ_d^N, $\hat{\gamma}_s^N$ and $\hat{\gamma}_d^N$ are converging to a value of approximately 10 which is close to the magnitude of the eigenvalue with the smallest magnitude for all values of N.

Table 3.2.2 – Stabilizability and Detectability Radii				
N	γ_s^N	$\hat{\gamma}_s^N$	γ_d^N	$\hat{\gamma}_d^N$
2	10.8333	10.6325	10.8036	10.6325
4	10.2512	9.9300	10.2001	9.9300
8	10.0631	9.6515	9.9708	9.6515
10	10.0499	9.6098	9.9373	9.6098
12	10.0509	9.5857	9.9180	9.5857
14	10.0590	9.5705	9.9060	9.5705
16	10.0711	—	9.8979	—

The optimal control that solves the LQR problem, (3.2.1)–(3.2.3), is given in feedback form

$$u^*(t) = -\int_0^1 g(x)y(t,x)dx \tag{3.2.17}$$

where the function $g(\cdot)$ belongs to $L_2(0,1)$. The optimal control $u^*(t)$ is completely determined when the functional gain $g(x)$ is known (see [7,19,24]). One approach to computing $g(x)$ is to replace the LQR problem by an approximate LQR problem governed by one of the approximating systems Σ_N, $\hat{\Sigma}_N$ or a reduced order model based on the model reduction scheme outlined in Section 2.3.

Given that the appropriate assumptions are satisfied by the approximation scheme, then it can be shown that this approach to estimating the functional gain $g(x)$ converges as $N \to \infty$ (see [7,19,24]). Moreover, the finite element scheme satisfies the conditions sufficient to imply convergence of this method. Convergence of these suboptimal functional gains has been well studied and we shall not address this issue.

We conducted a number of numerical experiments where various reduced order models were used to compute approximate functional gains. *Figure 3.2.25* illustrates a typical result. The solid line is the approximate functional gain computed by using the full (raw) finite element model with $N = 24$ elements. We note that this is a "converged" solution in that $g(x)$ computed by $N = 32$ and $N = 64$ elements are identical to the $N = 24$ case. Hence, we have that the solid curve represents the true optimal functional gain.

For comparison, the dotted line is the approximate functional gain computed using the full (raw) finite element model of dimension 6. The other two approximations were based on the reduction scheme given above. We constructed the $N = 12$ raw finite element model, balanced this model and then eliminated 6 (i.e. kept 6) states and 8 (i.e. kept 4) states to produce 6 and 4 dimensional design models, respectively.

Observe that the reduced order models of dimension 6 and 4 produced a better estimate of $g(x)$ than the full raw $N = 6$ finite element model. Thus, a model of dimension 4, obtained by the model reduction scheme, produced a better design than the raw finite element model of dimension 6.

At first glance, this may seem like a much improved approach to computing functional gains. However, note that the controllability and observability radii approach zero as $N \rightarrow \infty$ so that balancing becomes numerically ill-conditioned. As noted above, BALREAL.M could not balance the $N = 16$ raw finite element model. On the other hand, the stabilizability and detectability radii for these systems are bounded away from zero. Hence, the LQR problem for the raw finite element model is numerically well-conditioned.

Examples of this nature provide some insight into the trade offs between the ability to solve "large" LQR problems based on "raw" finite element models and the ability to balance and/or reduce these models.

CONTROLLABILITY SURFACE FOR THE HEAT EQUATION
N=4: RAW FE MODEL

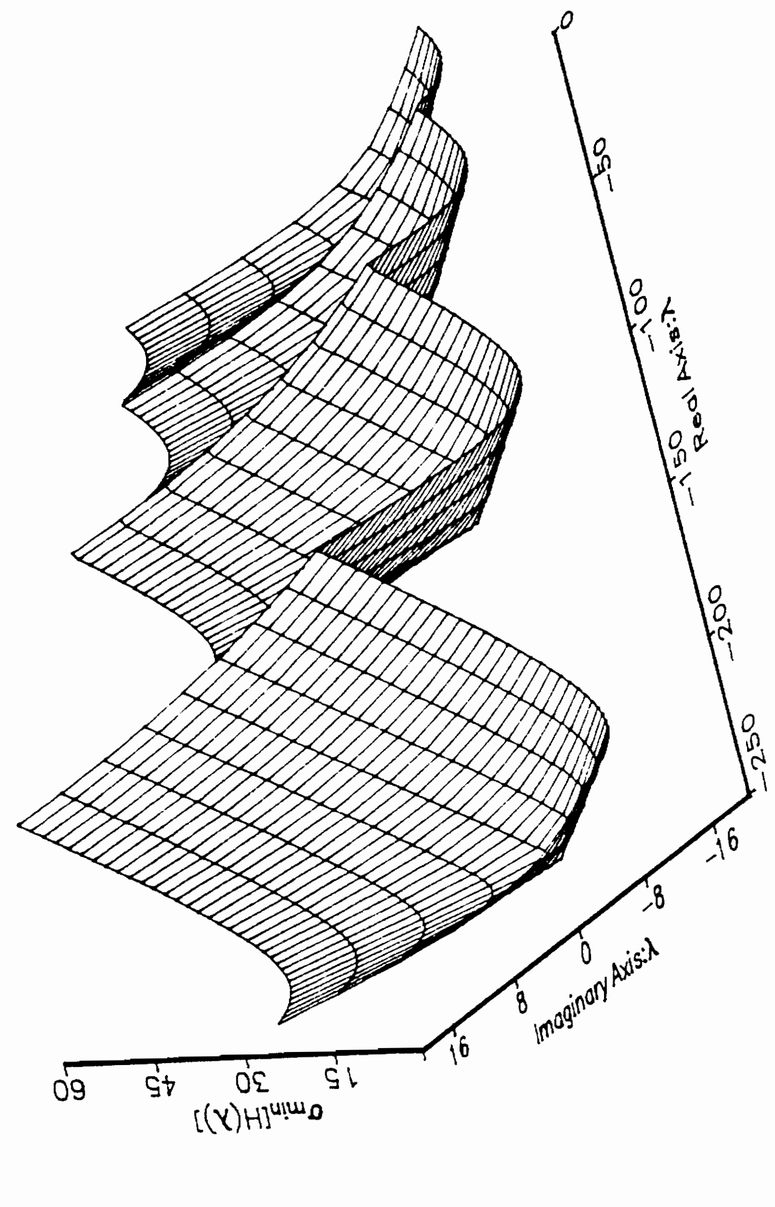

FIGURE 3.2.1

PLOT OF $\mathcal{F}(\lambda)$ FOR REAL λ

N=4: RAW FE MODEL

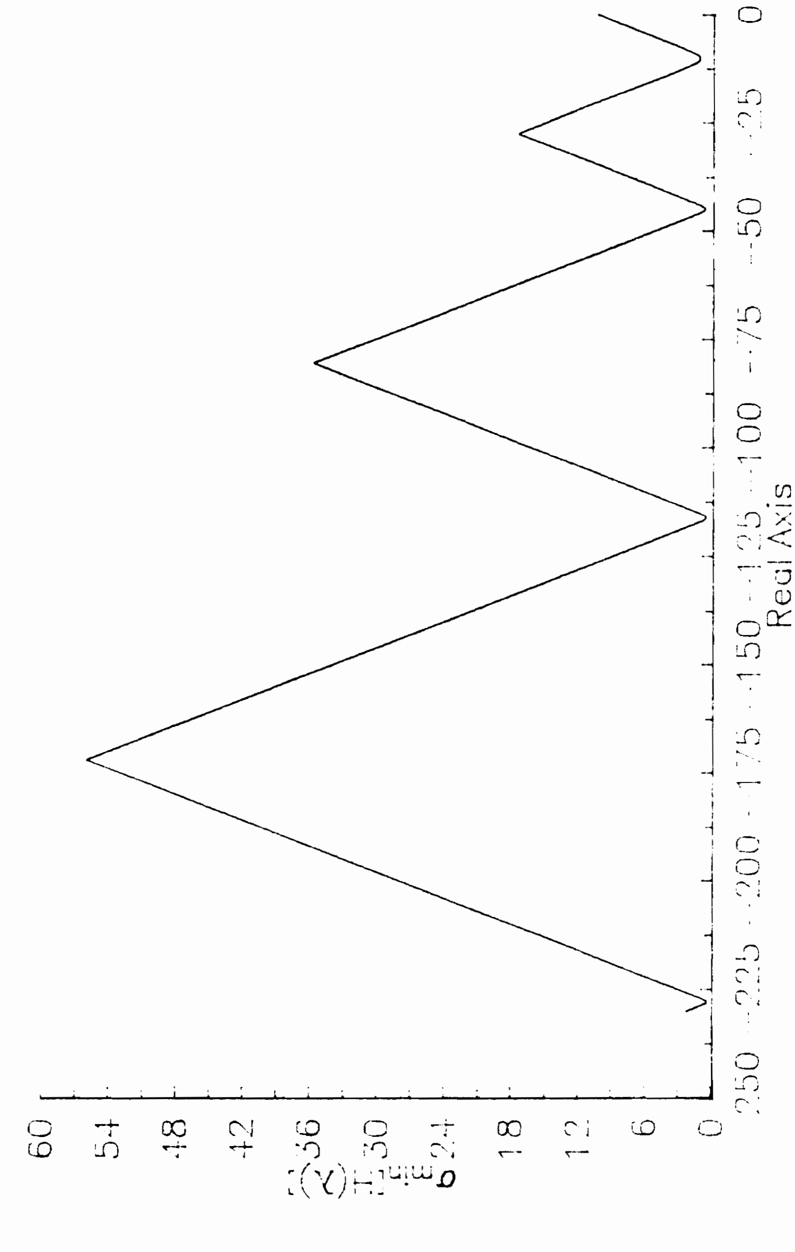

FIGURE 3.2.2

PLOT OF $\mathscr{F}(\lambda)$ FOR REAL λ

N=4: RAW FE MODEL

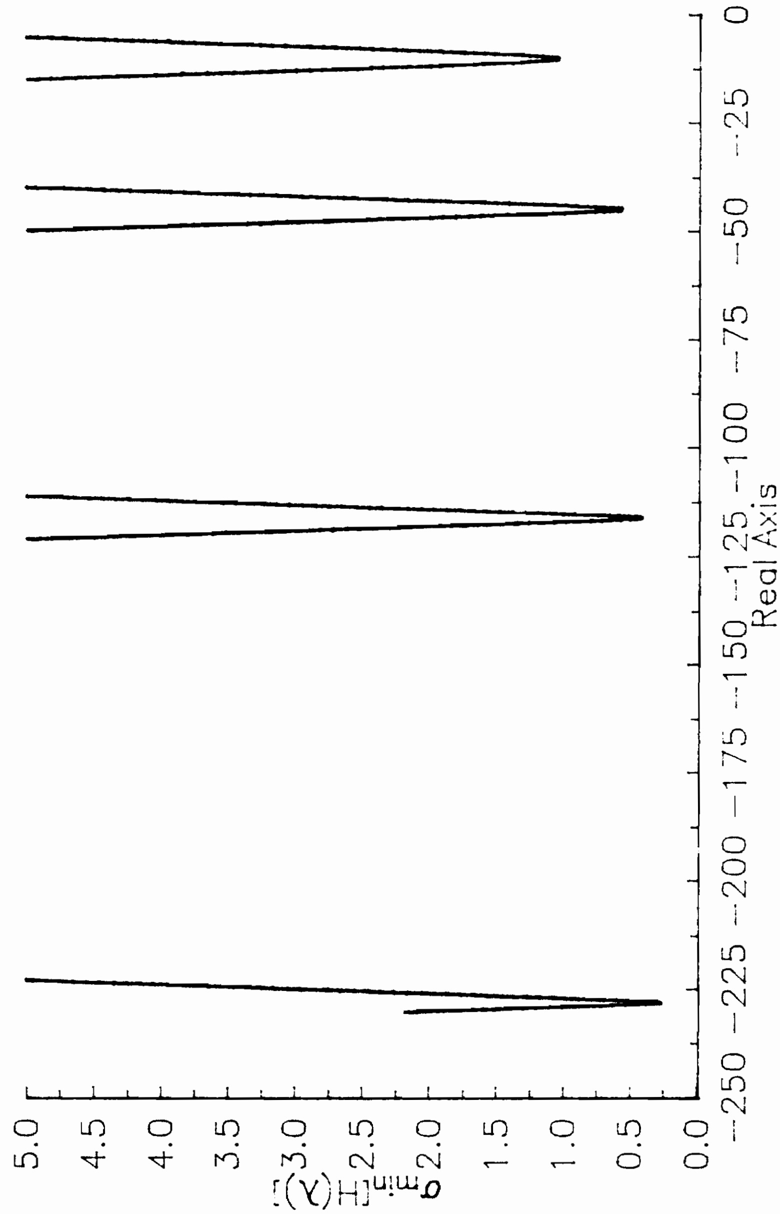

FIGURE 3.2.3

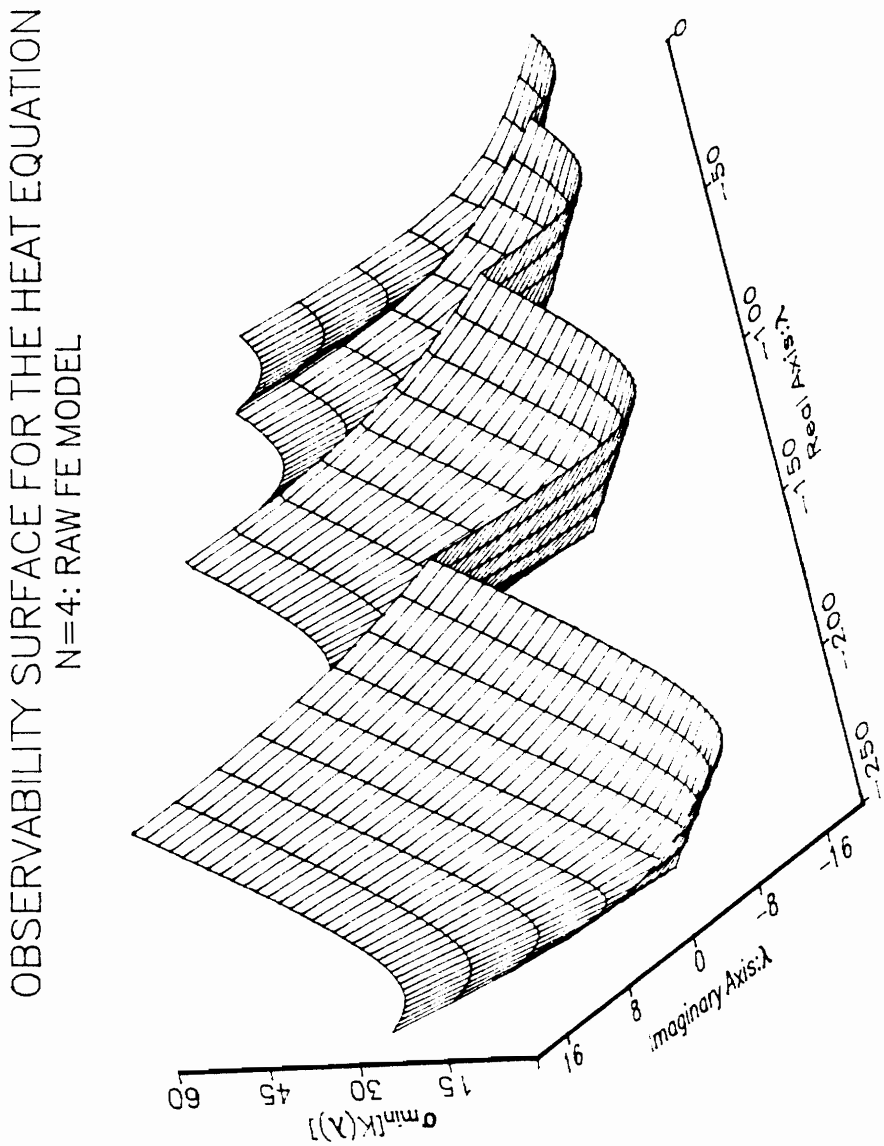
OBSERVABILITY SURFACE FOR THE HEAT EQUATION
N=4: RAW FE MODEL
Real Axis:λ
Imaginary Axis:λ
$\sigma_{min}[K(\lambda)]$
0
-50
-100
-150
-200
-250
16
8
0
-8
-16
60
45
30
15

FIGURE 3.2.4

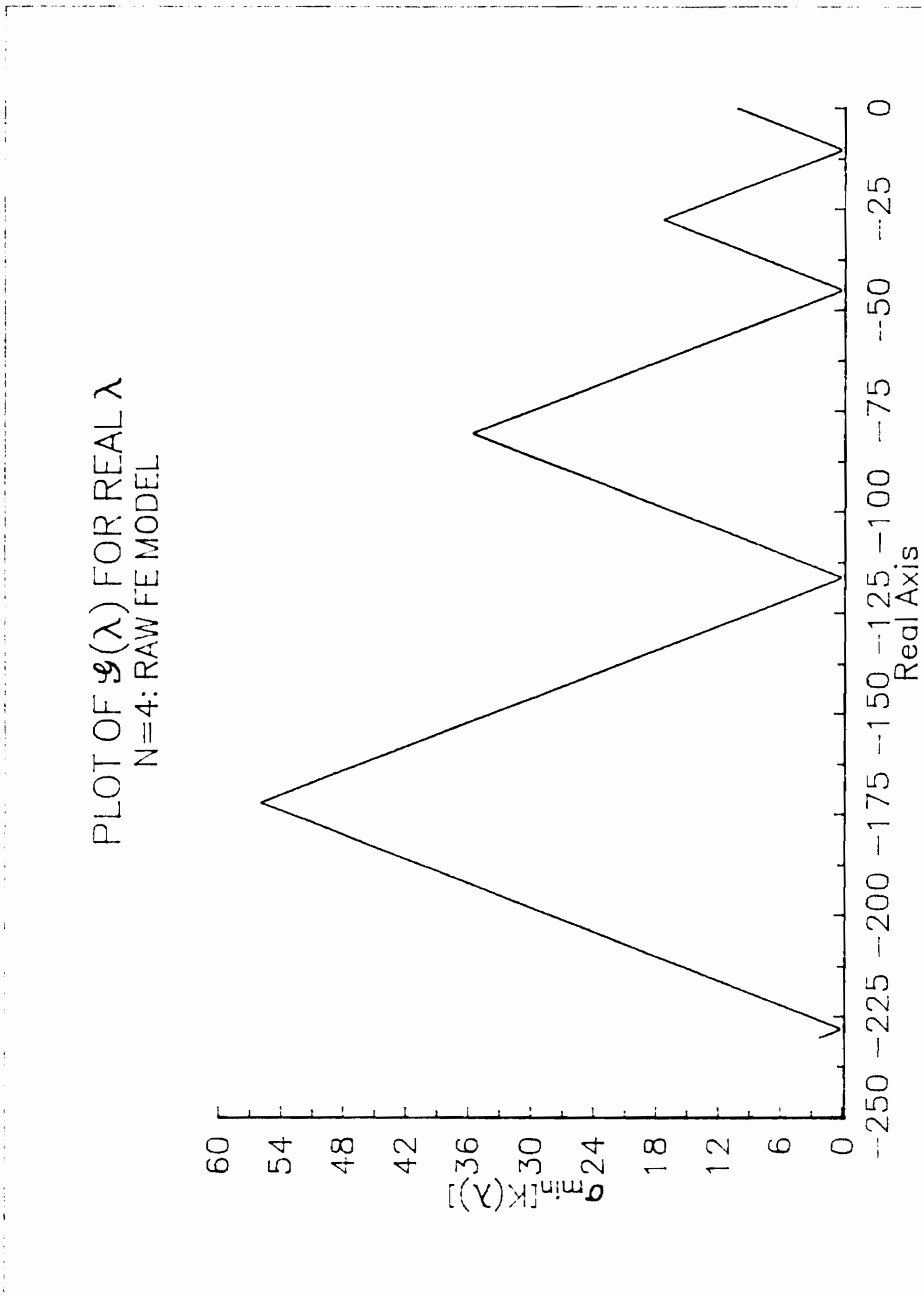
PLOT OF $\mathcal{G}(\lambda)$ FOR REAL λ
N=4: RAW FE MODEL
$\sigma_{min}[K(\lambda)]$
60
54
48
42
36
30
24
18
12
6
0
−250 −225 −200 −175 −150 −125 −100 −75 −50 −25 0
Real Axis

FIGURE 3.2.5

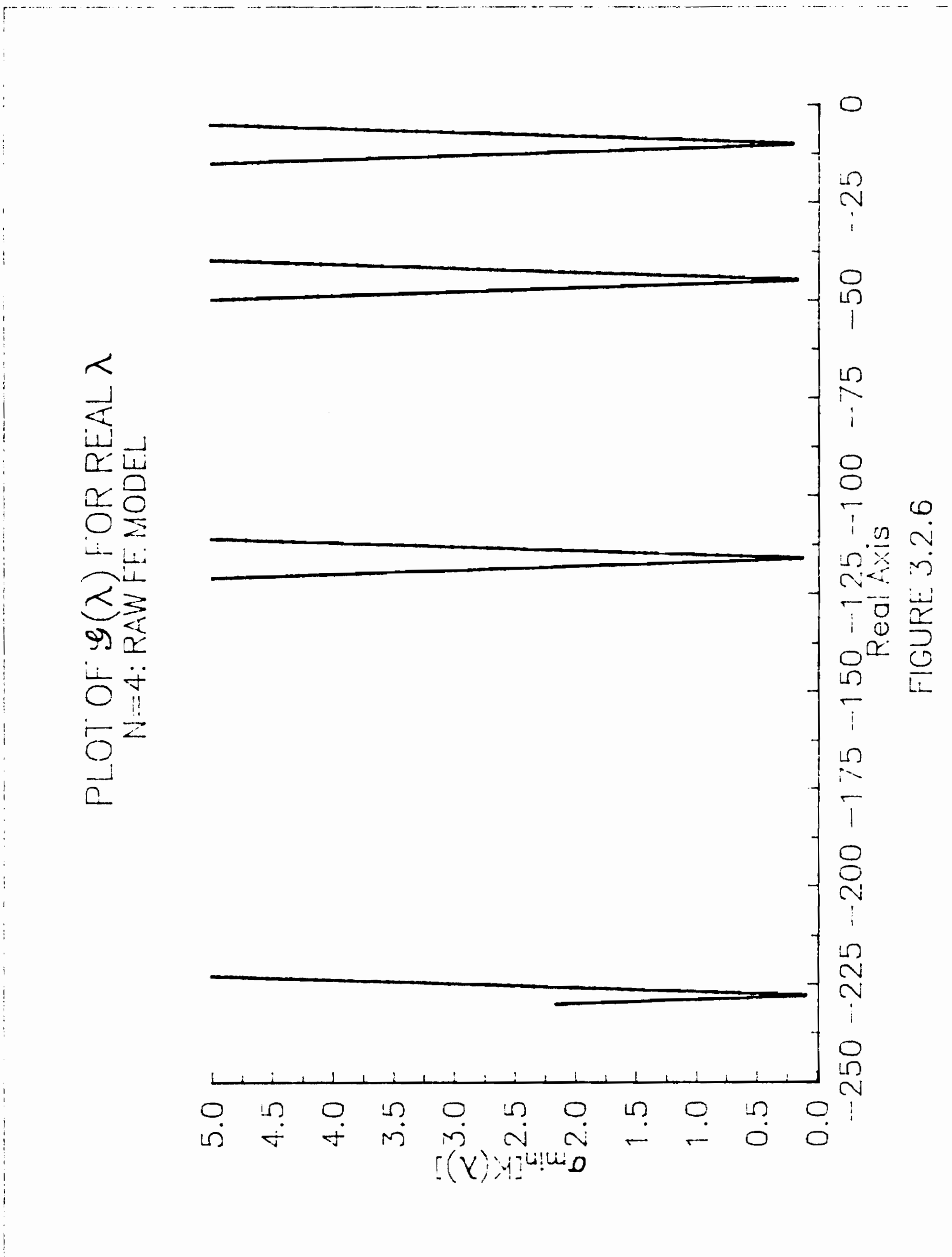
PLOT OF $\mathcal{G}(\lambda)$ FOR REAL λ
N=4: RAW FE MODEL
5.0
4.5
4.0
3.5
3.0
2.5
2.0
1.5
1.0
0.5
0.0
$g_{min}[K(\lambda)]$
-250 -225 -200 -175 -150 -125 -100 -75 -50 -25 0
Real Axis

FIGURE 3.2.6

CONTROLLABILITY SURFACE FOR THE HEAT EQUATION
N=8: RAW FE MODEL

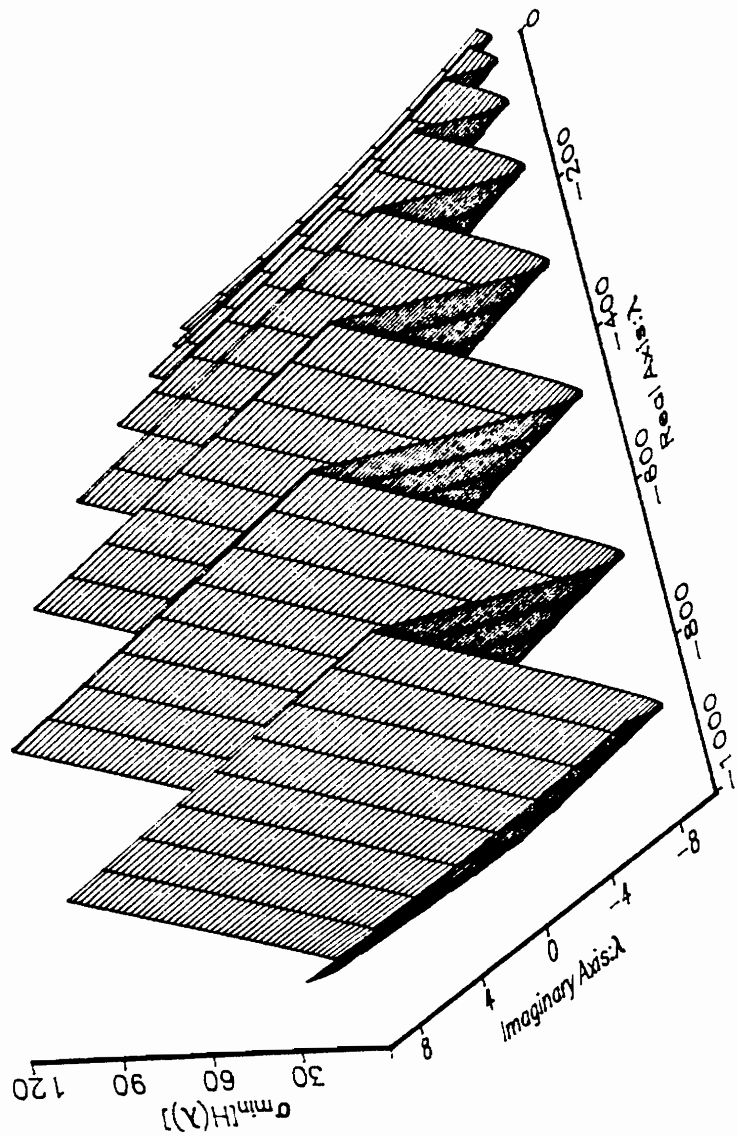

FIGURE 3.2.7

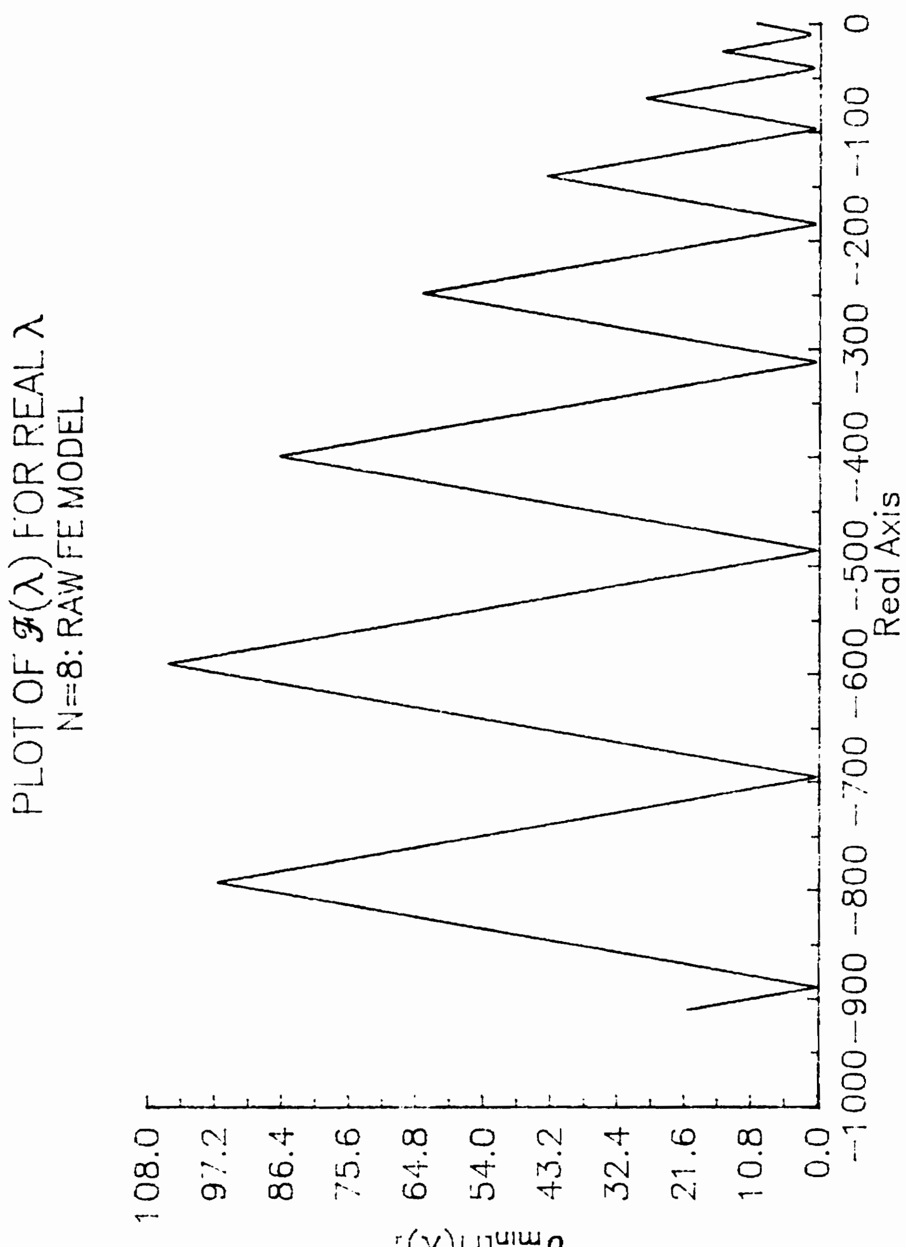
PLOT OF $\mathcal{F}(\lambda)$ FOR REAL λ
N=8: RAW FE MODEL
$\sigma_{min}[H(\lambda)]$
108.0
97.2
86.4
75.6
64.8
54.0
43.2
32.4
21.6
10.8
0.0
−1000 −900 −800 −700 −600 −500 −400 −300 −200 −100 0
Real Axis

FIGURE 3.2.8

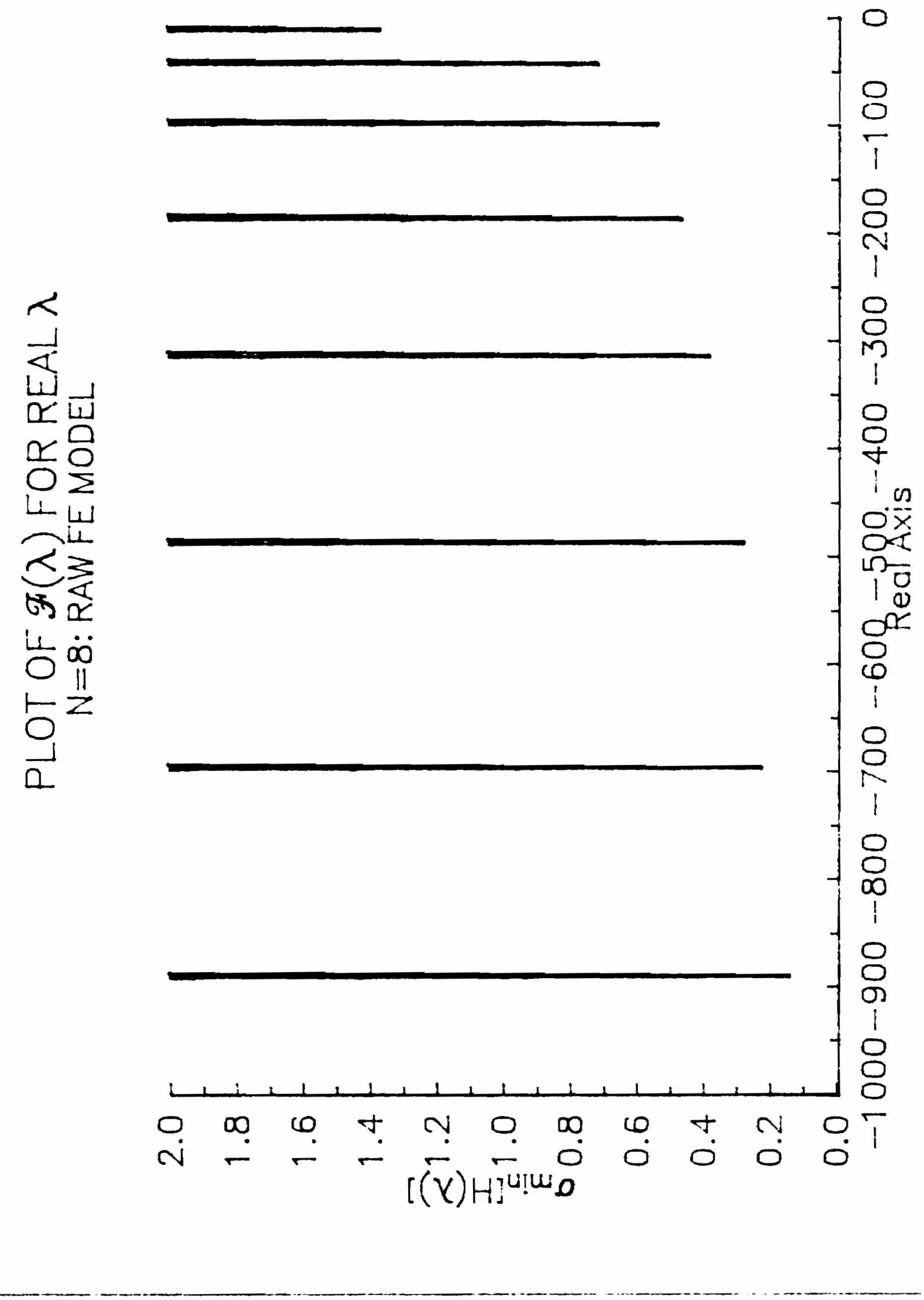
PLOT OF $\mathcal{F}(\lambda)$ FOR REAL λ
N=8: RAW FE MODEL
$\sigma_{min}[H(\lambda)]$
2.0
1.8
1.6
1.4
1.2
1.0
0.8
0.6
0.4
0.2
0.0
−1000
−900
−800
−700
−600
−500
−400
−300
−200
−100
0
Real Axis

FIGURE 3.2.9

OBSERVABILITY SURFACE FOR THE HEAT EQUATION
N=8: RAW FE MODEL

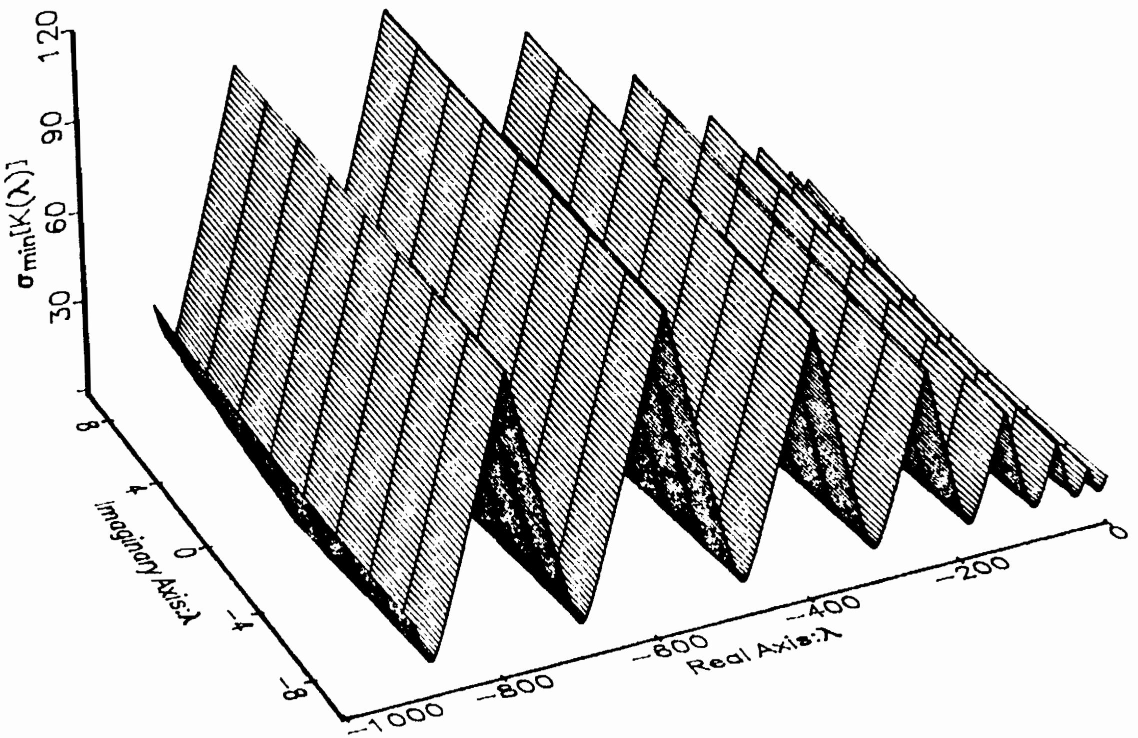

FIGURE 3.2.10

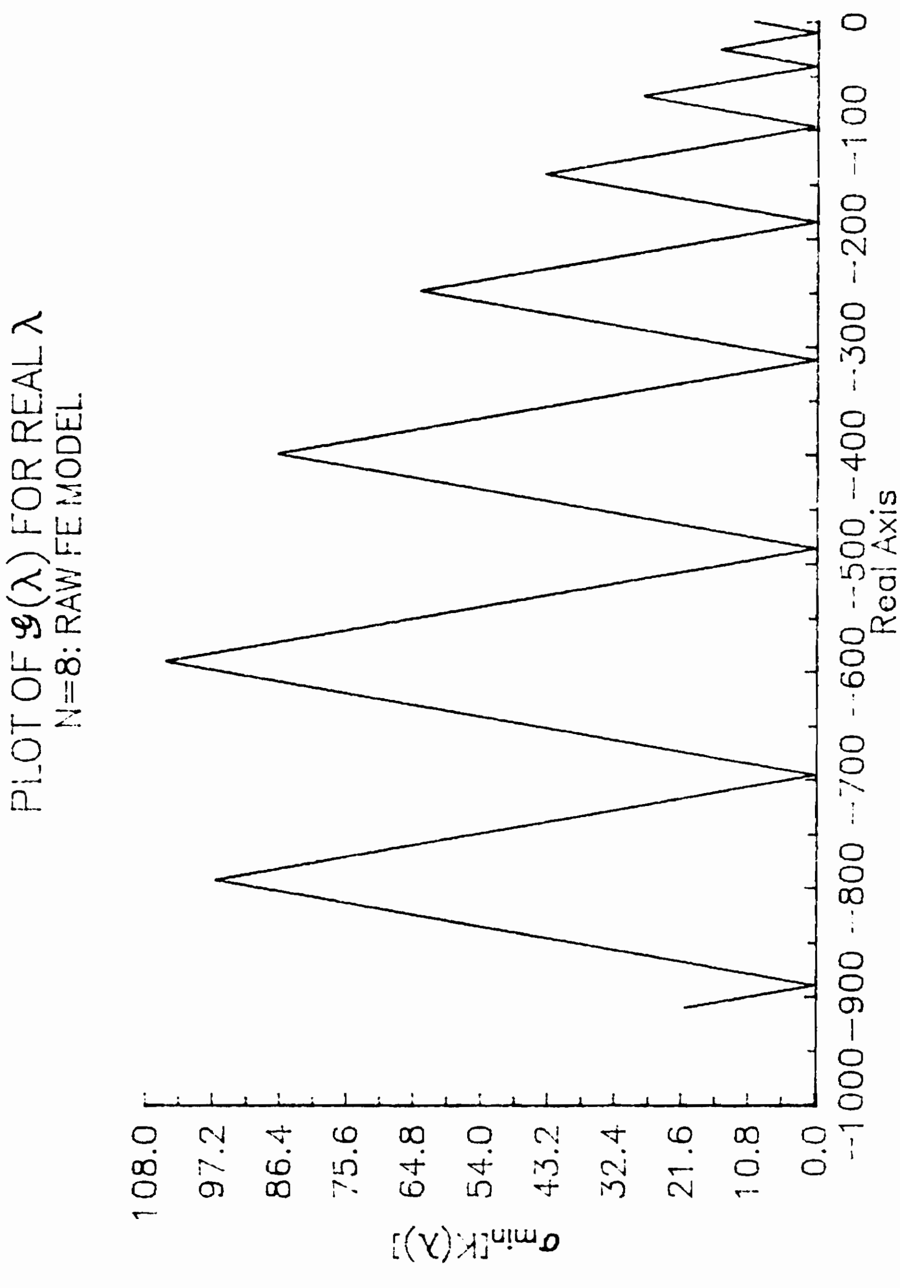
PLOT OF $\mathcal{G}(\lambda)$ FOR REAL λ
N=8: RAW FE MODEL
$\sigma_{min}[K(\lambda)]$
108.0
97.2
86.4
75.6
64.8
54.0
43.2
32.4
21.6
10.8
0.0
-1000 -900 -800 -700 -600 -500 -400 -300 -200 -100 0
Real Axis

FIGURE 3.2.11

CONTROLLABILITY SURFACE FOR THE HEAT EQUATION
N=4: BALANCED FE MODEL

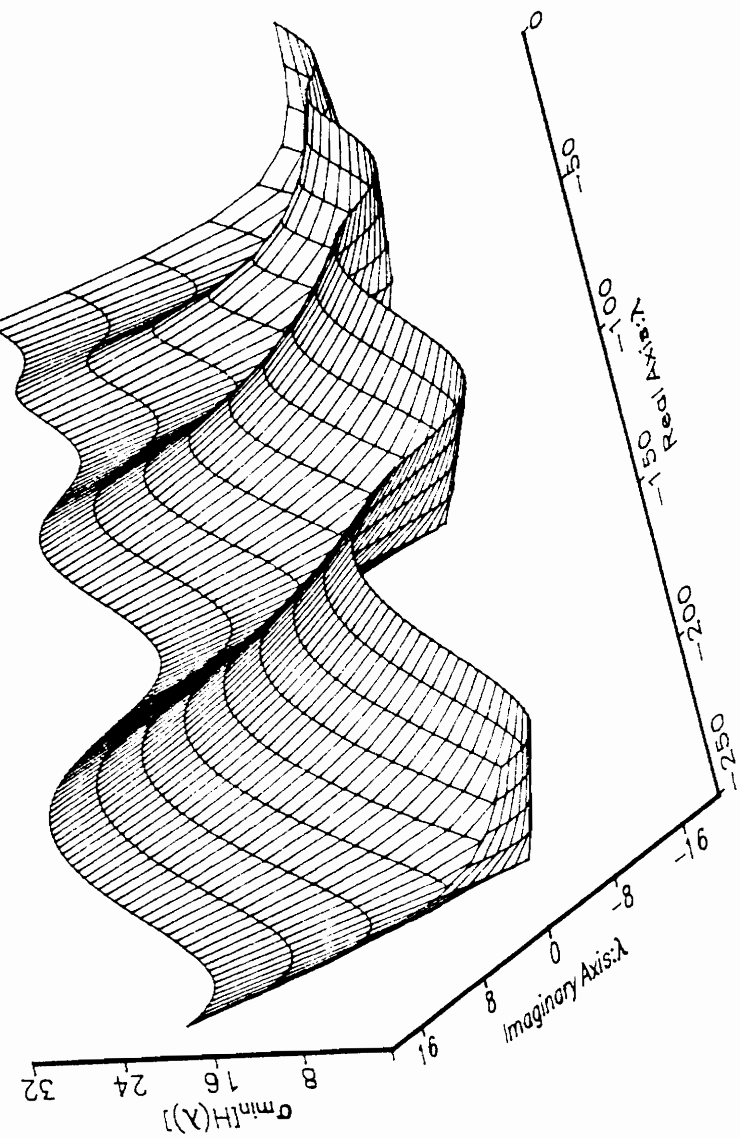

FIGURE 3.2.12

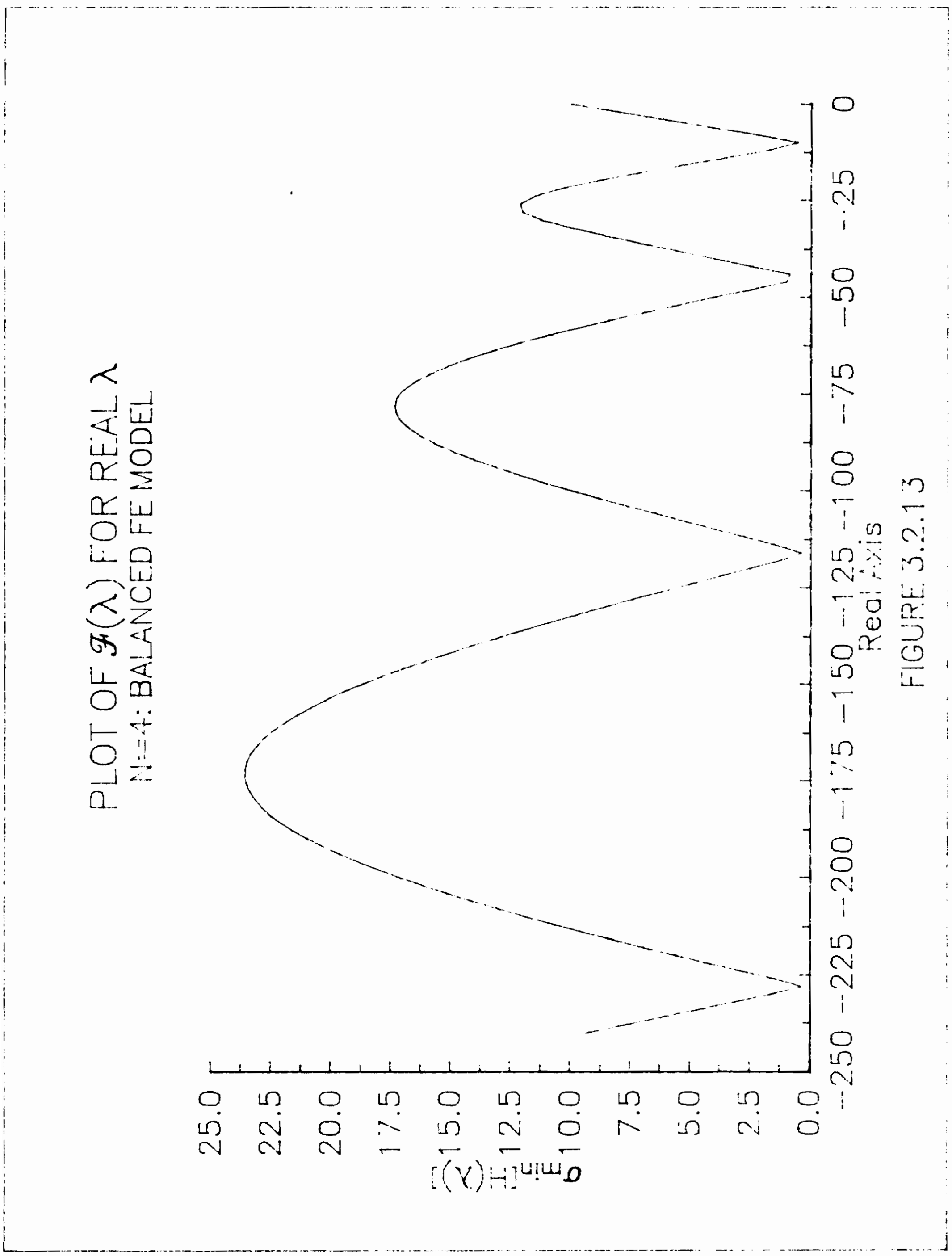

PLOT OF $\mathcal{F}(\lambda)$ FOR REAL λ
N=4: BALANCED FE MODEL
25.0
22.5
20.0
17.5
15.0
12.5
10.0
7.5
5.0
2.5
0.0
$\sigma_{min}[\mathcal{F}(\lambda)]$
−250 −225 −200 −175 −150 −125 −100 −75 −50 −25 0
Real Axis

FIGURE 3.2.13

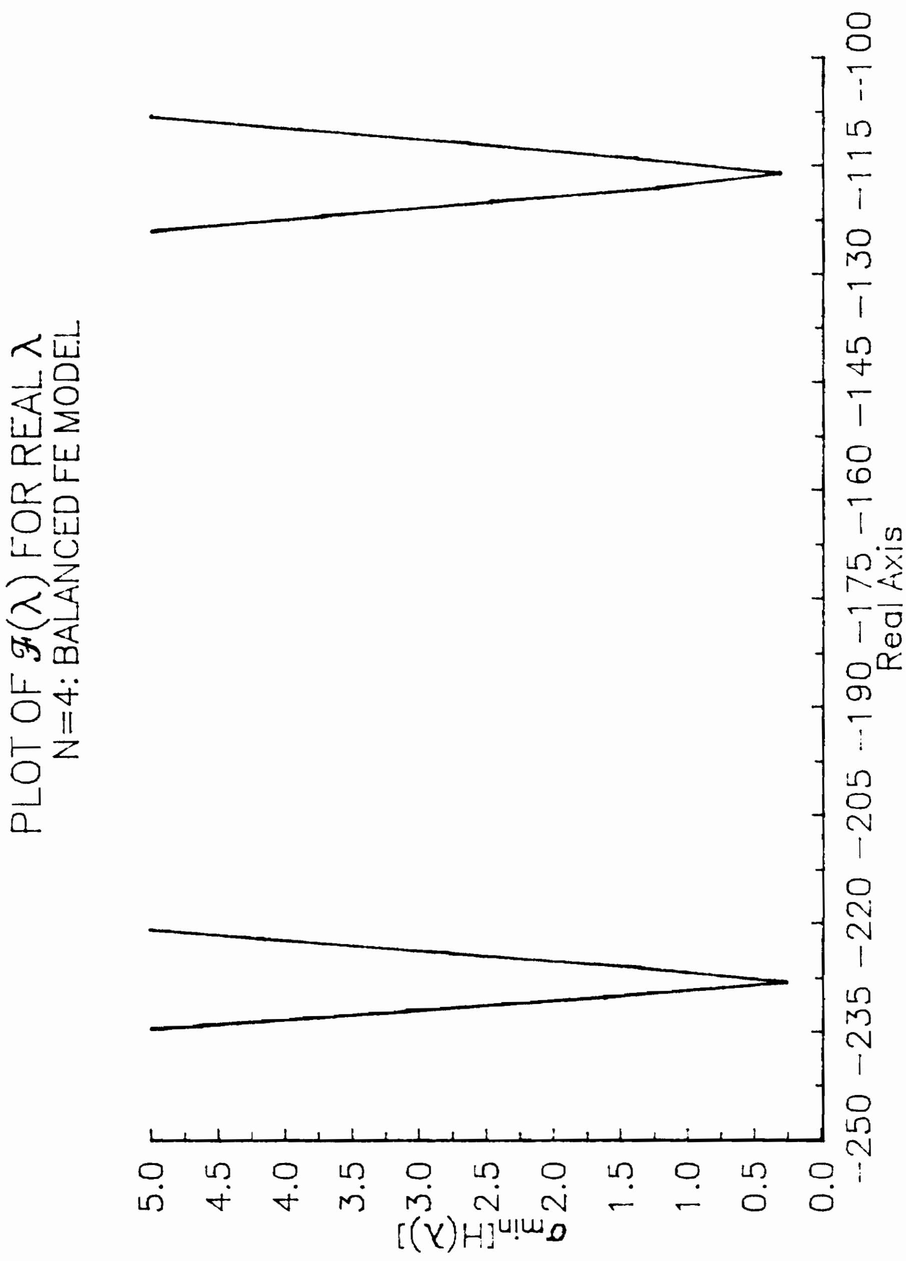
PLOT OF $\mathcal{F}(\lambda)$ FOR REAL λ
N=4: BALANCED FE MODEL
$\sigma_{min}[H(\lambda)]$
5.0
4.5
4.0
3.5
3.0
2.5
2.0
1.5
1.0
0.5
0.0
-250 -235 -220 -205 -190 -175 -160 -145 -130 -115 -100
Real Axis

FIGURE 3.2.14

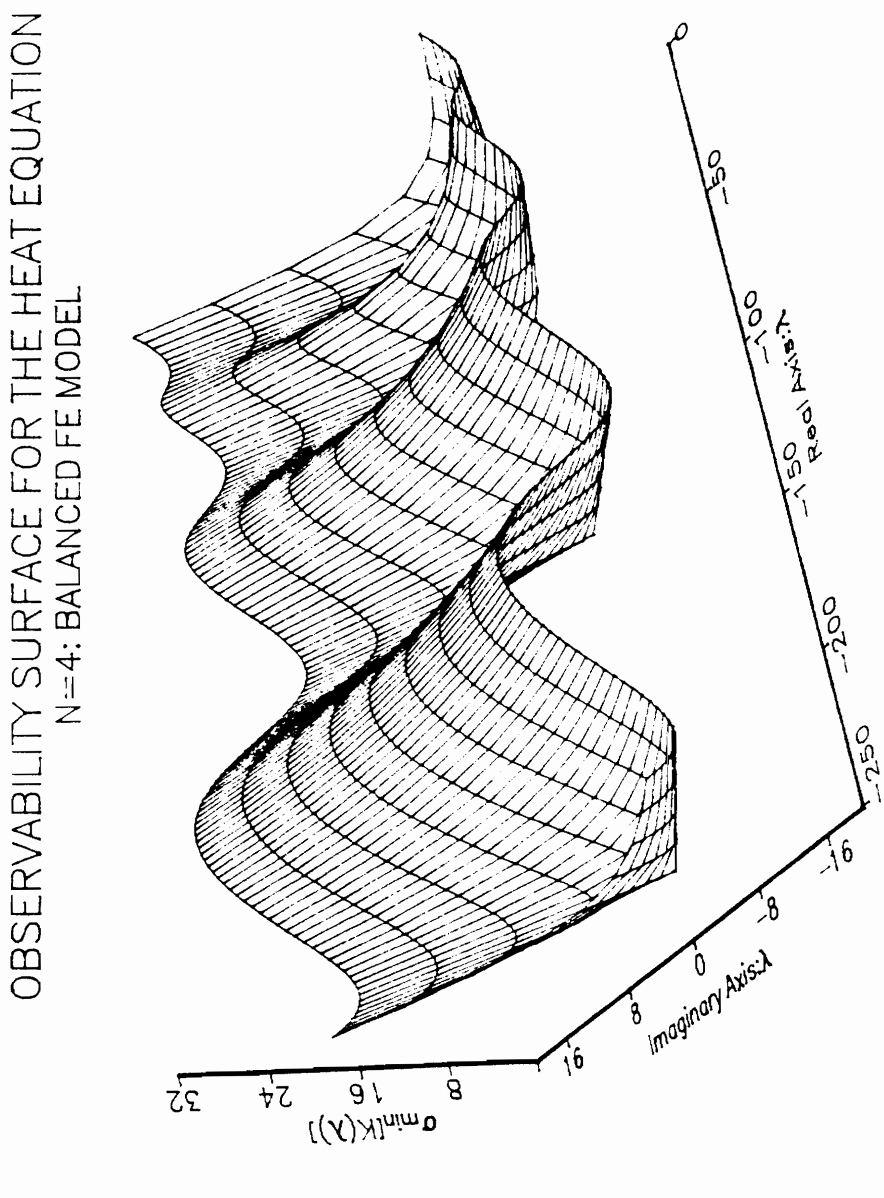
OBSERVABILITY SURFACE FOR THE HEAT EQUATION
N=4: BALANCED FE MODEL
$\sigma_{min}[K(\lambda)]$
8
16
24
32
16
8
0
-8
-16
Imaginary Axis:λ
-250
-200
-150
-100
-50
0
Real Axis:λ

FIGURE 3.2.15

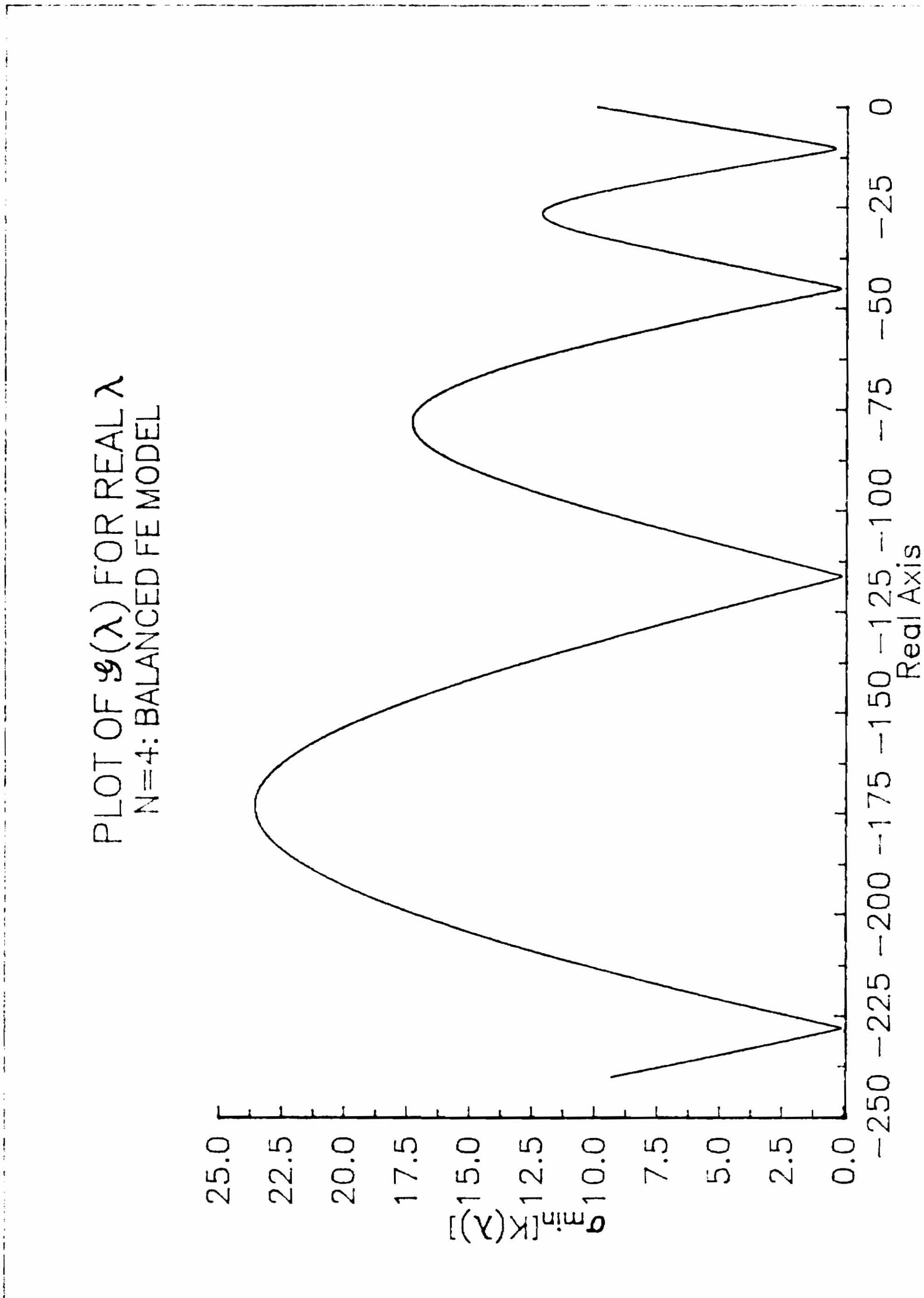
PLOT OF $\mathcal{G}(\lambda)$ FOR REAL λ
N=4: BALANCED FE MODEL
$\sigma_{min}[K(\lambda)]$
25.0
22.5
20.0
17.5
15.0
12.5
10.0
7.5
5.0
2.5
0.0
−250
−225
−200
−175
−150
−125
−100
−75
−50
−25
0
Real Axis

FIGURE 3.2.16

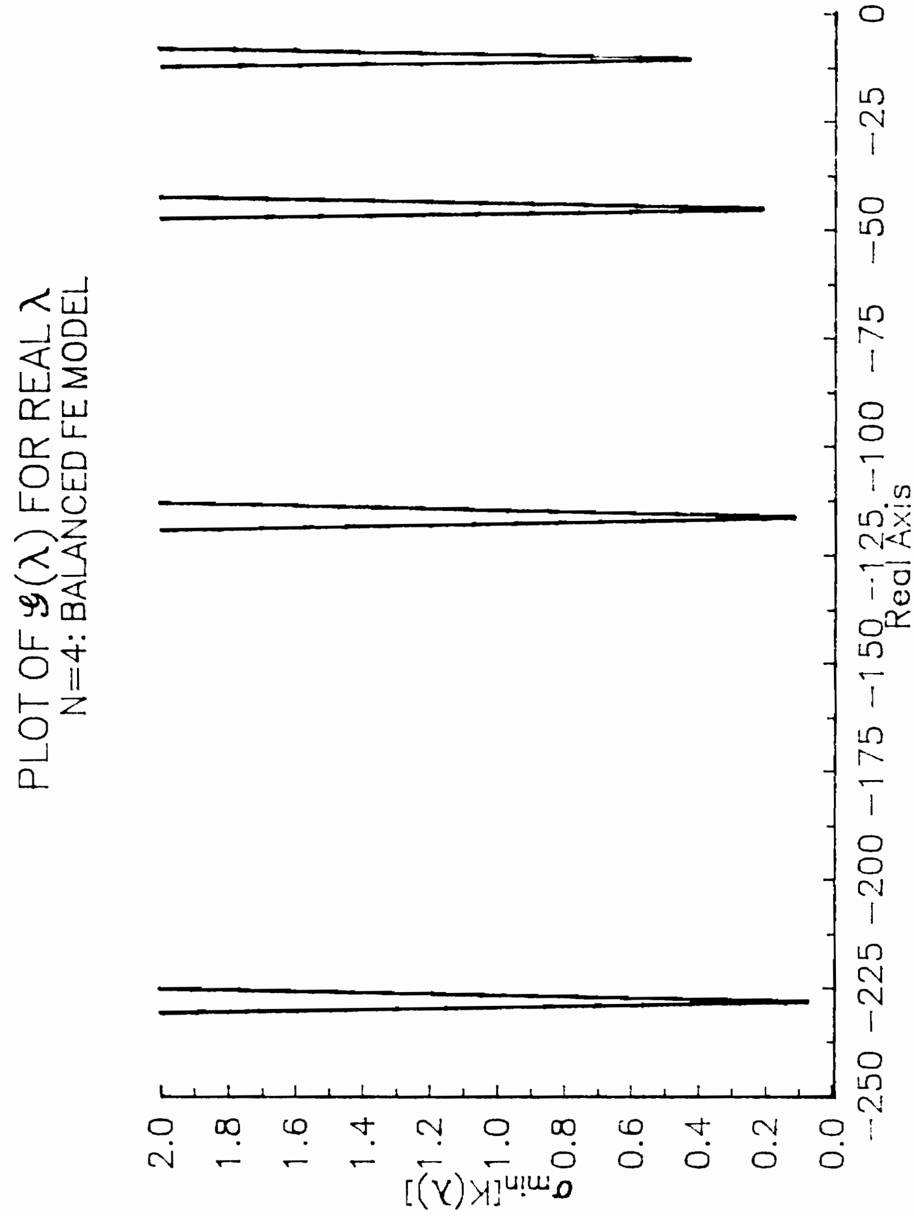
PLOT OF $\mathcal{G}(\lambda)$ FOR REAL λ
N=4: BALANCED FE MODEL
$\sigma_{min}[K(\lambda)]$
2.0
1.8
1.6
1.4
1.2
1.0
0.8
0.6
0.4
0.2
0.0
−250
−225
−200
−175
−150
−125
−100
−75
−50
−25
0
Real Axis

FIGURE 3.2.17

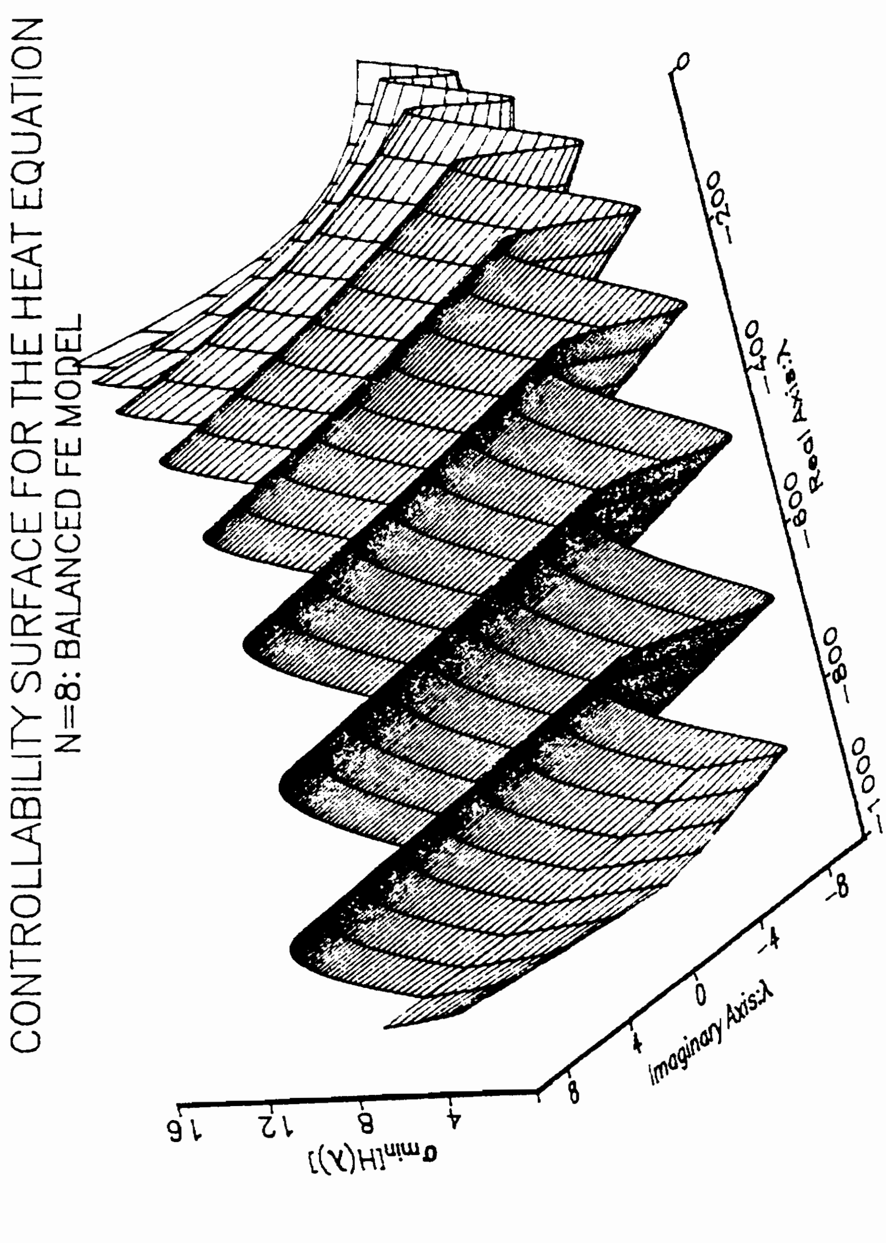
CONTROLLABILITY SURFACE FOR THE HEAT EQUATION
N=8: BALANCED FE MODEL
Real Axis:λ
0
−200
−400
−600
−800
−1000
Imaginary Axis:λ
8
4
0
−4
−8
σmin[H(λ)]
4
8
12
16

FIGURE 3.2.18

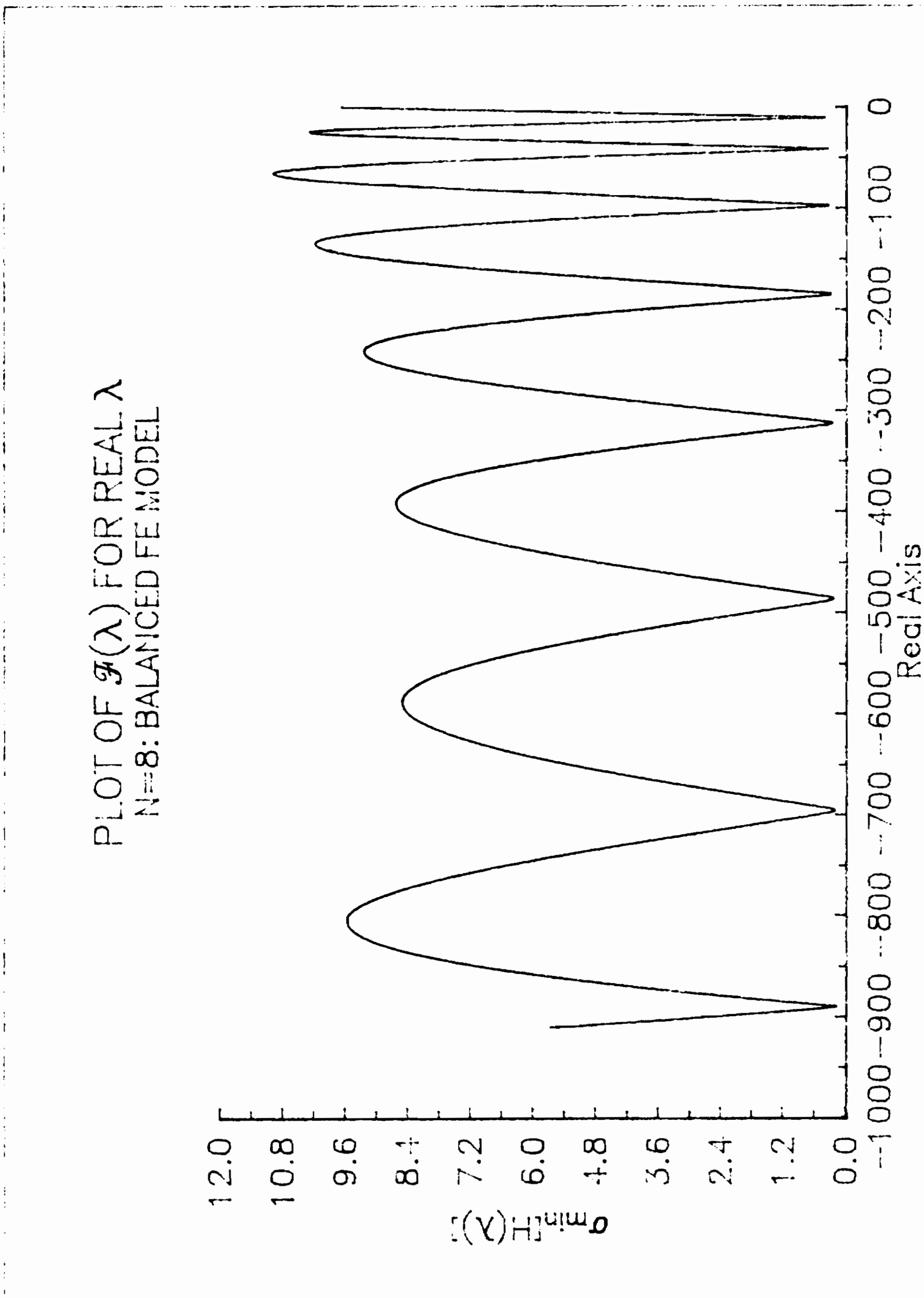
PLOT OF $\mathcal{F}(\lambda)$ FOR REAL λ
N=8: BALANCED FE MODEL
$\sigma_{min}[H(\lambda)]$
12.0
10.8
9.6
8.4
7.2
6.0
4.8
3.6
2.4
1.2
0.0
−1000
−900
−800
−700
−600
−500
−400
−300
−200
−100
0
Real Axis

FIGURE 3.2.19

PLOT OF $\mathcal{F}(\lambda)$ FOR REAL λ
N=8: BALANCED FE MODEL

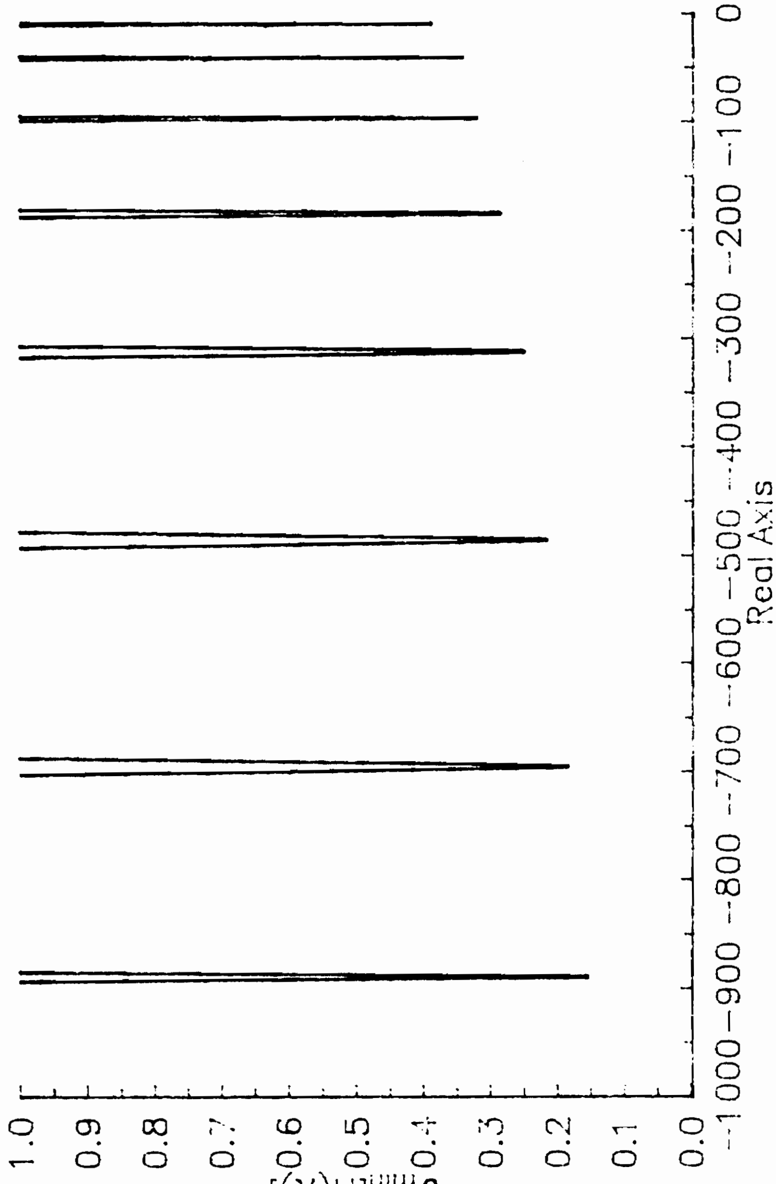

FIGURE 3.2.20

OBSERVABILITY SURFACE FOR THE HEAT EQUATION

N=8: BALANCED FE MODEL

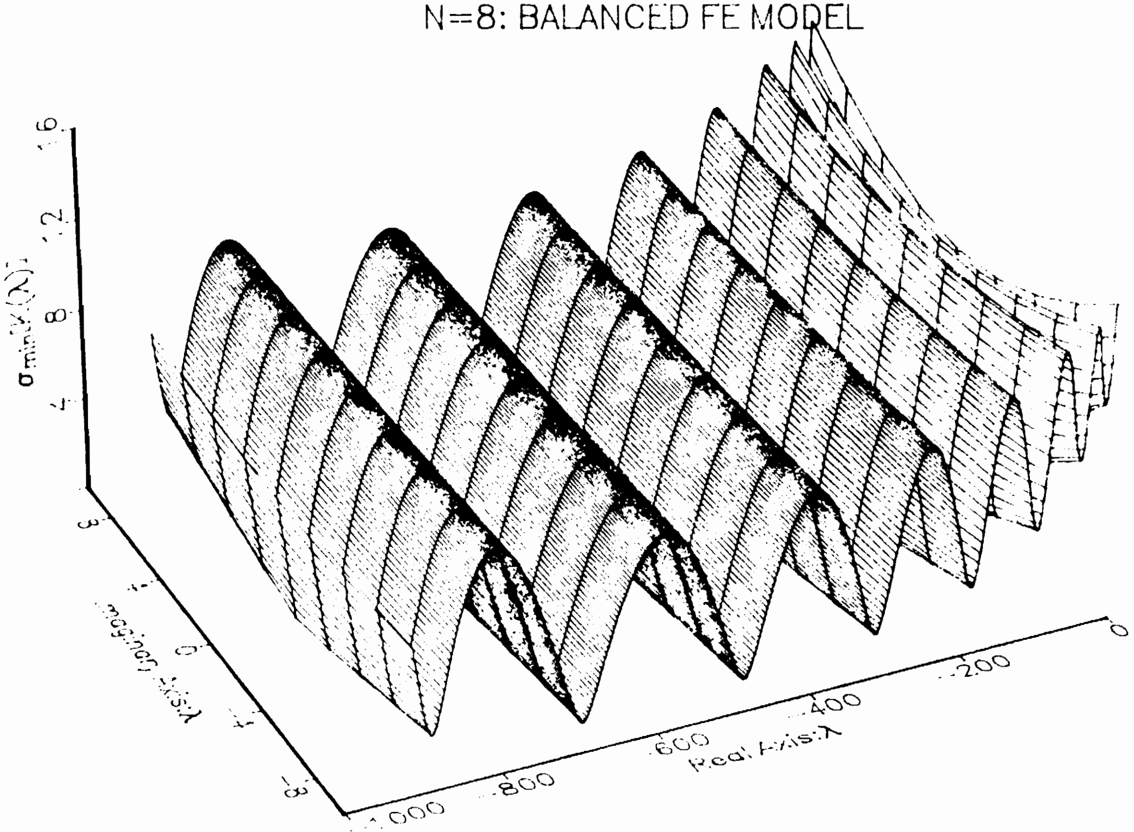

FIGURE 3.2.21

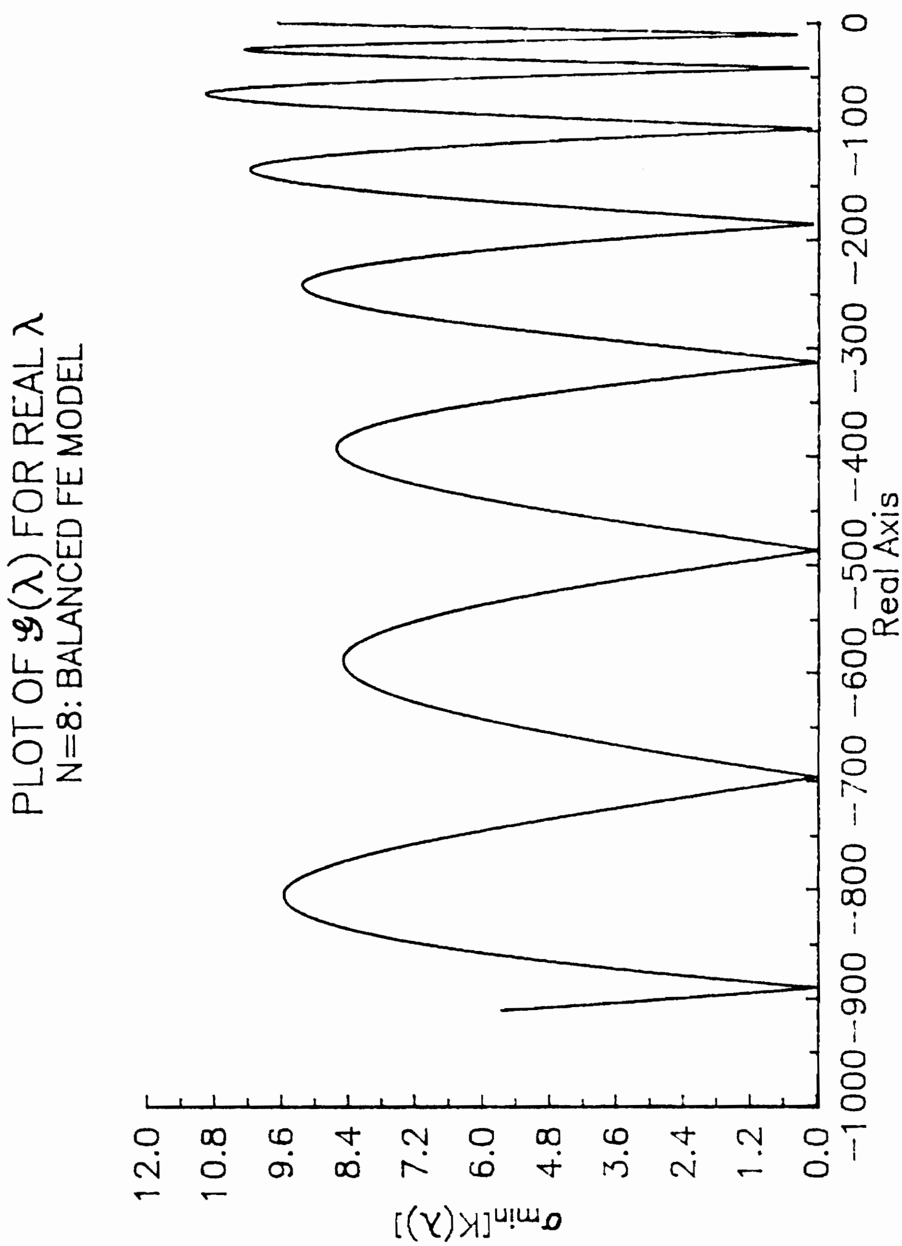
PLOT OF $\mathcal{G}(\lambda)$ FOR REAL λ
N=8: BALANCED FE MODEL
$\sigma_{min}[K(\lambda)]$
12.0
10.8
9.6
8.4
7.2
6.0
4.8
3.6
2.4
1.2
0.0
−1000 −900 −800 −700 −600 −500 −400 −300 −200 −100 0
Real Axis

FIGURE 3.2.22

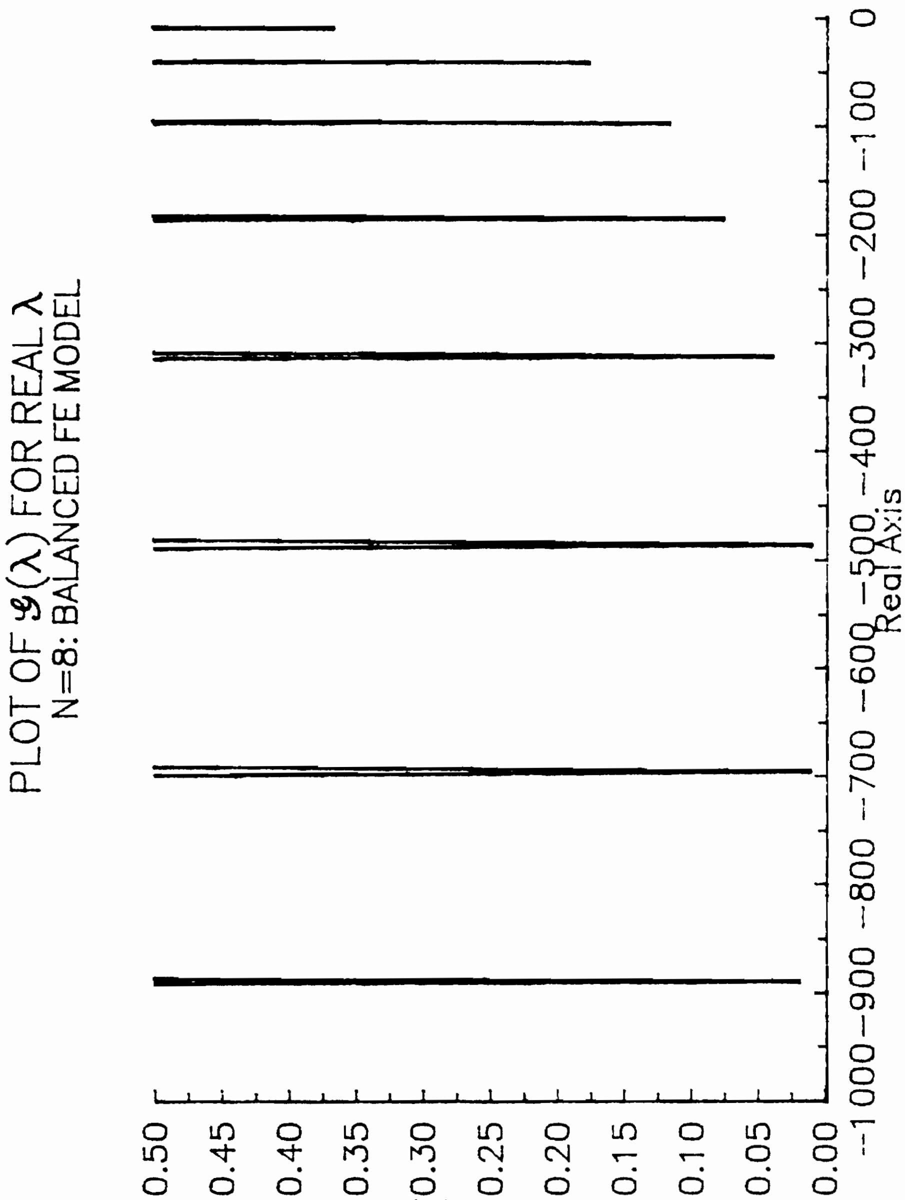
PLOT OF $\mathcal{G}(\lambda)$ FOR REAL λ
N=8: BALANCED FE MODEL
0.50
0.45
0.40
0.35
0.30
0.25
0.20
0.15
0.10
0.05
0.00
$\sigma_{min}[K(\lambda)]$
−1000 −900 −800 −700 −600 −500 −400 −300 −200 −100 0
Real Axis

FIGURE 3.2.23

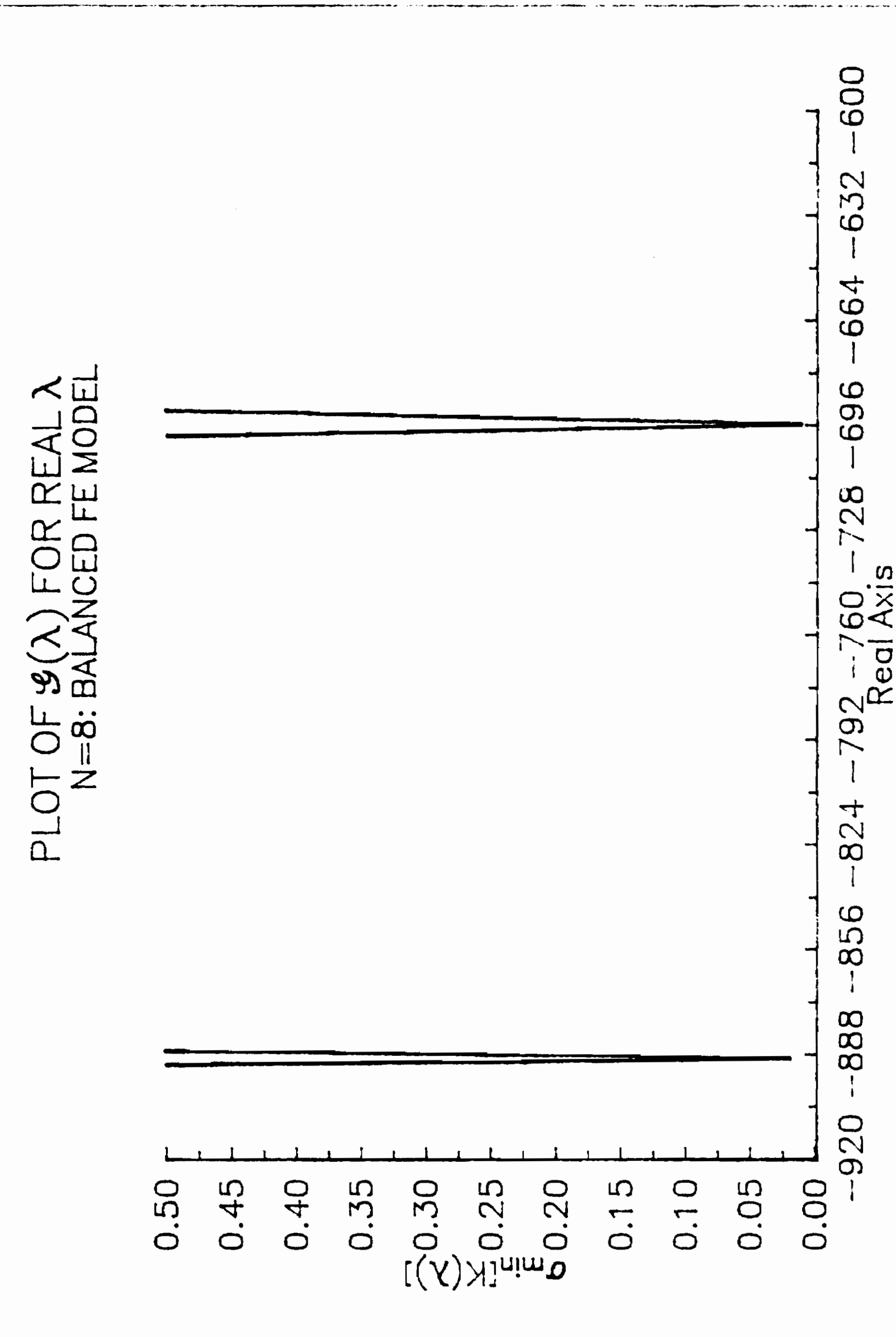
PLOT OF $\mathcal{G}(\lambda)$ FOR REAL λ
N=8: BALANCED FE MODEL
0.50
0.45
0.40
0.35
0.30
0.25
0.20
0.15
0.10
0.05
0.00
$\sigma_{min}[K(\lambda)]$
−920
−888
−856
−824
−792
−760
−728
−696
−664
−632
−600
Real Axis

FIGURE 3.2.24

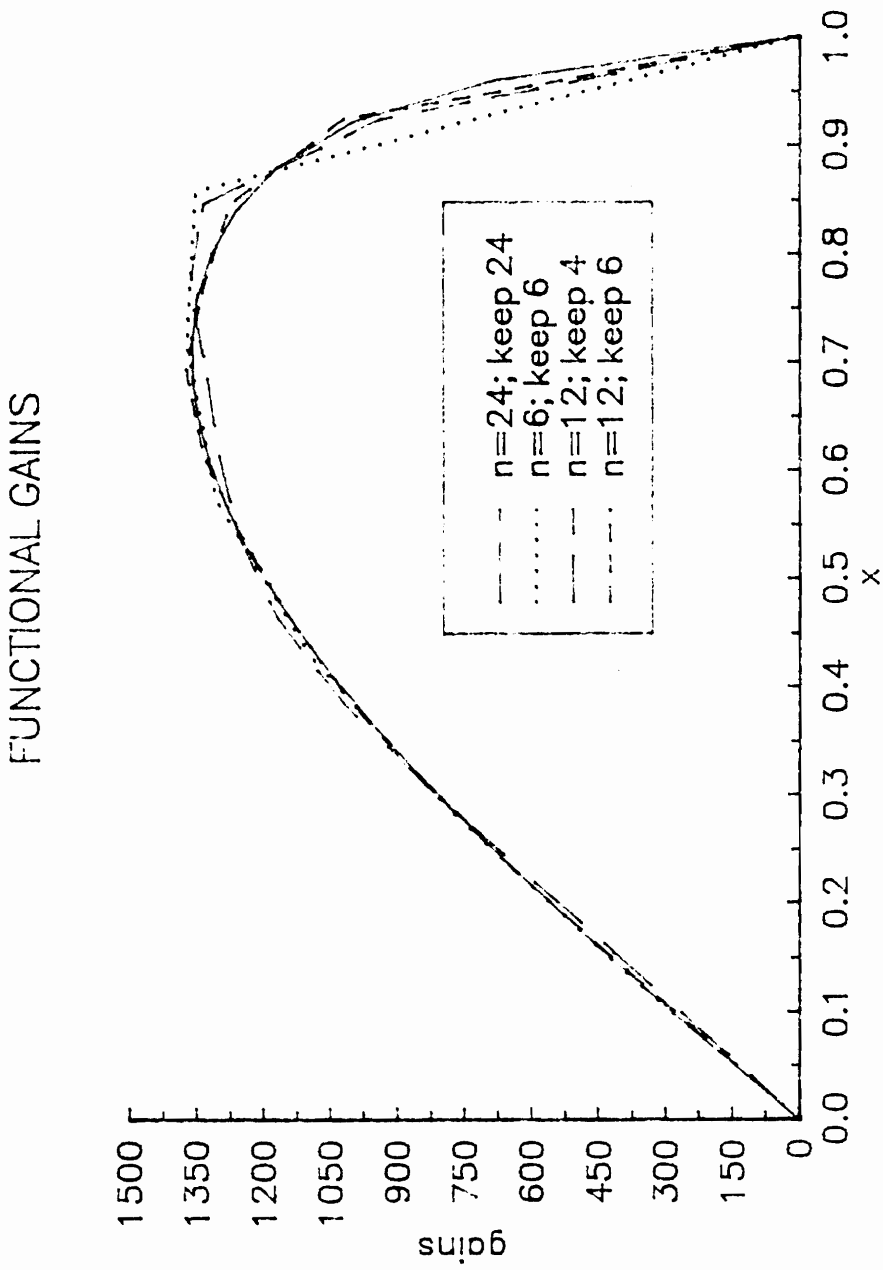
FUNCTIONAL GAINS
gains
1500
1350
1200
1050
900
750
600
450
300
150
0
0.0
0.1
0.2
0.3
0.4
0.5
0.6
0.7
0.8
0.9
1.0
x
n=24; keep 24
n=6; keep 6
n=12; keep 4
n=12; keep 6

FIGURE 3.2.25

3.3. The Wave Equation.

The problem we consider here is the control problem for the wave equation. In particular, we consider the problem

$$\frac{\partial}{\partial t^2} y(t,x) = \frac{\partial^2}{\partial x^2} y(t,x) + x u(t), \tag{3.3.1}$$

$0 < x < 1$, $t > 0$, with Dirichlet boundary conditions

$$y(t,0) = y(t,1) = 0 \tag{3.3.2}$$

and cost function

$$J(u(\cdot)) = \frac{1}{2}\int_0^\infty \left\{ \left\| \frac{\partial}{\partial t} y(t,\cdot) \right\|_{L_2}^2 + \left\| \frac{\partial}{\partial x} y(t,\cdot) \right\|_{L_2}^2 + R|u(t)|^2 \right\} dt \tag{3.3.3}$$

where $R = 1.0 \times 10^{-6}$.

If one applies the finite element method, as described in Section 1.2, then the approximate control problem is governed by the "raw finite element model"

$$\begin{aligned} \dot{z}^N(t) &= \begin{bmatrix} 0 & I_N \\ -[M_N^E]^{-1} K_N^E & 0 \end{bmatrix} z^N(t) + \begin{bmatrix} 0 \\ [M_N^E]^{-1} G_N^E \end{bmatrix} u(t) && (3.3.4) \\ &= A_N^E z^N(t) + B_N^E u(t) && (3.3.5) \end{aligned}$$

$$\begin{aligned} y^N(t) &= \begin{bmatrix} K_N^E & 0 \\ 0 & M_N^E \end{bmatrix} z^N(t) && (3.3.6) \\ &= C_N^E z^N(t) && (3.3.7) \end{aligned}$$

where the mass matrix, M_N^E; the stiffness matrix, K_N^E, and the input matrix, G_N^E, are given by (1.2.27)–(1.2.29) (see [3]).

In particular, if $A_N = A_N^E$, $B_N = B_N^E$ and $C_N = C_N^E = Q_N$, then the finite element system of dimension $2N$ is given by

$$\Sigma_N = (A_N, B_N, C_N) \tag{3.3.8}$$

We shall also make use of the transformed system

$$\tilde{\Sigma}_N = (\tilde{A}_N, \tilde{B}_N, \tilde{C}_N) \tag{3.3.9}$$

defined in (2.3.4)–(2.3.6) where

$$T = \begin{bmatrix} [K_N^E]^{-\frac{1}{2}} & 0 \\ 0 & [M_N^E]^{-\frac{1}{2}} \end{bmatrix}. \tag{3.3.10}$$

Thus by (2.3.4)

$$\tilde{A}_N = \begin{bmatrix} 0 & [K_N^E]^{\frac{1}{2}}[M_N^E]^{\frac{1}{2}} \\ -[M_N^E]^{\frac{1}{2}}[K_N^E]^{\frac{1}{2}} & 0 \end{bmatrix}. \tag{3.3.11}$$

We will make use of the matrices

$$H_N(\lambda) = [\lambda I - A_N, B_N], \tag{3.3.12}$$

$$K_N(\lambda) = [\lambda I - A_N^T, C_N^T], \tag{3.3.13}$$

$$\tilde{H}_N(\lambda) = [\lambda I - \tilde{A}_N, \tilde{B}_N] \tag{3.3.14}$$

and

$$\tilde{K}_N(\lambda) = [\lambda I - \tilde{A}_N^T, \tilde{C}_N^T]. \tag{3.3.15}$$

The functions that compute the corresponding minimum singular values are denoted by

$$\mathcal{F}_N(\lambda) = \sigma_{\min}[H_n(\lambda)], \tag{3.3.16}$$

$$\mathcal{G}_N(\lambda) = \sigma_{\min}[K_n(\lambda)], \tag{3.3.17}$$

$$\tilde{\mathcal{F}}_N(\lambda) = \sigma_{\min}[\tilde{H}_N(\lambda)] \tag{3.3.18}$$

and

$$\tilde{\mathcal{G}}_N(\lambda) = \sigma_{\min}[\tilde{K}_N(\lambda)], \tag{3.3.19}$$

respectively.

Observe that since $\tilde{A}_N = -[\tilde{A}_N]^T$, Theorem 2.2.4, part (ii) yields

$$\tilde{\gamma}_c^N = \gamma_c(\tilde{\Sigma}_N) = \min_{\lambda \in \mathbb{R}} \tilde{\mathcal{F}}_N(i\lambda) \tag{3.3.20}$$

and by duality,

$$\tilde{\gamma}_o^N = \gamma_o(\tilde{\Sigma}_N) = \min_{\lambda \in \mathbb{R}} \tilde{\mathcal{G}}_N(i\lambda). \tag{3.3.21}$$

We note that $A_N \neq -A_N^T$ and hence Theorem 2.2.4 cannot be applied to compute the radii

$$\gamma_c^N = \gamma_c(\Sigma_N)$$

and

$$\gamma_o^N = \gamma_o(\Sigma_N).$$

The same code (CONT2.M) mentioned in the last section was used for computing $\mathcal{F}_N(\lambda)$, $\mathcal{G}_N(\lambda)$, $\tilde{\mathcal{F}}_N(\lambda)$ and $\tilde{\mathcal{G}}_N(\lambda)$ for λ in a specified rectangle in the complex plane. *Table 3.3.1* contains values for γ_c^N, γ_o^N, $\tilde{\gamma}_c^N$ and $\tilde{\gamma}_o^N$ for increasing values of N. Observe that γ_c^N, γ_o^N and $\tilde{\gamma}_c^N$ are converging to 0 as $N \to \infty$. However, $\tilde{\gamma}_o^N$ does not appear to be converging to 0 nearly as rapidly as γ_c^N, γ_o^N and $\tilde{\gamma}_c^N$. In fact $\tilde{\gamma}_o^N$ was only reduced by approximately 7.0×10^{-9} from $N = 4$ to $N = 16$. The transformation improves γ_c^N and greatly improves γ_o^N.

Figures 3.3.6 and *3.3.8* show, as expected from Theorem 2.24, that the transformed controllability and observability radii are given by (3.3.20) and (3.3.21), respectively. The minimum always occurs on the imaginary axis and is near an eigenvalue of $\tilde{A}_N$. *Figure 3.2.7* contains the plot of $\tilde{\mathcal{F}}_8(i\lambda)$ for real λ satisfying $0 \leq \lambda \leq 32$. A similar plot for $\tilde{\mathcal{G}}_8(i\lambda)$ is given in *Figure 3.3.9.* The same series of plots for the original finite element case are presented in *Figures 3.3.1–3.3.5.*

It is interesting to note that although Theorem 2.2.4 cannot be applied to the original finite element system Σ_N, the minima of $\mathcal{F}_N(\lambda)$ and $\mathcal{G}_N(\lambda)$ also occur on the imaginary axis. Observe that for the raw finite element model the minimum defining γ_c^8 and γ_o^8 occur near the eigenvalue whose norm is of largest magnitude. However, this is not the case for the transformed system $\tilde{\Sigma}_8$ where $\tilde{\gamma}_o^8$ is obtained near an eigenvalue of smaller magnitude. It is also interesting to note that all of the local minima for $\tilde{\mathcal{G}}_8(\lambda)$ are almost equal.

Based on our numerical results, even though Theorem 2.2.4 does not apply to the raw finite element model, we conjecture that the minimum of $\mathcal{F}_N(\lambda)$ and $\mathcal{G}_N(\lambda)$ occur on the imaginary axis.

Table 3.3.1 – Controllability and Observability Radii

N	γ_c^N	$\tilde{\gamma}_c^N$	γ_o^N	$\tilde{\gamma}_o^N$
4	.01702	.05152	.39567	1.00000
8	.00393	.01647	.27941	1.00000
16	.00081	.00472	.19943	1.00000

CONTROLLABILITY SURFACE FOR THE WAVE EQUATION
N=8: RAW FE MODEL

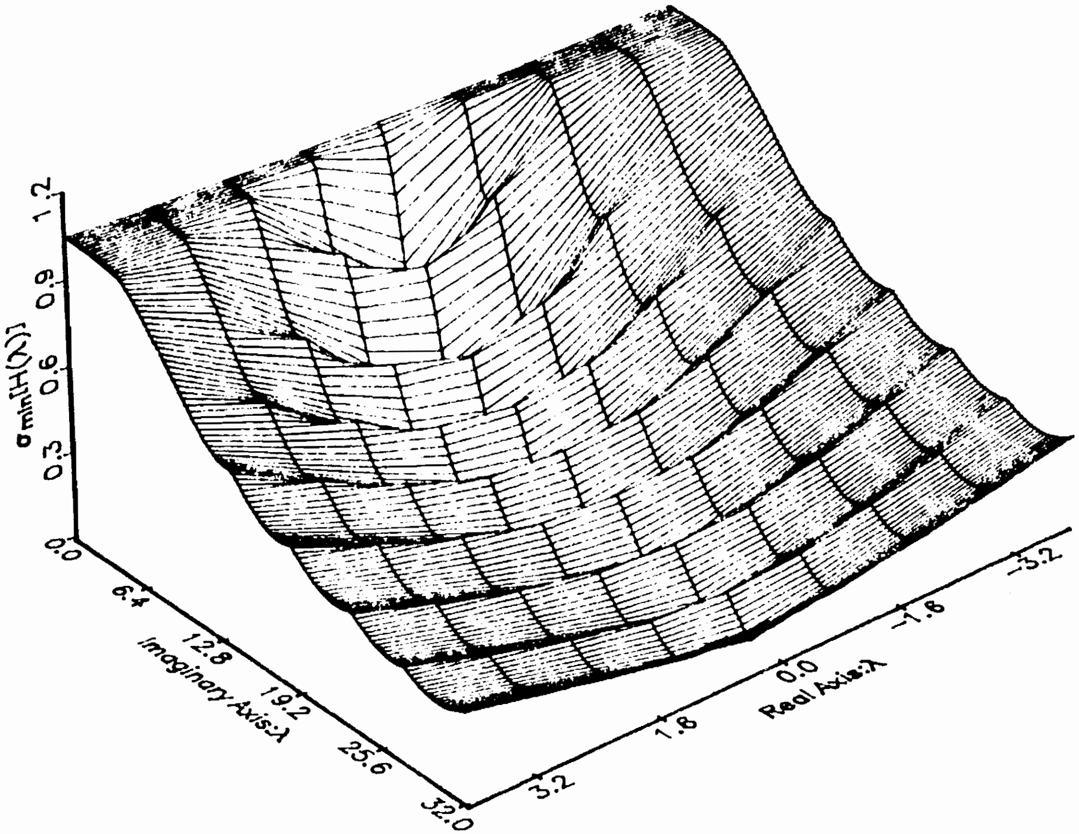

FIGURE 3.3.1

PLOT OF $\mathcal{F}(i\lambda)$ FOR REAL λ
N=8: RAW FE MODEL

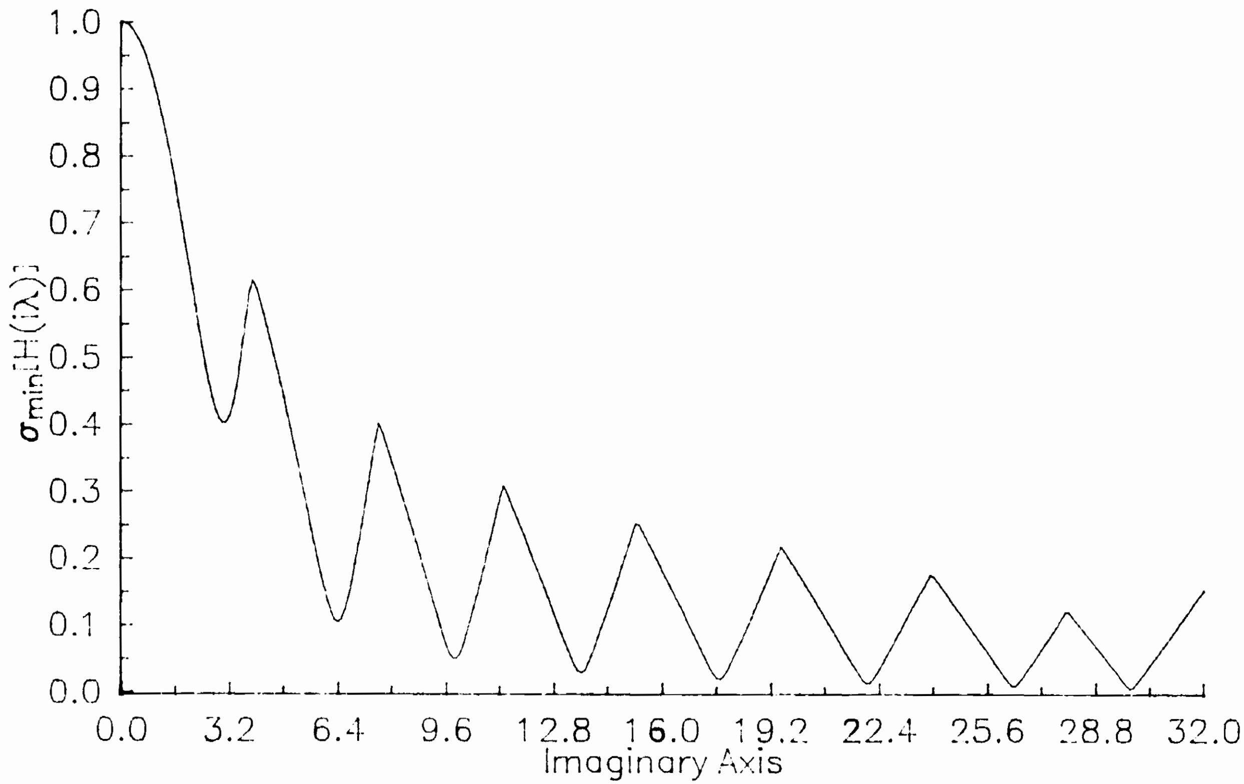

FIGURE 3.3.2

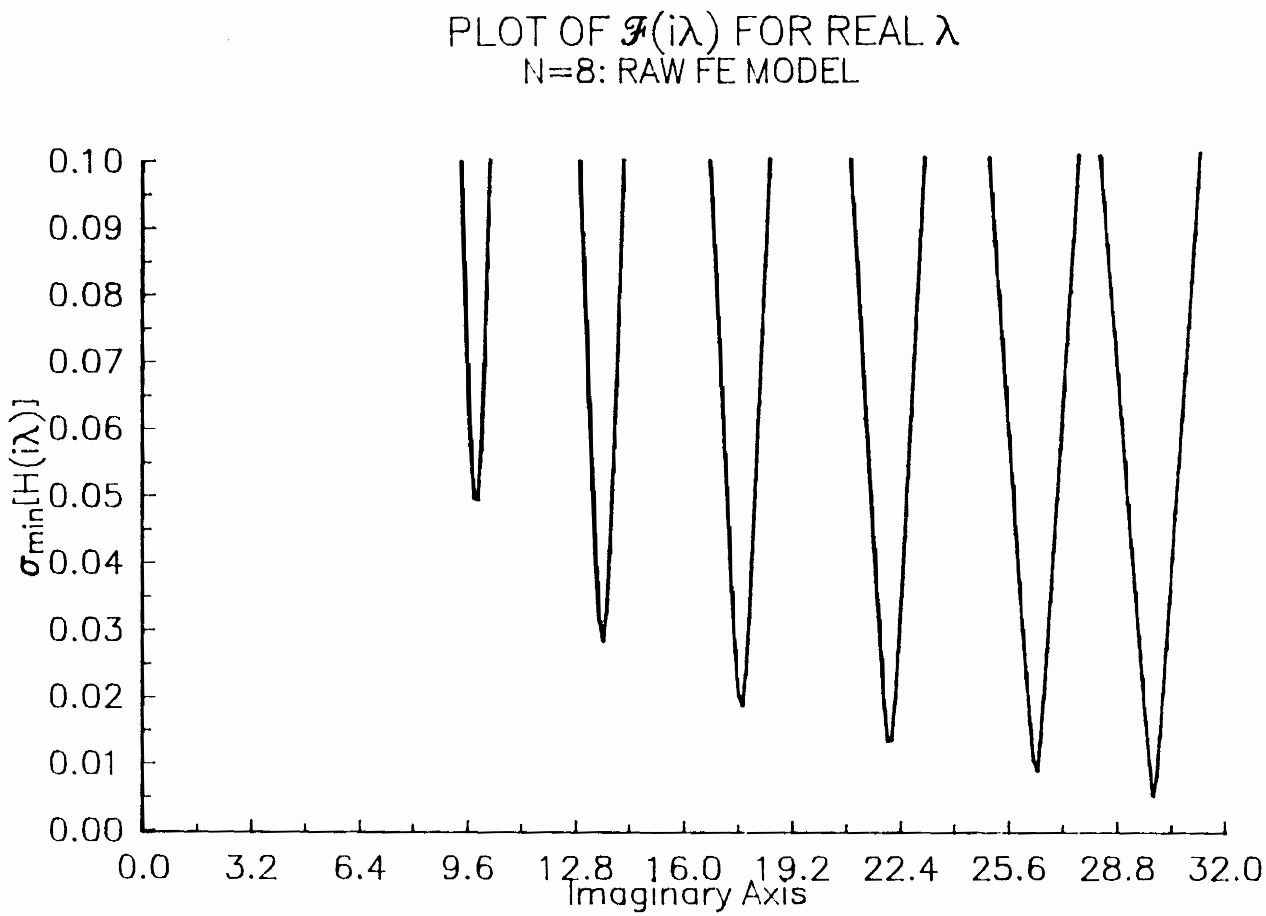
PLOT OF $\mathcal{F}(i\lambda)$ FOR REAL λ
N=8: RAW FE MODEL
$\sigma_{min}[H(i\lambda)]$
0.10
0.09
0.08
0.07
0.06
0.05
0.04
0.03
0.02
0.01
0.00
0.0
3.2
6.4
9.6
12.8
16.0
19.2
22.4
25.6
28.8
32.0
Imaginary Axis

FIGURE 3.3.3

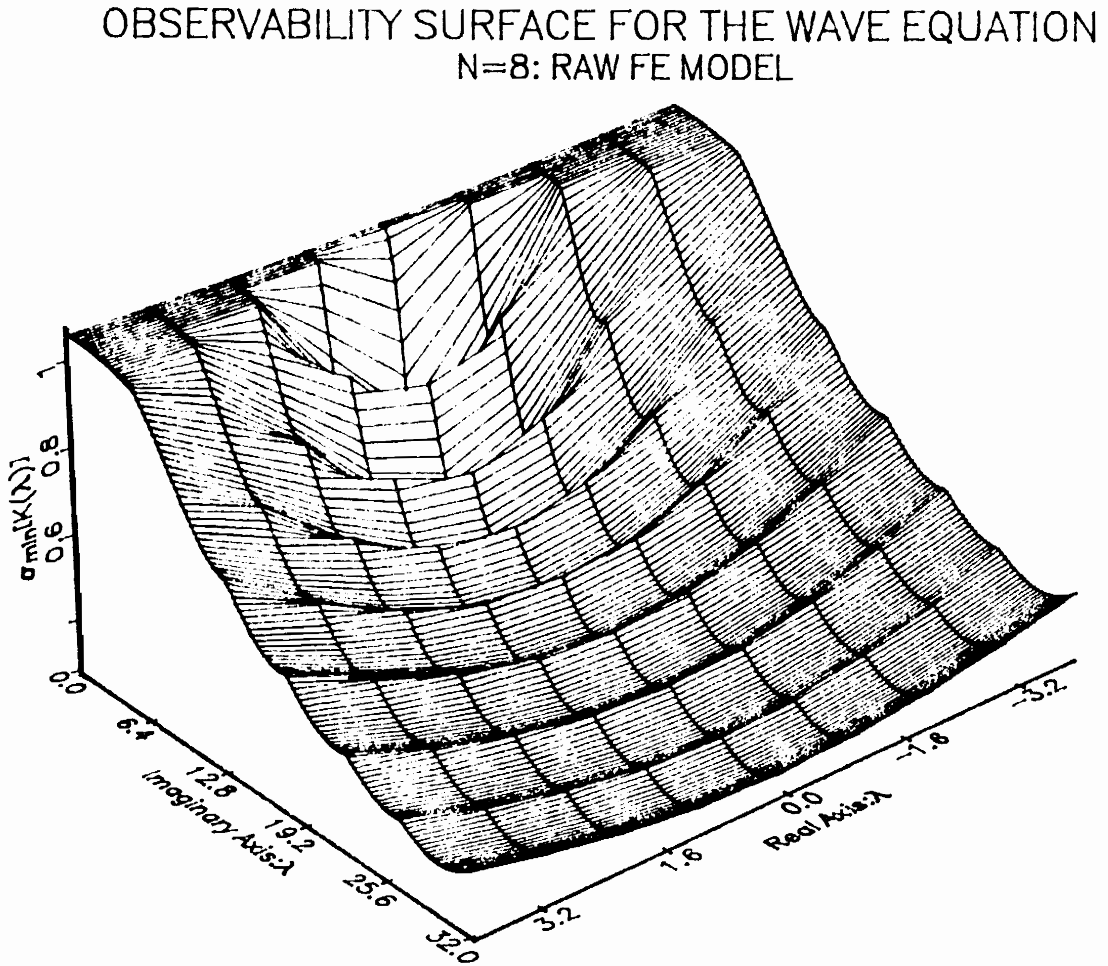
OBSERVABILITY SURFACE FOR THE WAVE EQUATION
N=8: RAW FE MODEL
$\sigma_{min}[K(\lambda)]$
0.0
0.6
0.8
1
6.4
12.8
19.2
25.6
32.0
Imaginary Axis:λ
3.2
1.6
0.0
-1.6
-3.2
Real Axis:λ

FIGURE 3.3.4

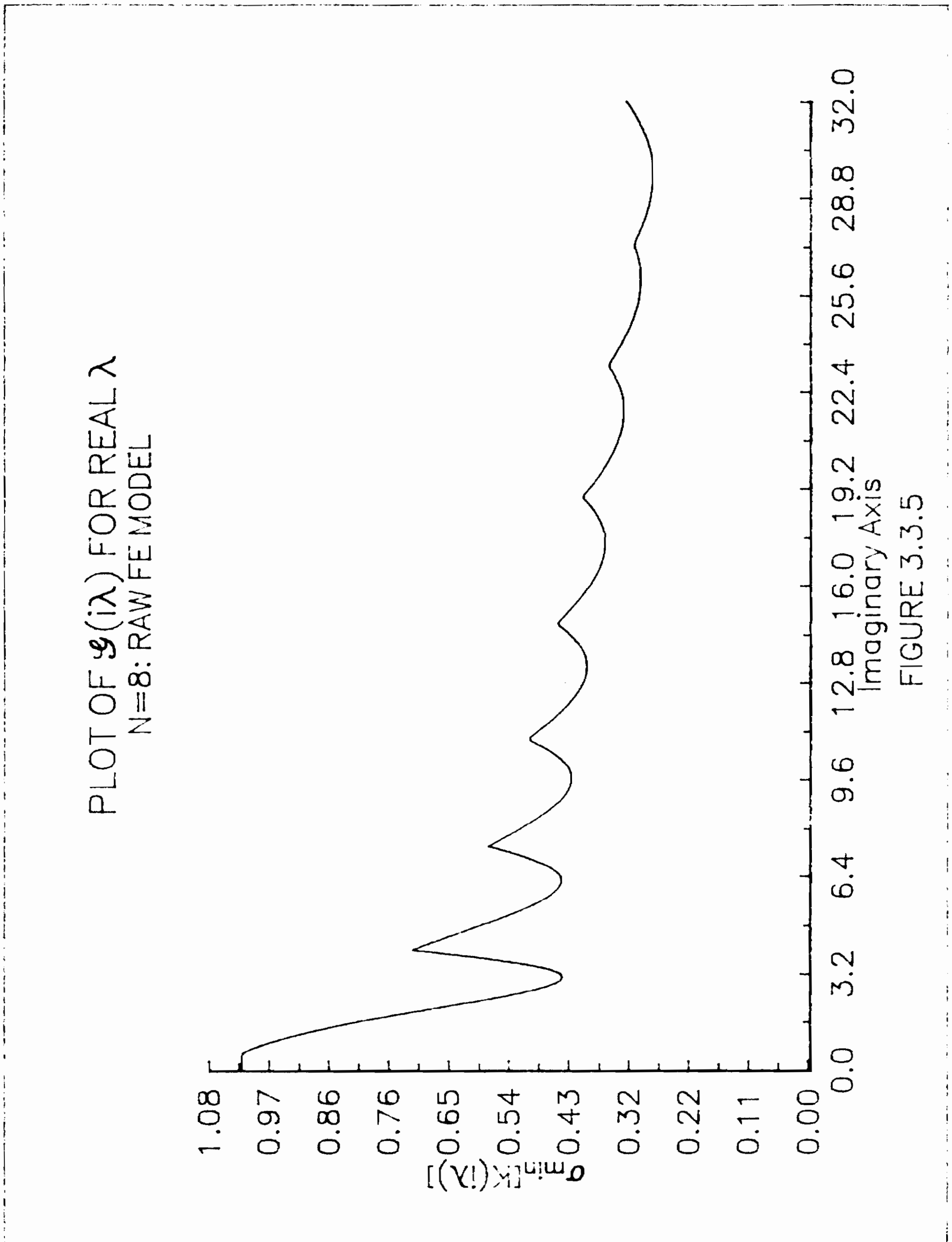
PLOT OF $\mathcal{G}(i\lambda)$ FOR REAL λ
N=8: RAW FE MODEL
$\sigma_{min}[K(i\lambda)]$
1.08
0.97
0.86
0.76
0.65
0.54
0.43
0.32
0.22
0.11
0.00
0.0
3.2
6.4
9.6
12.8
16.0
19.2
22.4
25.6
28.8
32.0
Imaginary Axis

FIGURE 3.3.5

CONTROLLABILITY SURFACE FOR THE WAVE EQUATION
N=8: TRANSFORMED FE MODEL

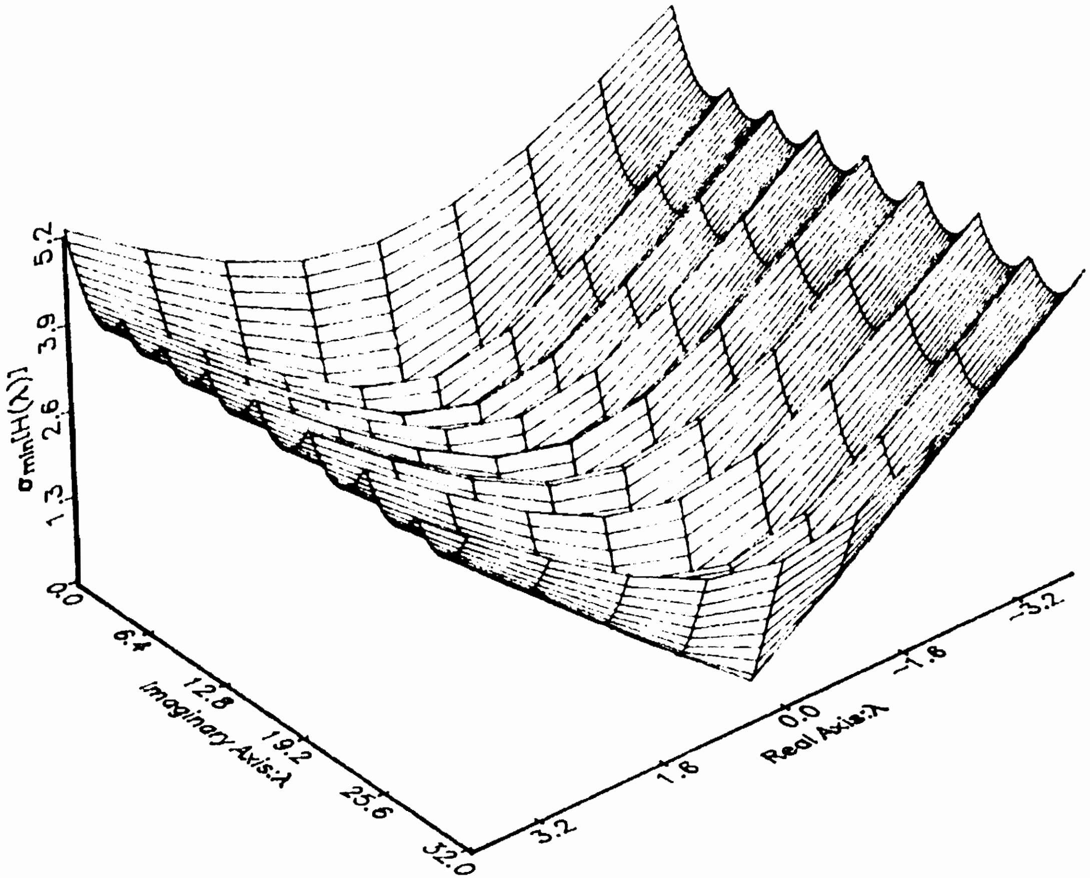

FIGURE 3.3.6

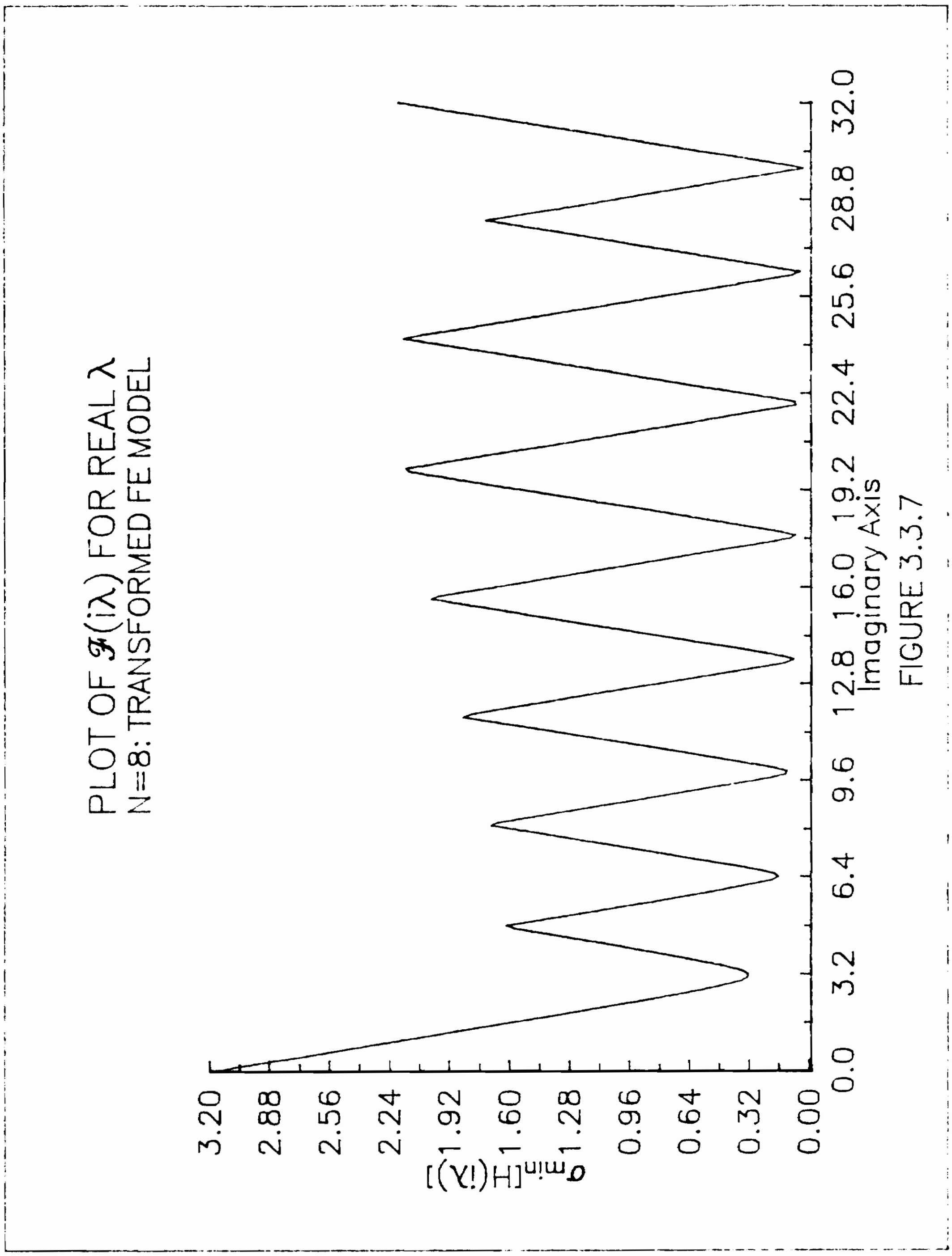
PLOT OF $\mathcal{F}(i\lambda)$ FOR REAL λ
N=8: TRANSFORMED FE MODEL
$\sigma_{min}[H(i\lambda)]$
3.20
2.88
2.56
2.24
1.92
1.60
1.28
0.96
0.64
0.32
0.00
0.0
3.2
6.4
9.6
12.8
16.0
19.2
22.4
25.6
28.8
32.0
Imaginary Axis

FIGURE 3.3.7

OBSERVABILITY SURFACE FOR THE WAVE EQUATION
N=8: TRANSFORMED FE MODEL

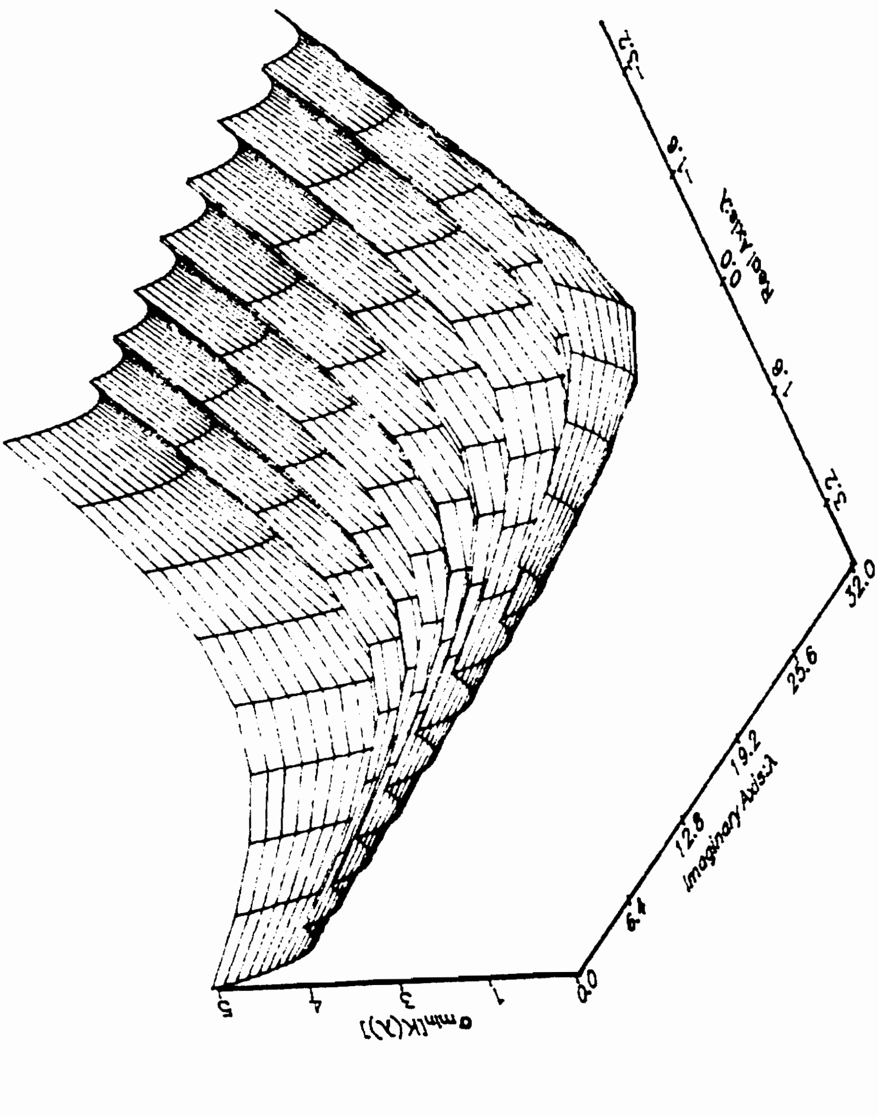

FIGURE 3.3.8

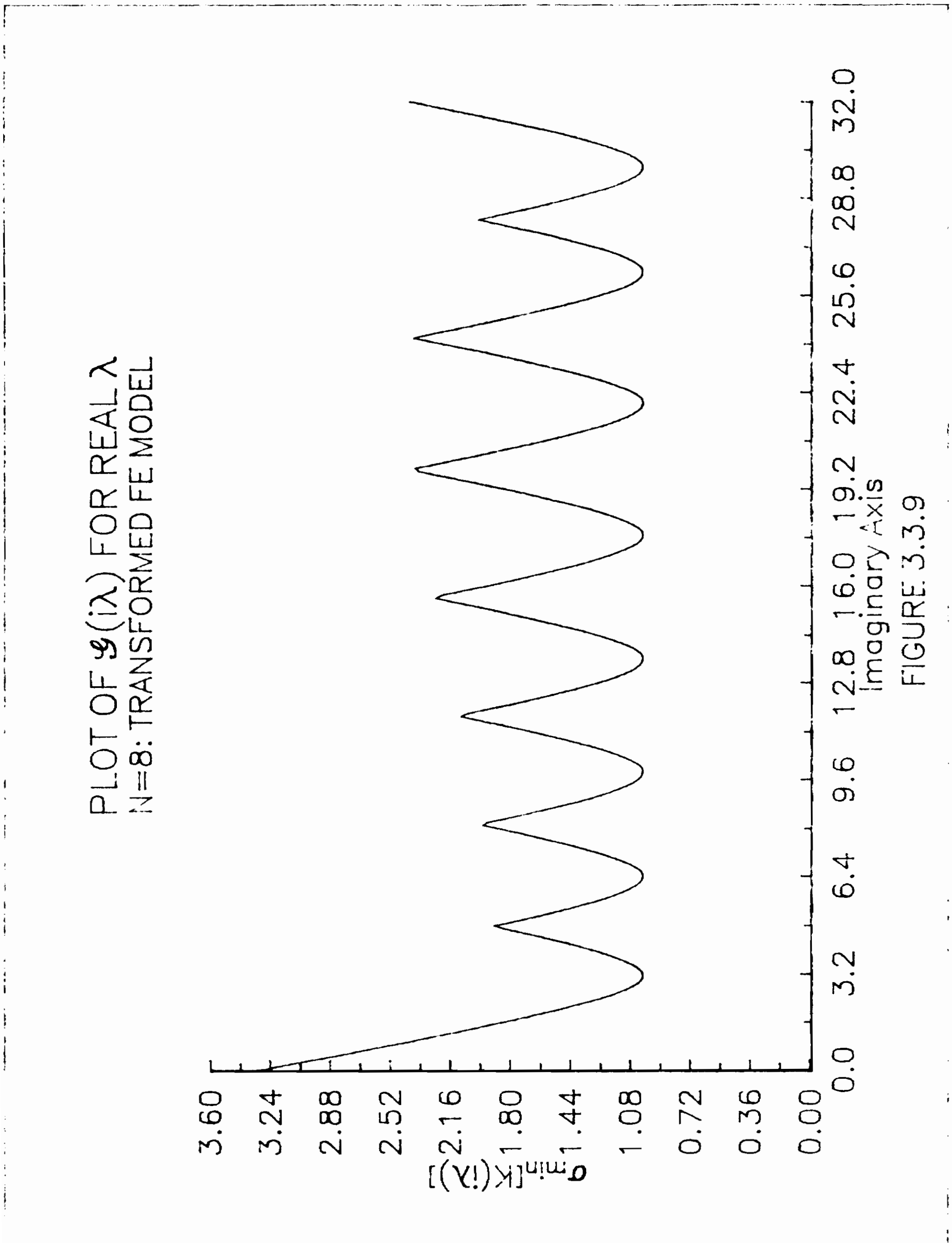
PLOT OF $\mathcal{G}(i\lambda)$ FOR REAL λ
N=8: TRANSFORMED FE MODEL
$\sigma_{min}[K(i\lambda)]$
3.60
3.24
2.88
2.52
2.16
1.80
1.44
1.08
0.72
0.36
0.00
0.0
3.2
6.4
9.6
12.8
16.0
19.2
22.4
25.6
28.8
32.0
Imaginary Axis

FIGURE 3.3.9

3.4. The Equations of Classical Thermoelasticity.

The problem we consider in this section is motivated by the paper [5,7,19,24,25]. The system consists of the basic equations of thermoelasticity with Kelvin–Voight damping terms. For a rod of length 1, the system governed by the hybrid system

$$\begin{aligned}\rho\frac{\partial^2}{\partial t^2}y(t,x) =&\frac{\partial}{\partial x}\left[(\lambda-2\mu)\frac{\partial}{\partial x}y(t,x)-\beta\frac{\partial^2}{\partial t\partial x}y(t,x)\right]\\ &-\alpha(3\lambda+2\mu)\frac{\partial}{\partial x}\theta(t,x)+b(x)u(t)\end{aligned}\tag{3.4.1}$$

$$\rho c\frac{\partial}{\partial t}\theta(t,x) =\mathcal{K}\frac{\partial^2}{\partial x^2}\theta(t,x)-\theta_o\alpha(3\lambda+2\mu)\frac{\partial^2}{\partial t\partial x}y(t,x)\tag{3.4.2}$$

where for $0<\beta<+\infty$, the term $\beta\frac{\partial^3}{\partial t\partial x^2}y(t,x)$ provides Kelvin–Voight damping. In the results presented below the numerical constants are chosen to be the same as used in [19] for an aluminum rod of length 1. In particular, $\rho = 9.82\times10^{-2}$, $\lambda = 2.06\times10^{-1}$, $\mu = 1.11\times10^{-1}$, $\alpha = 1.29\times10^{-3}$, $c = 5.40\times10^{-1}$, $\mathcal{K} = 7.02\times10^{-7}$, $\theta_o = 68$, $q = 30$ and $\beta = 1.8\times10^{-4}$. For these values, $\alpha(3\lambda+2\mu) = 1.085\times10^{-3}$ is the coupling parameter between (3.4.1) and (3.4.2) and represents the "amount of coupling" between the "hyperbolic equation", (3.4.1), and the "parabolic equation", (3.4.2).

The input function $b(x)$ is given by

$$b(x)=\begin{cases}1\ , & .4\le x\le .435\\ 0\ , & elsewhere\end{cases}\tag{3.4.3}$$

and is the same as used in [19]. The boundary conditions for (3.4.1)–(3.4.2) are (Dirichlet)

$$y(t,0)=y(t,1)=\theta(t,0)=\theta(t,1)=0\tag{3.4.4}$$

and the "output operator" is the identity (see [7,19] for details).

A finite element scheme (piecewise linear in $y(t,x)$ and $\theta(t,x)$) was used to construct a finite dimensional model of (3.4.1)–(3.4.4). The finite element model has the form

$$\dot{z}^N(t) = A_N z^N(t) + B_N u(t) \tag{3.4.5}$$

$$y^N(t) = C_N z^N(t) \tag{3.4.6}$$

where A_N is a $3(N-1) \times 3(N-1)$ real matrix. The system matrix A_N is neither symmetric nor skew symmetric. However, $\langle A_N x, x \rangle$ is always real and negative.

We denote the $3(N-1)$ dimensional system by

$$\Sigma_N = (A_N, B_N, C_N). \tag{3.4.7}$$

We shall also make use of the balanced realization of (3.4.7) which we denote, as in Section 3.2, by

$$\hat{\Sigma}_N = (\hat{A}_N, \hat{B}_N, \hat{C}_N). \tag{3.4.8}$$

If k is an integer with $1 \leq k \leq N$, then the reduced order obtained by eliminating k states of the balanced system $\hat{\Sigma}_N$ is denoted by

$$\hat{\Sigma}_N^k = (\hat{A}_N^k, \hat{B}_N^k, \hat{C}_N^k, D_N^k) \tag{3.4.9}$$

Observe that $\hat{\Sigma}_N^k$ has dimension $3(N-1) - k$.

As in Section 3.2, we shall make use of the matrices

$$H_N(\lambda) = [\lambda I - A_N, B_N], \tag{3.4.10}$$

$$K_N(\lambda) = [\lambda I - A_N^T, C_N^T], \tag{3.4.11}$$

$$\hat{H}_N(\lambda) = [\lambda I - \hat{A}_N, \hat{B}_N] \tag{3.4.12}$$

$$\hat{K}_N(\lambda) = [\lambda I - \hat{A}_N^T, \hat{C}_N^T]. \tag{3.4.13}$$

$$\hat{H}_N^k(\lambda) = [\lambda I - \hat{A}_N^k, \hat{B}_N^k] \tag{3.4.14}$$

and

$$\hat{K}_N^k(\lambda) = [\lambda I - [\hat{A}_N^k]^T, [\hat{C}_N^k]^T]. \tag{3.4.15}$$

Also, the functions that compute the corresponding minimum singular values are denoted by

$$\mathcal{F}_N(\lambda) = \sigma_{\min}[H_n(\lambda)], \tag{3.4.16}$$

$$\mathcal{G}_N(\lambda) = \sigma_{\min}[K_n(\lambda)], \tag{3.4.17}$$

$$\hat{\mathcal{F}}_N(\lambda) = \sigma_{\min}[\hat{H}_N(\lambda)] \tag{3.4.18}$$

$$\hat{\mathcal{G}}_N(\lambda) = \sigma_{\min}[\hat{K}_N(\lambda)], \tag{3.4.19}$$

$$\hat{\mathcal{F}}_N^k(\lambda) = \sigma_{\min}[\hat{H}_N^k(\lambda)] \tag{3.4.20}$$

and

$$\hat{\mathcal{G}}_N^k(\lambda) = \sigma_{\min}[\hat{K}_N^k(\lambda)], \tag{3.4.21}$$

respectively.

The LQR problem for the model (3.4.1)–(3.4.4) was solved in [7,19] by using the finite element scheme to produce (3.4.5)–(3.4.6). As noted in [7], convergence of the approximating functional gains is highly dependent on the damping parameter β. We used the value, $\beta = 1.8 \times 10^{-4}$, that corresponds to "large damping". *Table 3.4.1* gives the various system radii for the raw finite element model and the value of λ^* where the minimum of $\mathcal{F}_N(\lambda)$ ($\mathcal{G}_N(zI)$, $\hat{\mathcal{F}}_N(\lambda)$, etc.) occurs.

Table 3.4.1 – Controllability and Observability Radii				
N	γ_c^N	λ^*	γ_o^N	λ^*
4	$4.1916e-05$	0	$5.1945e-04$	0
8	$3.3624e-05$	0	$3.3915e-04$	0
10	$3.2527e-05$	0	$2.8696e-04$	0

Figure 3.4.1 is a plot of the controllability surface $\mathcal{F}_N(\lambda) = \sigma_{\min}[H_N(\lambda)]$ for $N = 8$ and complex λ in the region

$$\{\lambda = \alpha + i\beta \mid -5 \leq \alpha \leq 5,\ -60 \leq \beta \leq 60\}.$$

Observe that the minimum of $\mathcal{F}_8(\lambda)$ occurs at $\lambda^* = 0$. *Figure 3.4.2* clearly shows that $\mathcal{F}_8(\lambda)$ is symmetric with respect to the real axis and hence since

$$\gamma_c^8 = \min_{\lambda\in\mathbb{C}} \mathcal{F}_8(\lambda) = \min_{Re(\lambda)\geq 0} \mathcal{F}_8(\lambda),$$
$$\gamma_s^8 = \min_{Re(\lambda)\geq 0} \mathcal{F}_8(\lambda),$$

and

$$\gamma_c^8 = \mathcal{F}(0),$$

then $\gamma_c^8 = \gamma_s^8 = \mathcal{F}(0)$. In other words, $\gamma_c^8 = \gamma_s^8$ can be calculated by evaluating $\mathcal{F}_8(\lambda)$ at $\lambda = 0$. The observability surface in *Figure 3.4.3* and the corresponding plot along the imaginary axis, *Figure 3.4.4*, show similar features.

Since the approximating system is exponentially stable, we were able to apply the balancing and model reduction algorithm described in Section 2.3. For $N = 8$, the raw finite element model has dimension $3(8-1) = 21$. We eliminated $k = 7$ states and produced a balanced model of dimension 14.

Table 3.4.2 gives the various system radii for the balanced system before model reduction was applied and the value of λ^*.

Table 3.4.2 – Controllability and Observability Radii				
N	$\hat{\gamma}_c^N$	λ^*	$\hat{\gamma}_o^N$	λ^*
4	$1.2112e-04$	0	$1.2123e-04$	0
8	$1.2091e-04$	0	$1.2108e-04$	0
10	—	—	—	—

Note that since the raw finite element system, Σ_N, was nearly uncontrollable and unobservable for $N = 10$, we could not balance Σ_{10}.

Table 3.4.3 gives the various system radii for the reduced order models $\hat{\Sigma}_4^3$ and $\hat{\Sigma}_8^7$ and the values of λ^*.

Table 3.4.3 – Controllability and Observability Radii				
N	$\hat{\gamma}_c^N$	λ^*	$\hat{\gamma}_o^N$	λ^*
4	.24293	$-.02 \pm 14.49i$	.24330	$-.02 \pm 14.49i$
8	.17000	$-.13 \pm 37.88i$	.17031	$-.13 \pm 37.88i$
10	—	—	—	—

The minima defining $\hat{\gamma}_c^N$ and $\hat{\gamma}_o^N$ for the reduced order models occur near an eigenvalue. *Figure 3.4.5* shows that the minimum of $\mathcal{F}_8(\lambda)$ occurs on the imaginary axis. However for that figure the step size along the real axis was 1. Thus when we refined the grid along the real axis we found that the minimum of $\mathcal{F}_8^7(\lambda)$ occurred close to the imaginary axis. *Figure 3.4.6* is a plot along the imaginary axis using the data from *Figure 3.4.5.* Observe that $\mathcal{F}_8^7(\lambda)$ is symmetric. Similar plots are given for observability in *Figures 3.4.7* and *3.4.8.*

After several numerical experiments of this type, we conjecture that the minimum of $\mathcal{F}_N(\lambda)$, $\mathcal{G}_N(\lambda)$, $\hat{\mathcal{F}}_N(\lambda)$ and $\hat{\mathcal{G}}_N(\lambda)$ occur at the origin. We also concluded, as in the heat equation, that balancing the raw finite element model as a first step to model reduction can be numerically ill–conditioned.

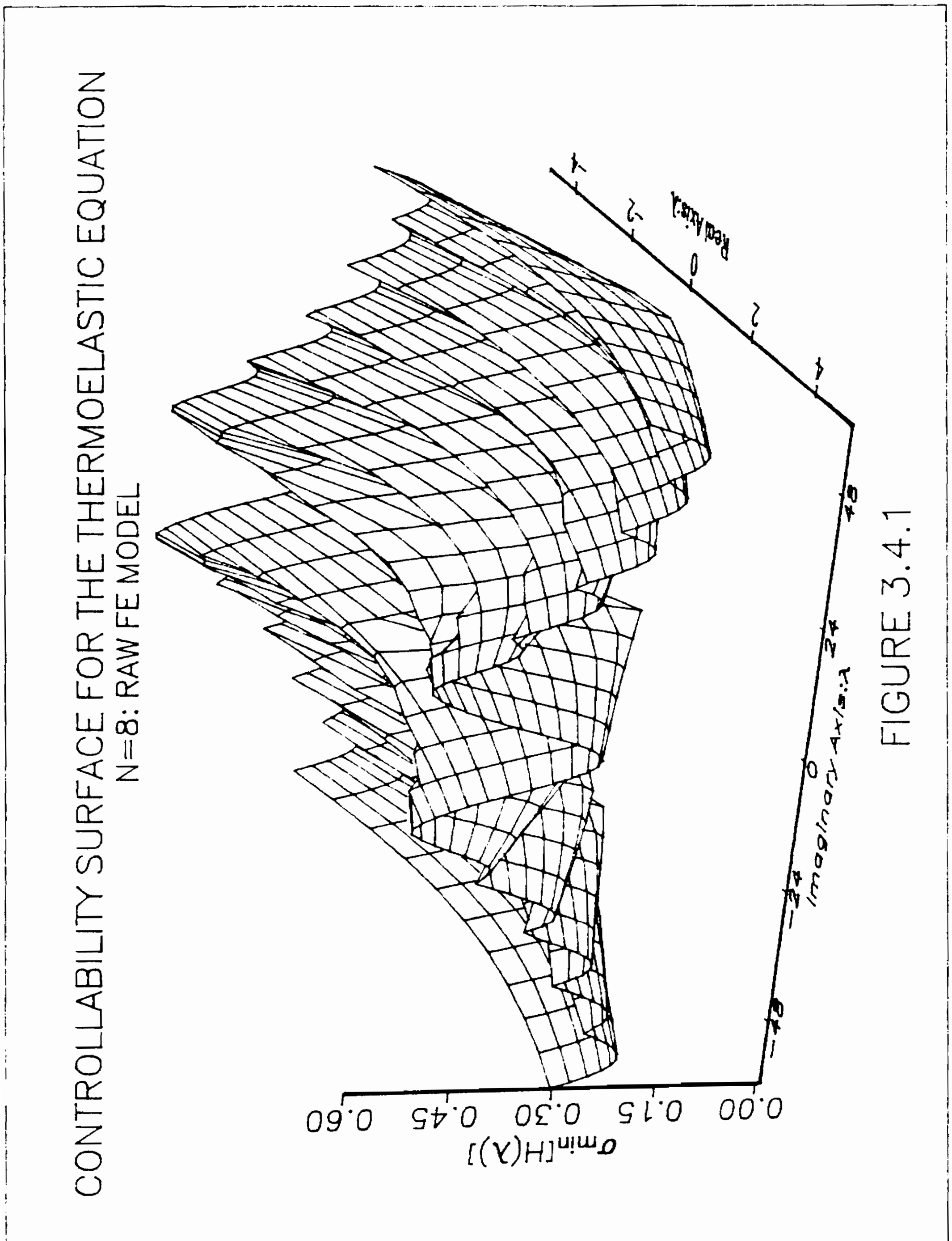
CONTROLLABILITY SURFACE FOR THE THERMOELASTIC EQUATION
N=8: RAW FE MODEL
$\sigma_{min}[H(\lambda)]$
0.00 0.15 0.30 0.45 0.60
-48 -24 0 24 48
Imaginary Axis:λ
-4 -2 0 2 4
Real Axis:λ

FIGURE 3.4.1

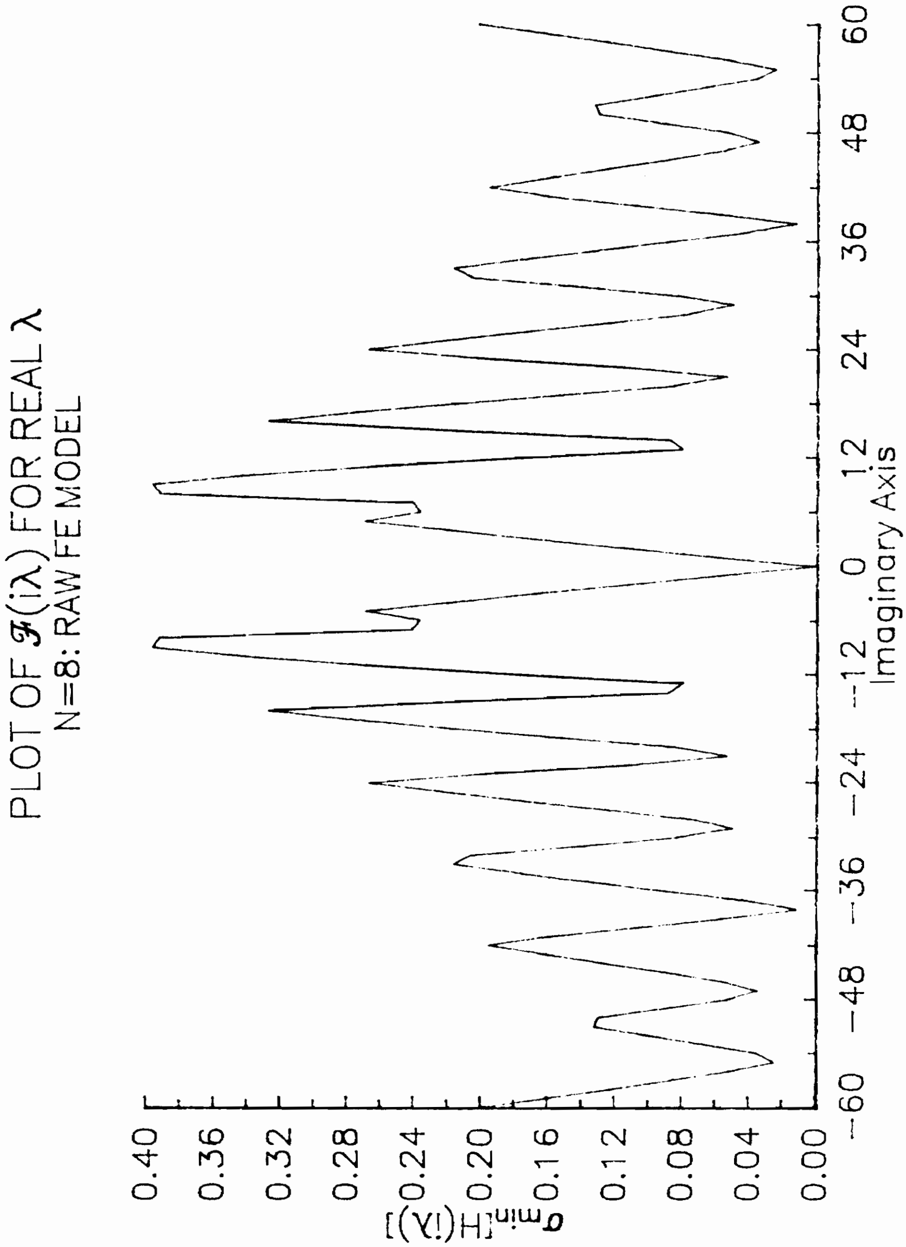
PLOT OF $\mathcal{F}(i\lambda)$ FOR REAL λ
N=8: RAW FE MODEL
$\sigma_{min}[H(i\lambda)]$
0.40
0.36
0.32
0.28
0.24
0.20
0.16
0.12
0.08
0.04
0.00
−60
−48
−36
−24
−12
0
12
24
36
48
60
Imaginary Axis

FIGURE 3.4.2

OBSERVABILITY SURFACE FOR THE THERMOELASTIC EQUATION
N=8: RAW FE MODEL

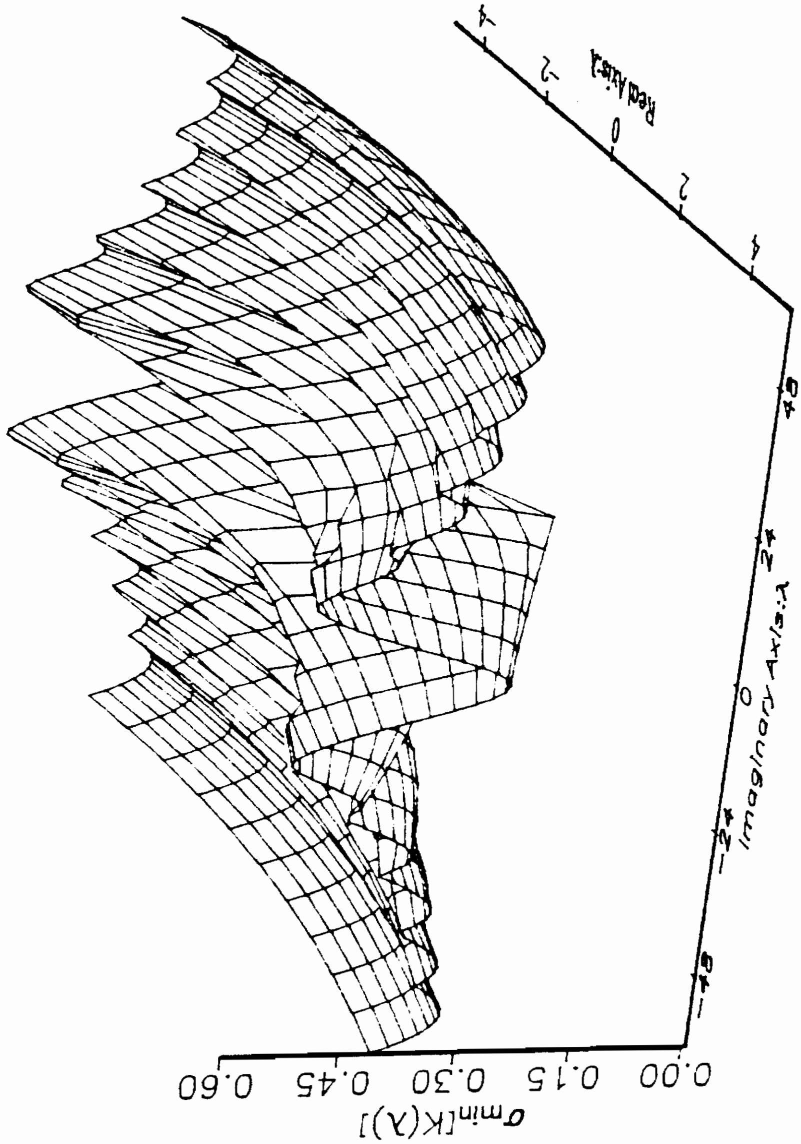

FIGURE 3.4.3

PLOT OF $\mathcal{G}(i\lambda)$ FOR REAL λ
N=8: RAW FE MODEL

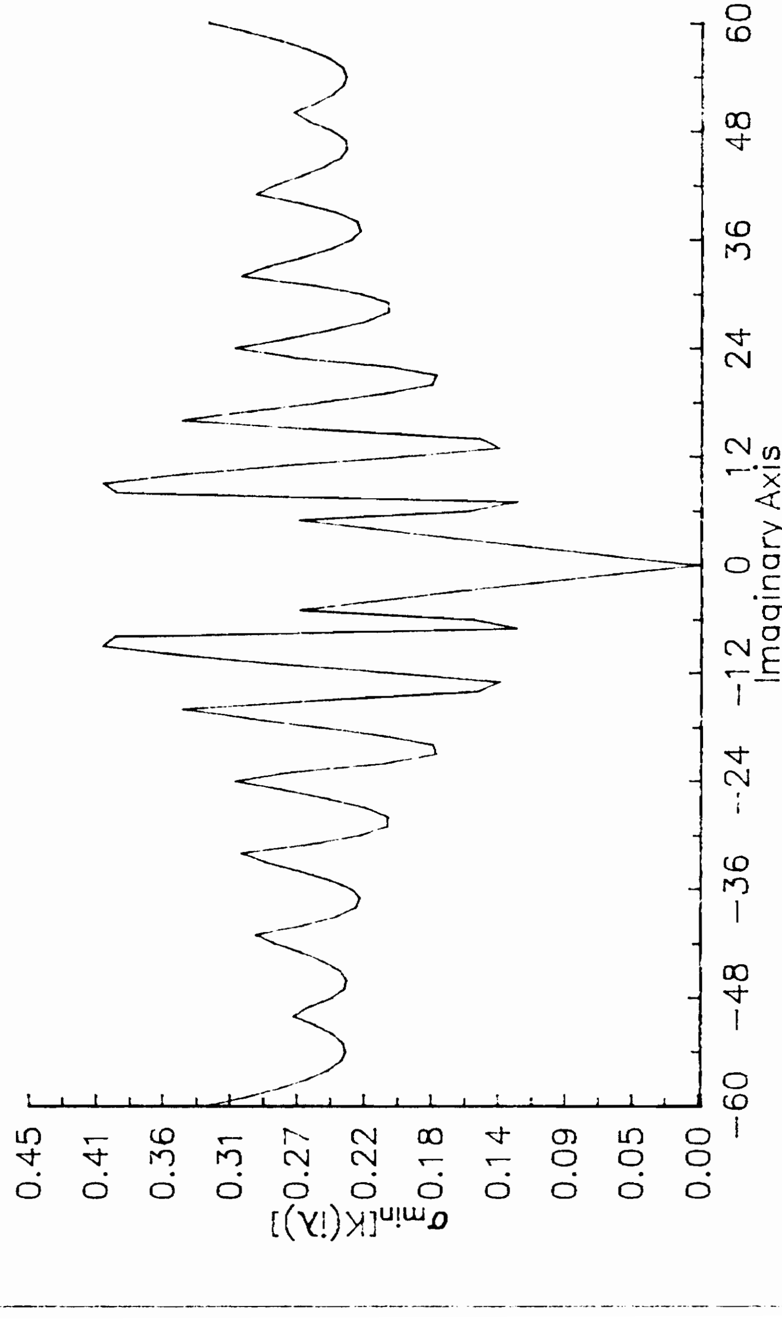

FIGURE 3.4.4

CONTROLLABILITY SURFACE FOR THE THERMOELASTIC EQUATION
N=8: MODEL REDUCED FE MODEL

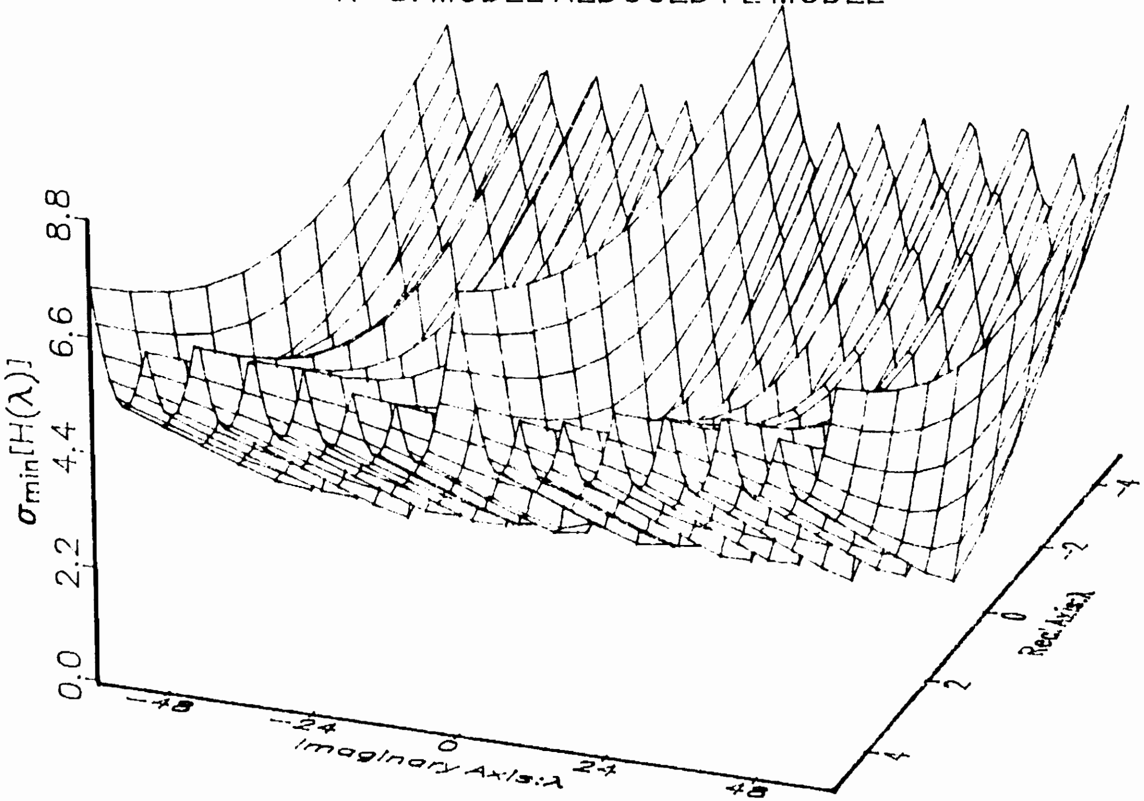

FIGURE 3.4.5

PLOT OF $\mathcal{F}(i\lambda)$ FOR REAL λ

N==8: REDUCED ORDER FE MODEL

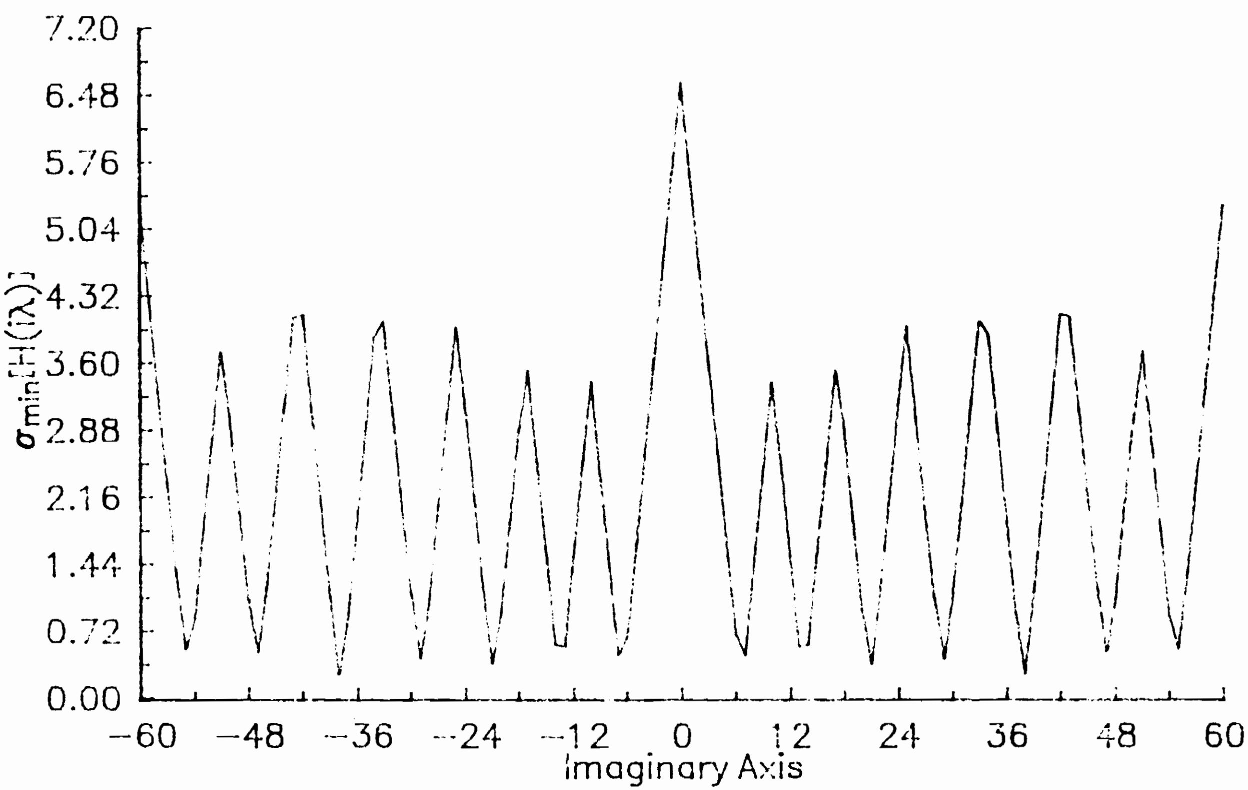

FIGURE 3.4.6

OBSERVABILITY SURFACE FOR THE THERMOELASTIC EQUATION
N=8: MODEL REDUCED FE MODEL

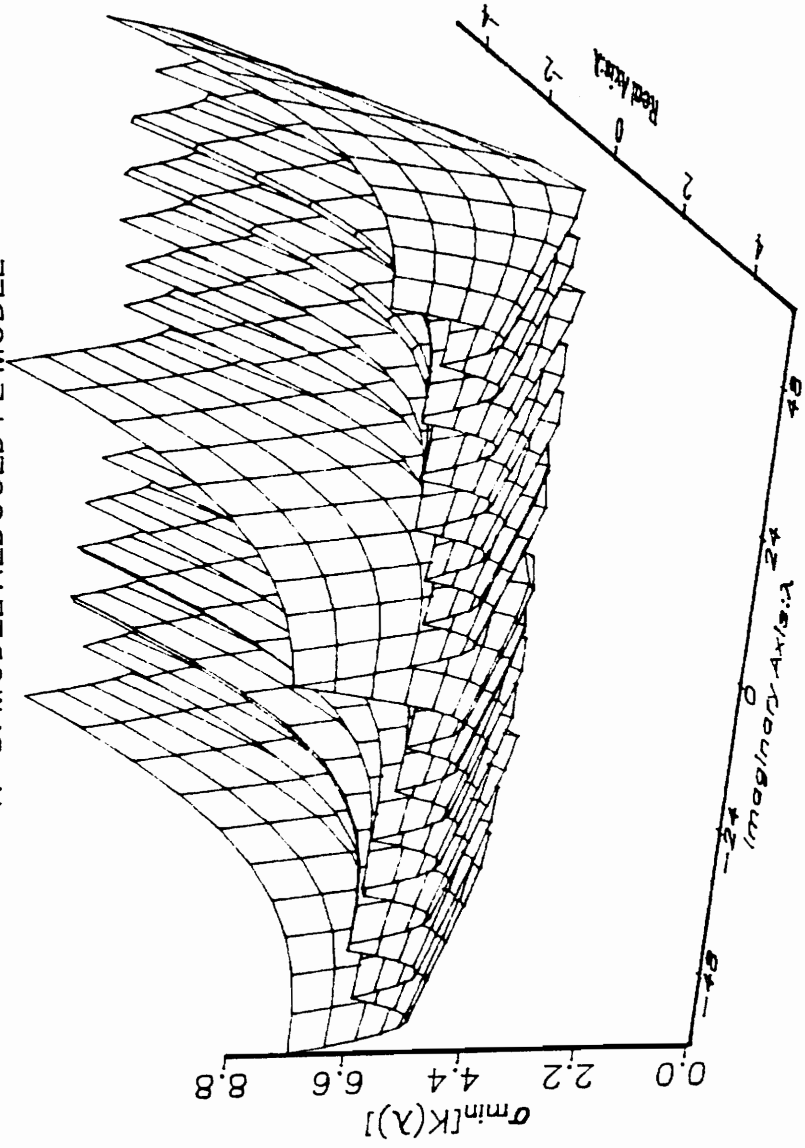

FIGURE 3.4.7

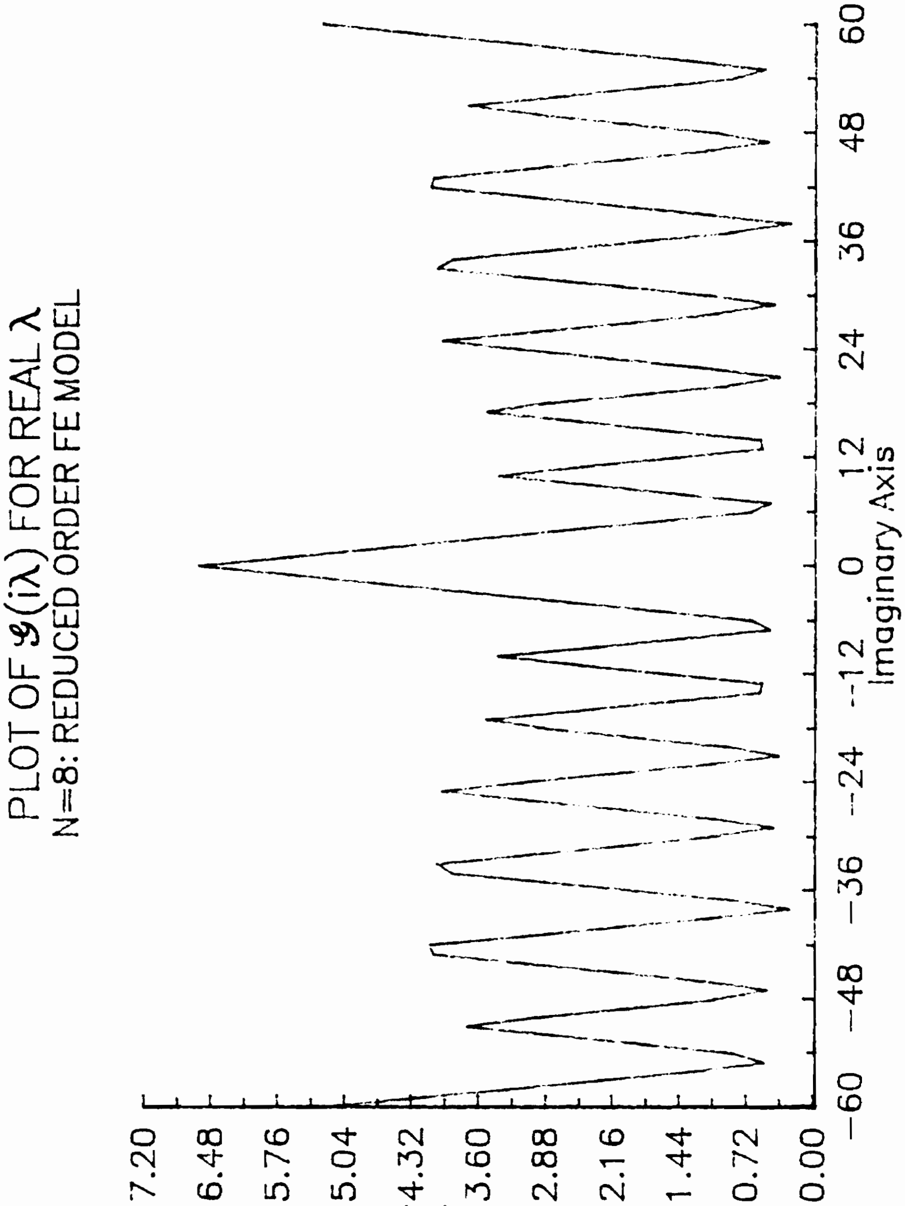
PLOT OF 𝒢(iλ) FOR REAL λ
N=8: REDUCED ORDER FE MODEL
$\sigma_{min}[K(i\lambda)]$
7.20
6.48
5.76
5.04
4.32
3.60
2.88
2.16
1.44
0.72
0.00
−60
−48
−36
−24
−12
0
12
24
36
48
60
Imaginary Axis

FIGURE 3.4.8

Chapter IV. Conclusions

In this paper we investigated the control system radii for finite dimensional systems that are produced by applying finite element schemes to partial differential equations. We also applied balancing and other state transformations to three systems to see how the system radii behaved under such transformations. Reduced order models were also considered. Three types of systems were studied: parabolic (heat equation), hyperbolic (wave equation) and mixed (equations of thermoelasticity).

Several numerical experiments were conducted. However, we have presented only those results that illustrate the following observations.

[1] It is sometimes possible to improve the control system radii by transforming the system. This was the case for the wave equation considered in Section 3.3.

[2] The balancing transformation does not always improve the system radii.

[3] Balancing and model reduction applied to raw finite element models can be highly ill-conditioned.

[4] Certain realizations of the finite element models have symmetries that allow Theorem 2.2.4 and Theorem 2.2.5 to be used to reduce the work needed to compute the system radii. Moreover, certain transformations produce systems that share this feature. For example, in the case of the heat equation, the balanced as well as the raw finite element model both have the minimum of $\mathcal{F}_N(\lambda)$ and $\mathcal{G}_N(\lambda)$ occuring on the negative real axis, even though the balanced system matrix $\hat{\mathcal{A}}_N$ is not symmetric. Similar observations were made for the finite element model of the wave equation and the skew symmetric form of the transformed system.

[5] The number of local minima of $\mathcal{F}_N(\lambda)$ (and $\mathcal{G}_N(\lambda)$) and the "roughness" of the surface $z = \mathcal{F}_N(\lambda)$ (and $z = \mathcal{G}_N(\lambda)$) may provide some indication why standard optimization algorithms have difficulty computing systim radii by using the representation (2.2.13) (see [4,28,31]).

References

[1] Arnold III, W. F., and A. J. Laub, *Generalized Eigenproblem Algorithms and Software for Algebraic Riccati Equations*, Proc. IEEE, 12 (1984), 1746-1754.

[2] Belevitch, V., "Classical Network Theory," Holden-Day, San Francisco, California, 1968, 413-414.

[3] Berdaguer, E. F., J. A. Burns, G. H. Peichl, and R. S. Sanchez Pena, *A note on computing system radii for galerkin approximations of elastic systems*, 29^{th} IEEE Conference on Decision and Control, 1990, 17-21.

[4] Boley, D. L., and W. S. Lu, *Measuring how far a controllable system is from an uncontrollable one*, IEEE Trans. Automat. Control, AC-31 (1986), 249-251.

[5] Burns, J. A., E. M. Cliff, Z. Y. Liu and R. E. Miller, *Control of a thermoviscoelastic system*, 27^{th} IEEE Conference on Decision and Control, 1988, 1249-1252.

[6] Burns, J. A., K. Ito and G. Propst, *On nonconvergence of adjoint semigroups for control systems with delays*, SIAM J. Control Opt., 26 (1988), 1442-1454.

[7] Burns, J. A., Z. Y. Liu and R. E. Miller, *Approximations of Thermoelastic and Viscoelasic Control Systems*, ICASE Report No. 90-43, June, 1990, NASA Langley Research Center, Hampton, Virginia.

[8] Burns, J. A., and G. H. Peichl, *A note on the asymptotic behavior of controllability radii for a scalar hereditary system*, "Control and Estimation of Distributed Parameter Systems," Kappel, F., Kunisch, K., Schappacher, W., Eds., Birkhäuser Verlag, 1989, 27-39.

[9] Burns, J. A., and G. H. Peichl, *On robustness of controllability for finite dimensional approximations of distributed parameter systems*, in "Proceedings of the IMACS/IFAC International Symposium on Modelling and Simulation of Distributed Parameter Systems," Sunahara, Y., Tzafestas, S. G., Futagami, T., Eds., Hiroshima Institute of Technology, Hiroshima (1987), 491-496.

[10] Burns, J. A., and G. H. Peichl, *Open questions concerning approximation and control of infinite dimensional systems*, preprint.

[11] Burns, J. A., and G. H. Peichl, *Preservation of controllability under approxi-*

mation and controllability radii for hereditary systems, Differential and Integral Equations, 2 (1989), 439-452.

[12] Demmell, J. W., *On condition numbers and the distance to the nearest illposed problem*, Numer. Math., 51 (1987), 251-289.

[13] Demmell, J. W., and B. Kagstrom, *Accurate solutions of illposed problems in control theory*, SIAM J. Matrix Anal. Appl., 9 (1988), 126-145.

[14] Eising, R., *The distance between a system and the set of uncontrollable systems*, Proc. MTNS-83, Beer Sheva, Lecture Notes in Control and Information Sciences, 58 (1984), 303-314, Springer, New York.

[15] El Jai, A., and A. J. Pritchard, "Sensor and Controls in the Analysis of Distributed Systems," Ellis Norwood Limited, England, 1988.

[16] Ewing, G. W., "Calculus of Variations with Applications," Dover Publications, New York, 1985.

[17] Gibson, J. S., *Linear-quadratic optimal control of hereditary differential systems: infinite dimensonal riccati equations and numerical approximations*, SIAM J. Control Opt., 21 (1983), 95-139.

[18] Gibson, J. S., and A. Adamian, *Approximation theory for LQG optimal control of flexible structures*, ICASE Report No. 88-48, August, 1988, NASA Langley Research Center, Hampton, VA.

[19] Gibson, J. S., I. G. Rosen and G. Tau, *Approximation in Control of thermoelastic systems*, 1989 IEEE ACC, June 21-23, Pittsburg, PA.

[20] Kailath, T., "Linear Systems," Prentice Hall, Englewood Cliffs, New Jersey, 1980.

[21] Kenney, C., and A. J. Laub, *Controllability and stability radii for companion form systems*, Math. Contr. Signals, Syst., 1 (1988), 239-256.

[22] Laub, A. J., *Computation of 'balancing' transformations*, Proc. JACC, paper FA8-E, 1980.

[23] Laub, A. J., *Numerical linear algebra aspects of control design computations*, IEEE Trans. Automat. Control, 30 (1985), 97-106.

[24] Liu, Z. Y., *Approximation and control of a thermoviscoelastic system*, Ph. D. Dissertation, Virginia Polytechnic Institute and State University, August, 1989.

[25] Miller, R. E., *Approximation of the LQR control problem for systems governed by partial differential equations*, Ph. D. Dissertation, Virginia Polytechnic Institute and State University, November, 1988.

[26] Moore, B. C., *Principle component analysis in linear systems: controllability, observability and model reduction*, IEEE Trans. Automat. Control, 26 (1981), 17-31.

[27] Pazy, A., "Semigroups of Linear Operators and Applications to Partial Differential Equations," New York, Springer, 1983.

[28] Paige, C. C., *Properties of numerical algorithms related to computing controllability*, IEEE Trans. Automat. Control, 26 (1981), 130-138.

[29] Rosenbrock, H. H., "State Space and Multivariable Theory," John Wiley and Sons, New York, 1970.

[30] Strong, G., and G. Fix, "An Analysis of the Finite Element Method," Prentice Hall, Englewood Cliffs, 1973.

[31] Wicks, M. W., and R. A. DeCarlo, *Computing the distance to an uncontrollable system*, IEEE Trans. Automat. Control, 36 (1991), 39-49.

VITA

Kimberly L. Oates was born in West Germany on July 16, 1967. She graduated from James Wood High School in Winchester, Virginia in 1985 and decided to continue her education at Virginia Tech. She received a B. S. degree in Mathematics from Virginia Tech in 1989 and a M. S. degree in Mathematics in August, 1991.

She is currently a member of the Society of Industrial and Applied Mathematics and Pi Mu Epsilon, Mathematics Honor Society.

She will start work with the John Hopkins Applied Physics Laboratory in September, 1991.